Clemson University
TigerPrints

All Dissertations | Dissertations

8-2011

THE EFFECTS OF FUNDAMENTAL MIXTURE PARAMETERS ON HOT-MIX ASPHALT PERFORMANCE PROPERTIES

Wenbin Zhao
Clemson University, yzsjswb.zhao@gmail.com

Follow this and additional works at: https://tigerprints.clemson.edu/all_dissertations

 Part of the Civil Engineering Commons

Recommended Citation
Zhao, Wenbin, "THE EFFECTS OF FUNDAMENTAL MIXTURE PARAMETERS ON HOT-MIX ASPHALT PERFORMANCE PROPERTIES" (2011). *All Dissertations*. 801.
https://tigerprints.clemson.edu/all_dissertations/801

This Dissertation is brought to you for free and open access by the Dissertations at TigerPrints. It has been accepted for inclusion in All Dissertations by an authorized administrator of TigerPrints. For more information, please contact kokeefe@clemson.edu.

THE EFFECTS OF FUNDAMENTAL MIXTURE PARAMETERS ON HOT-MIX ASPHALT PERFORMANCE PROPERTIES

A Dissertation
Presented to
the Graduate School of
Clemson University

In Partial Fulfillment
of the Requirements for the Degree
Doctor of Philosophy
Civil Engineering

---

by
Wenbin Zhao
August 2011

Accepted by:
Dr. Bradley J. Putman, Committee Chair
Dr. James L. Burati
Dr. C. Hsein Juang
Dr. Prasada Rao Rangaraju

ABSTRACT

Asphalt pavements are composed of three components: aggregate, asphalt binder, and air. In the process of plant production and on-site construction, the construction quality can vary in the three components and the variability can further affect a pavement's future performance. This research identifies aggregate gradation, binder content, and air voids content as the fundamental parameters. Understanding the fundamental parameters' influence on the HMA mixture's performance properties can provide valuable information on how to improve the current quality insurance practice. The objective of this study is to investigate how mix gradation, air voids and small range binder content deviation from design binder content can affect, individually and collectively, the performance properties (rutting, cracking, and moisture susceptibility) of asphalt concrete in the context of construction variations.

In this study, three aggregate sources were utilized, and two gradations (fine-graded and coarse-graded) were tested from each aggregate source. Two levels of binder content and air voids content were used to represent the construction variability levels of binder content and density, respectively. The three aspects of mixture performance that were evaluated include rutting, tensile cracking and moisture susceptibility.

It is found that aggregate gradation is significant to rutting and IDT performance. In rutting, the gradation effect is aggregate specific. The effect of gradation on ITS can be reflected by the design binder content, which is closely related to the VMA value of the aggregate gradation. Therefore, the rutting performance seems more sensitive to gradation variation than the tensile strength of a mixture. Binder content variation in a permissible range can significantly affect the rutting and IDT strength properties based on the results of statistical analysis. A "binder content

window" is determined from a fracture energy point of view; however, the rutting performance should not be compromised. On pavement density variation, the study showed that reducing air voids content can increase the mixtures' engineering properties, both rutting and ITS.

Several statistical regression models were developed using the fundamental parameters as the predictors. The equations can effectively summarize the experimental data set, creating quantitative relationships that can possibly be used to predict the response variables.

DEDICATION

I would like to dedicate this work to my wife, Hao Gu, and my daughter, Raina Zhao.

ACKNOWLEDGEMENTS

I would like to acknowledge my committee members for their contribution to this dissertation. First, I thank Dr. Bradley Putman, my academic advisor, for all his guidance. He is completely devoted to helping me finish this study. There were so many times that he put his thoughts into this research that it is impossible to keep track of all, but many of these mentoring occasions will be deeply impressed in my memory and will be a source of inspiration for me over my lifetime. Without his specific advice and detailed instruction, the work would never reach such a quality. Secondly, the same appreciation is extended to committee members: Dr. James Burati, who was also my academic advisor for my Master's study here in Clemson University, Dr. Prasada Rangaraju, and Dr. Hsein Juang. They took valuable time to review my manuscripts, giving constructive advice, correcting the problems of them. This research would not have been completed in a timely manner, if their collective efforts were not there.

I would like to express my sincere gratitude to Dr. Serji Amirkhanian, who was my former academic advisor and directed me the first two years of my Ph.D. Study. He introduced the area of asphalt concrete to me and created the opportunity for me to study this material. Working with him is not only nourishing, but also enjoyable.

Thanks are given to the professors, staff, researchers, and fellow students who work or worked at the Asphalt Rubber Technology Service (ARTS) and the Department of Civil Engineering. They gave me a lot of help and support and made my life easier during the course of my study.

Finally, I will thank my wife for her love and support for my study over the last several years. Also, the financial support and love from my parents-in-law to my family is greatly appreciated.

TABLE OF CONTENTS

Page

TITLE PAGE……...i

ABSTRACT……ii

DEDICATION……...iv

ACKNOWLEDGEMENTS……v

LIST OF TABLES……..x

LIST OF FIGURES……..xii

CHAPTER I: INTRODUCTION……1

Research Objective……..6
Scope of Work……6
Significance of Work……..7
Organization of the Dissertation……8

CHAPTER II: LITERATURE REVIEW……10

Aggregate Gradation……10
Binder Content……..12
Mat Density……...14
Permanent Deformation……19
Tensile Cracking……....20
Moisture Susceptibility……..…23

CHAPTER III: EXPERIMENTAL METHODS AND MATERIALS……..……25

Experimental Plan for Rutting Assessment……...…27
Experimental Plan for Tensile Cracking……...……31
Experimental Plan for Moisture Susceptibility……..…36

Table of Contents (Contitued)

Page

Materials Properties……...……38

CHAPTER IV: STATISTICAL ANALYSIS……...……41

Analysis of Variance…….……41
Tukey's Method for Multiple Comparisons…….....47
Analysis of Covariance……48
Factorial Experiment Design……49
Linear Regression Analysis……..50

CHAPTER V: PERMANENT DEFORMATION……54

Gradation and Mix Design……54
Interpretation of Gradation and Aggregate Interaction…….57
Aggregate Source Effect……...62
Gradation Effect……62
Air Voids Level Effect……..71
Binder Content Effect……72
Main Parameter Sensitivity Analysis……74
2-Way Interaction Effect……...75
3-Way Interaction Effect……...79
Statistical Models……..82

CHAPTER VI: TENSILE CRACKING RESULTS AND DISSCUSIONS……91

Gradation and Mix Design……91
Aggregate Gradation Effect Analysis……96
Binder Content Variation Effect Analysis……...101
Air Voids Content Effect Analysis……..103
2-Way and 3-Way Interaction Effects…….106

Table of Contents (Contitued)

Page

Aggregate Source Effect Analysis……..106
ITS Model Development…….109
Deformation Model…….113
Fracture Energy Model……116
Contour Plot of FE……..117

CHAPTER VII: MOSITURE SUSCEPTIBILITY RESULTS AND DISSCUSIONS……..120

Tensile Strength for Wet-Conditioned Samples…….120
ITS strength model for wet conditioned samples……121
TSR Results…….122
Deformation and Fracture Energy Results……..126

CHAPTER VIII: SUMMARY, CONCLUSIONS AND RECOMMENDATIONS……..128

Conclusions/ Findings for Rutting Performance……129
Conclusions/ Findings for Indirect Tensile Cracking…….131
Conclusions/ Findings for Moisture Susceptibility…….132
Recommendations……...132
Contributions and Applications……...133

APPENDICES……136

Appendix A: Binder Volume and Weight Conversion……...137
Appendix B: Aggregate Gradations……139
Appendix C: Linear Contrasts Construction for 2^{4th} factorial Design…….141
Appendix D: Minitab Statistical Results—Rutting…….142
Appendix E: Minitab Statistical Results—Tensile Cracking……..…...147
Appendix F: Minitab Statistical Results—Stripping……...156

Table of Contents (Contitued)

Page

Appendix G: Mechanical Test Results……....158

REFERENCES……164

LIST OF TABLES

Table Page

Table 1.1 In-Place Density Specification of State A and B…….3

Table 1.2 Pay Factor Determination for the Demonstrative Example…….4

Table 2.1 Effect of Compaction of Pavement Performance (after R.N. Linden et al.)……..…16

Table 3.1 Experiment Design Levels and Code Designation for Rutting Assessment..... 29

Table 3.2 Experiment Design Levels and Code Designation for Tensile Cracking 33

Table 3.3 the Properties of PG 64-22 Asphalt Binder 39

Table 3.4 Physical Properties of Aggregates (after SC DOT, 2010; 2011)..... 40

Table 4.1 the ANOVA (1-way) Table Format..... 46

Table 5.1 Mix Design Parameters in Rutting Assessment..... 57

Table 5.2 New Aggregate Gradation Classifications..... 60

Table 5.3 ANOVA Table for Rutting Results 61

Table 5.4 Design Parameters vs. Gradation Rut depth Correlation Analysis..... 65

Table 5.5 The Values for Parameters in the Correlation Analysis 68

Table 5.6 Treatment Level Means and Sensitivity Analysis for the Main Factors..... 75

Table 5.7 Hypothetical Gradation and Binder Content Interaction due to Gradation Deviation in the Construction Process..... 78

Table 5.8 Tukey's Multiple Comparisons Results..... 80

Table 5.9 Statistical Rutting Model Using Volumetric Variables 84

Table 6.1 Mix Design Volumetric Parameters in Cracking Evaluation 94

Table 6.2 ANOVA Results of Main Factors and Treatment Levels..... 95

List of Tables (Continued)

Table Page

Table 6.3 ANOVA Results of Aggregate Effect 95

Table 7.1 TSR Results 123

Table 7.2 Single Sample ANOVA Analysis Table for TSR..... 124

Table 7.3 Comparison between Experimental and Predicted TSRs 125

Table 8.1 A Summary of the Influence of Fundamental Mixture Parameters…….135

LIST OF FIGURES

Figure Page

Figure 1.1 Illustration of Various In-Place Density Distributions…….....4

Figure 2.1 Establishing a Roller Pattern Using a Test Strip 17

Figure 2.2 Failure (Flow) Zones under Tire Load (after Oh and Coree, 2004) 20

Figure 3.1 Experimental Plan Flow Chart for Rutting Evaluation 30

Figure 3.2 Experimental Plan Flow Chart for Tensile Cracking Evaluation 32

Figure 3.3 Theoretical Stress Distributions on the Vertical Diametrical Plane in IDT Test (After Yoder And Witczak, 1975) 35

Figure 3.4 A Typical Load-Displacement Curve 36

Figure 3.5 Experimental Flow Chart for Moisture Susceptibility Evaluation 37

Figure 4.1 Graphic Illustration of the Treatment Effects Model (After Toler, 2008) 43

Figure 4.2 An Example of F Distribution with Rejection Region 45

Figure 5.1 Gradation Charts: (a) Aggregate A; (b) Aggregate B 56

Figure 5.2 Interaction Plot between Aggregate Source and AASHTO Gradation 58

Figure 5.3 Interaction Plot between Aggregate Source and Performance Gradation 60

Figure 5.4 Four Gradation Rutting Performances at 4% and 7% AV Level 64

Figure 5.5 The gradation rutting effect reflected by $P_{ba,n}$ 68

Figure 5.6 The gradation rutting effect reflected by $SSA*P_{ba,n}$ 69

Figure 5.7 Binder Content Treatment Effect 72

Figure 5.8 Rut Depths at 4% Air Voids with Lower Binder Content 74

Figure 5.9 Aggregate Source and AV Interaction Effect 77

List of Figures (Continued)

Figure Page

Figure 5.10 Gradation And Binder Content Combination Effect: (a) at 4% AV; (b) at 7% AV. (Note: the side-by-side bars are aggregate A and B.) 81

Figure 5.11 Measured and Predicted Rut Depths by Eq 5.5 86

Figure 5.12 Rut Depth vs. Air Voids Content by Using Eq 5.5 87

Figure 5.13 Relationship between Rut Depth and Volume Content of Effective Binder: (a) AV=4.0%; (b) AV=7.0% 89

Figure 6.1 Gradation Charts in Cracking Evaluation: (a) aggregate A; (b) aggregate B; (c) aggregate C 93

Figure 6.2 Aggregate and Gradation Effect on IDT Test: (a) ITS Values; (b) Deformation; (c) Fracture Energy 97

Figure 6.3 Correlation of the ITS with Design Binder Content for the Six Gradations 98

Figure 6.4 Correlation of the Deformation with Design Binder Content for the Six Gradations. 100

Figure 6.5 Binder Content Effects on IDT Test: (a) ITS Values; (b) Deformation; (c) Fracture. Note: (High: OBC+0.25%; Low: OBC-0.25%) 103

Figure 6.6 Air Voids Effect on IDT Test: (a) ITS Values; (b) Deformation; (c) Fracture Energy 105

Figure 6.7 Aggregate Effect on IDT Test parameters: (a) ITS Values; (b) Deformation; (c) Fracture Energy 108

Figure 6.8 Measured Vs. Predicted ITS 111

List of Figures (Continued)

Figure Page

Figure 6.9 Rut depth Prediction Using Eq 6.1: (a) BC=5.3%, AV=Independent Variable; (b) AV=4%, BC=Independent Variable; (c) AV=7%, BC=Independent Variable 112

Figure 6.10 Scatter Plot of Predicted vs. Measured Deformation 114

Figure 6.11 Scatter Plot of ITS vs. Deformation 115

Figure 6.12 Contour Plot of Fracture Energy 118

Figure 7.1 ITS Values of Wet-conditioned Samples 121

Figure 7.2 Predicted vs. Measured ITS for Wet samples 122

Figure 7.3 Graphic Illustration of TSR Results 123

Figure 7.4 Predicted vs. Experimental TSR Values 125

Figure 7.5 Deformation Results for Wet-conditioned Samples 126

Figure 7.6 Fracture Energy Results for Wet-conditioned Samples 127

CHAPTER I: INTRODUCTION

Asphalt pavements are a significant part of the transportation infrastructure system in the United States. They assume a vital role in moving goods and services from place to place. Of the 4-million miles of pavements, 2.3-million miles are paved; approximately 94% of the paved roads are surfaced with asphalt concrete. Every year, more than 550-million tons of hot-mix asphalt (HMA) are produced and placed, with a total expenditure of more than $25 billion (Asphalt Pavement Research and Technology, 2007).

Starting in 1987, the Strategic Highway Research Program (SHRP) developed the Superpave method for asphalt concrete mix design with the intent to address the rutting problems witnessed rampantly on the roads that experienced heavy traffic in the United States, especially during and after the 1970s due to the increase in truck tire pressure. The new system primarily consists of improvements in three areas: the performance-based binder grading system, the introduction of mineral aggregate property criteria (consensus and source), and the Superpave mix design method (Asphalt Institute, 1996). The new mix design method tends to use a coarse-graded aggregate gradation, because it is believed that the aggregate packing characteristics in a coarser gradation can provide an increased aggregate internal friction angle, hence reducing the rutting susceptibility problem; meanwhile, the method tends to produce mixes having leaner binder contents, compared to the precursor Marshall mix design method.

Alongside the mix design specifications are quality assurance (QA) programs. QA refers to those tests necessary to make a decision on the acceptance of a project, and hence to make sure the HMA material used in a pavement project is constructed in conformity to the design parameters and the quality control requirements. According to a 1997 study, 60% of the states

have a QA program in place (Cominsky et al., 1998). A good QA program is essential to the quality of a pavement, because it is the last defense to make sure the parameters and construction standards stipulated by a good mix design document are met during construction.

Pay factors (PF) in a QA program are used as incentives or disincentives to promote better specification compliance. Based on the evaluation of how well a contractor has complied with their requirements, PFs are assigned to the evaluated items or parameters, such as voids in mineral aggregate (VMA), binder content (BC), etc. If a contractor does a good job—the as-constructed values of the evaluated parameters fall in the target tolerance range—he or she will receive a high PF (sometimes PF>1) as a reward (or compensation) for compliance to the specifications; on the other hand, a poor job will incur a partial PF as a penalty to the contractor. PFs serve the goals of both contractors and highway agencies—capital gain and better pavement products, respectively.

One problem that can occur in a QA program is that the assignment of PFs only considers the specification compliance, yet good compliance sometimes has little or no relevance to the final pavement performance. There have been incidences that reflect such a discontinuity between the assigned PF values and the true pavement quality. For example, the contractor who constructed a section of pavement on I-25 in Colorado received bonuses because of good material quality and smoothness; however, within one year after completion, the pavement started to show some longitudinal cracking and the deterioration accelerated in the following years (Harmelink et al., 2008).

The following example shows the PFs for three pavements with hypothetical mat density distributions calculated based on the QA specifications from two states. The purpose of the

example aims to make a point, rather than commenting on the specific quality acceptance approaches; so, they are referred as State A and State B. Table 1.1 includes the PF calculation formulas for in-place mat density for high volume roads with an HMA surface course. Both states use the same density level (around 92%) as the minimum requirement. State A uses a percentage within limits (PWL) approach for quality acceptance, while State B does not use PWL. Three hypothetical mats with different mean density values but the same standard deviation are mat A, B, and C, as shown in Figure 1.1 and the calculated pay factors are shown in Table 1.2.

Three interesting points can be found from the comparisons between the results: (1) for the same mat density property, the PF assigned could differ by as much as 11.4%, as seen by mat B; (2) for the same PF assigned per the State A specification, the density property is different, as seen by mats A and B; the same goes for mats B and C per the State B specification; (3) for the given mats, PFs assigned per the State B specification are generally higher than State A.

Table 1.1 In-Place Density Specification of State A and B

State A			State B	
			% Density	Pay Factor
Lower Spec Limit (%):	92.2		93.6 and above	1.04
Target (%):	94		93.1-93.5	1.02
Upper Spec Limit (%):	96.0		92.0-93.0	1.00
Total Percent Within Limits (TPWL, %)	= (LPWL + UPWL) – 100		91.0-91.9	0.98
			90.5-90.9	0.95
Pay factor (PF, %)	= 55 + 0.5(TPWL)		90.0-90.4	0.91
			89.5-89.9	0.85

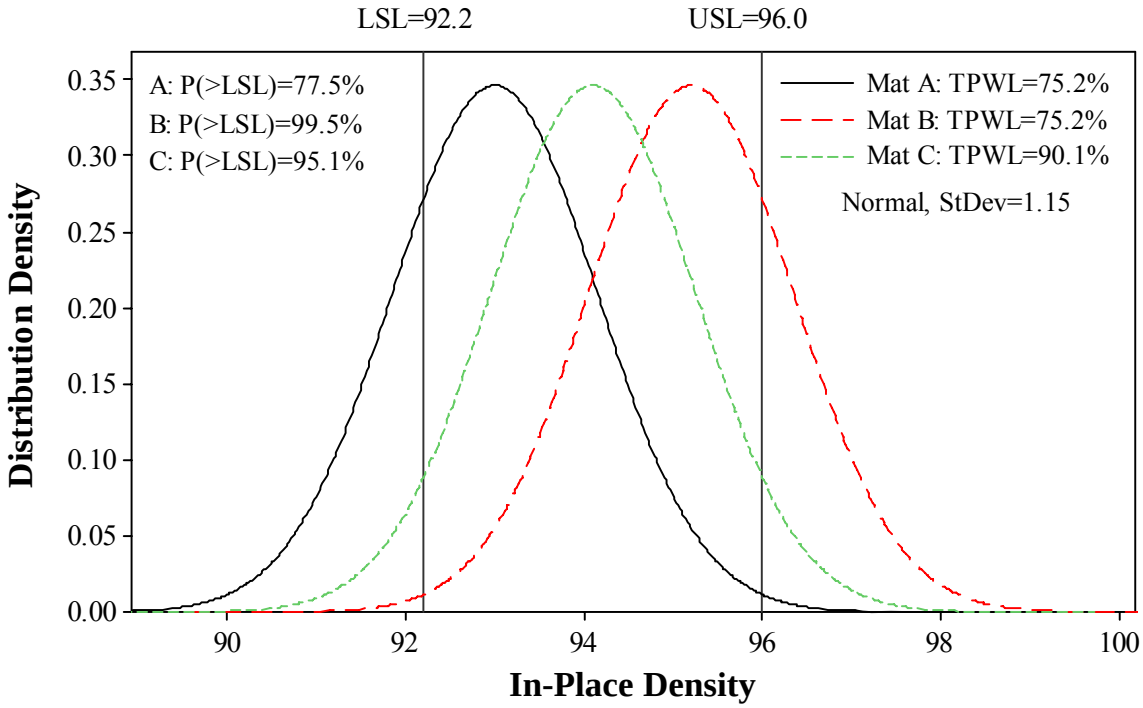

Figure 1.1 Illustration of Various In-Place Density Distributions

Table 1.2 Pay Factor Determination for the Demonstrative Example

Mat	In-place Mat Density (%)		TPWL (%)	Percentage larger than LSL	State A PF	State B PF
	Mean	Standard Deviation				
A	92.2	1.15	75.2	77.5	0.926	1.00
B	96.0	1.15	75.2	99.5	0.926	1.04
C	94.1	1.15	90.1	95.7	1.0005	1.04

Many factors may contribute to the differences in the results, including the quality acceptance approach and PF calculation methods. For example, the PF difference between States A and B for mat B lies in the fact that State B does not use the PWL approach to calculate pay factors. The purpose of this example is not to address the reasons for the differences, but to emphasize

that the pavement performance is an underlining issue in a QA program. It is almost certain that there will be some performance difference between the mats, as their densities are different. From the stand point of promoting fairness, the mat with better performance should be assigned a higher PF; and vice versa. However, as illustrated by this example, no correspondence between PFs and the predicted performance can be clearly perceived. Further, to establish such a reliable relationship between the PFs and predicted performance, it is necessary to address the material properties within the context of construction variations.

To establish the link between the future performance of a pavement and the way the pay factors are assigned, the material properties in terms of the QA parameters should be addressed such that the degree of compliance with the QA parameters could potentially reflect the future performance of a pavement. The HMA material in a pavement is composed of three components, namely aggregate, binder, and air voids. In QA programs, many parameters are used to measure or give an indication of the state or variations of the three components. These parameters include aggregate gradation, mat density, VMA, voids filled with asphalt (VFA), binder content, air voids (AV) content, among others. Why they are selected as the parameters or how they are used in practice are beyond the scope of this study. However, to fundamentally understand the effects of the three components on HMA material's properties, the "raw, primary" terms are used to represent the true state of the three components: aggregate gradation, binder content, and air voids. To distinguish the three parameters from the parameters used in QA programs, in this study these three parameters are generally referred to as "fundamental parameters".

Moreover, each of the three fundamental factors varies within a certain range as allowed by a QA specification; as a result, there will be numerous scenarios due to the combination of the

values of the parameters. The interaction of the fundamental factors has not been adequately addressed in the literature.

RESEARCH OBJECTIVE

The previous example demonstrated that varied pay factor results can be assigned to a pavement with the same constructed quality, depending upon the specific QA program. At least some improvement can be made to one of the QA specifications, or both. The improvement, however, should be based on the understanding of HMA material properties, and reliable future performance related to the material.

The objective of this research was to investigate how aggregate source, mix gradation, air voids and small range binder content deviation from the job mix formula can affect, individually and collectively, the performance properties (rutting, cracking, and moisture susceptibility) of asphalt concrete in the context of construction variations. These parameters are integral parts of the characteristics of a pavement; leaving any one out of the equation will miss out on the true understanding of some fundamental influences of them. Previously, researchers have not put them into one picture. In this research the three parameters were treated as being independent of each other; the effects of the three parameters and the interaction factors were partitioned out. The study variables were put into the context of construction variability, and the outcomes implicitly aim at providing the knowledge to provide a stepping off point to potentially tie pavement performance into QA programs in the future.

SCOPE OF WORK

Three performance characteristics of asphalt concrete were examined in this study: permanent deformation (rutting), tensile cracking, and moisture susceptibility. The treatment levels were

carefully selected to represent reasonable expected values in an asphalt pavement. Each of the factors was put into the context of the presence of other factors such that mixtures with various combinations of the main factors could be analyzed and evaluated. More importantly, this factorial experiment allowed the interaction effects between the different variables to be evaluated.

The specific objectives of this study were achieved by completing the following tasks:

1. Conducting a literature review on the related topics, including the three fundamental parameters (gradation, air void content, and binder content), pavement rutting, tensile cracking and moisture susceptibility.
2. Evaluating the effect of aggregate gradation on asphalt mixture rutting, tensile cracking, and moisture susceptibility.
3. Evaluating the effect of small binder content variations on asphalt mixture rutting, tensile cracking, and moisture susceptibility.
4. Evaluating the effect of air voids content (mat density) on asphalt mixture rutting, tensile cracking, and moisture susceptibility.

SIGNIFICANCE OF WORK

As discussed in the Introduction and Literature Review chapters, the three fundamental mix parameters are very important to the field performance of an HMA mixture. Previous research evaluated their effects separately, or just focused on one aspect of the asphalt concrete performance, leaving some important issues unexamined, such as the interaction effects between the factors. Further, the impacts of the fundamental parameters on HMA properties are the direct technical resource making improvements to current QA programs. However, due to the nature

and complexity of the issue and the inadequacy of previous research, there is no direct and fathomable technical support for agencies to wade through and fine-tune their requirements.

This research examines the critical asphalt concrete performance measures in a holistic way by putting three parameters into one picture; not only individual effects but also the interaction effects will be investigated. It aims to provide direct technical support to agencies. The specific significance of work could be as follows:

- Will provide agencies and asphalt pavement practitioners with the direct information about the effects of individual mix property parameters on rutting performance, and tensile cracking of pavement; the individual effects due to those factors are properly separated.
- Will investigate the interaction effects of the parameters on pavement performance, which could be more important than the individual effects.
- Even though the study is put in the context of construction variation effect and with the purpose of aiming to improve construction quality, the knowledge gained here can be utilized in the mix design process. Mix design engineers will be able to compare the predictive performance of various mixes, and make sure the best mix will be chosen for the project.
- Other information revealed from this study, although it is not germane to the objective of the research, will aid in a better understanding of asphalt pavement's properties and the related laboratory test methods.

ORGANIZATION OF THE DISSERTATION

This dissertation is divided into eight chapters. Chapter I contains an introduction to this topic, research objectives and the scope of work. Chapter II is the literature review on the related subject areas. Chapter III describes the methodology used to fulfill the research objectives,

experimental plans, and the materials involved in the study. The statistical analysis methods that were used to analyze the experimental results are detailed in Chapter IV. Chapters V, VI, and VII elaborate on the experimental results and discussions with regard to permanent deformation, tensile cracking, and moisture susceptibility, respectively. The dissertation is concluded with Chapter VIII, where the findings, conclusions, and recommendations from this study are included.

CHAPTER II: LITERATURE REVIEW

This research covers a wide range of topics: three mixture construction variation parameters—aggregate gradation, binder content variation, and as-constructed density variation; and three performance evaluating characteristics—permanent deformation, tensile cracking and moisture susceptibility. This chapter provides a comprehensive up-to-date literature review regarding these topics.

AGGREGATE GRADATION

Gradation is the most significant characteristic for a HMA mixture. Superpave once introduced the restricted zone to the aggregate gradation, because the expert panel was concerned with the mix tenderness rendered by the sand materials in that sieve size range. A gradation below the restricted zone was encouraged because it was believed to have better shear resistance provided by the coarse aggregate skeleton (Asphalt Institute, 1996). Back then, aggregate gradation was classified as above, through, and below the restricted zone. Previous research on the rutting potential of dense-graded mixtures showed improved rutting performance with gradation through the restricted zone (TRZ) compared to the other two types (Kandhal & Mallick, 2001). Many studies in the literature showed similar conclusions (Kandhal & Cooley, 2002; Zhang et al., 2004). With the restricted zone withdrawn from the AASHTO specification (AASHTO, 2004), agencies are using a master band (or broad band) to confine the specific aggregate size into a certain range, as evidenced by the SCDOT specifications (SCDOT, 2009). Now, the classification for aggregate gradation is coarse-graded and fine-graded. Depending on the mixture nominal maximum aggregate size (NMAS), a primary control sieve (PCS) is determined for the aggregate mixture. A combined aggregate gradation passing below the PCS is

comprised primarily of coarse aggregate and is classified as coarse-graded; if the gradation curve passes above the PCS, it is classified as fine-graded (AASHTO, 2004).

Now, most agencies are explicitly specifying that it is the contractors' responsibility to conduct the gyratory asphalt concrete mix design in accordance with the current specifications. The gradation broad band gives contractors the freedom of developing a master gradation curve that can meet all the mix design parameter requirements, such as VMA, VFA, or even film thickness. However, the band is also large enough to allow two types of aggregate gradations to be designed with the same aggregate source for a pavement project: coarse-graded and fine-graded. Due to these two gradations, the mix properties could be distinctly different. Contractors might prefer one type of gradation to another type just because the selected one could be easier to comply with the gradation requirements of the QA program. This raises the concern that a gradation with better performance, such as higher rutting resistance would not be selected by the contractor. Therefore, to produce a good performing pavement, it seems equally important to address the aggregate gradation issue by selecting a proper gradation in the mix design phase and to control the gradation deviation in the production phase.

Elliott et al. conducted research on the effect of aggregate gradation variation on asphalt concrete mix properties, which specifically aimed at the effects of typical construction variability (1991). Four types of variation from job mix formula (JMF) gradation curves were selected; they represented the extremes encountered on actual construction projects. One of the conclusions drawn from the results stated that coarse gradation variations produced the lowest tensile strength; whereas, the JMF gradation generally exhibited the highest value. Another conclusion

that is worth noting is that within the range of variations normally encountered, air void content had more sensitive influence on the tensile strength than gradation variation.

BINDER CONTENT

The binder content of a mixture should be differentiated between two phases: one is determined by the mix design, often known as the optimum binder content (OBC), which is on the reported JMF; another one is the as-constructed binder content, which may deviate from the target value due to production variations.

The optimum binder content is the ultimate outcome of an asphalt mixture design. In general, the binder content is leaner after a Superpave mix design compared to the traditional Marshall mix design, because the Superpave gyratory compactor (SGC) is more effective at compacting the aggregate into a small space, and the leaner binder content is attributed to increased rutting resistance. During mix design, many factors affect the resulting binder content, such as gyration number and the design air voids content.

The gyration number used in a design reflects the projected level of future traffic. Design for higher volume roads requires a higher gyration number. For example, in the SCDOT mix design technical specification the gyration number is 100 for a Surface Type A mix (interstates and intersections), while the Surface Type B (primary roads) requires 75 gyrations (SCDOT, 2009). The higher compactive effort input can result in a more compacted aggregate skeleton or reduced VMA, thus a lower binder content will be required to fill the voids to reach the specified air voids level (Harmelink et al., 2007).

Another factor that affects the OBC outcome is the air voids content specified in mix design, corresponding to which the OBC will be determined. According to NCHRP report 567

(Christensen & Bonaquist, 2006), many agencies have modified the Superpave 4% air voids criteria and broadened it to a range from 3% to 5%. Based on their findings, it appears reasonable to allow design air voids for Superpave mixtures to vary within the range from about 3% to 5%; however, engineers should understand how such a change can affect HMA performance. If a larger air voids criterion is adopted in the mix design, the portion of VMA that needs to be filled up by asphalt binder is smaller compared to that of a smaller air voids criterion, resulting in a leaner binder content. Therefore, the outcome of a design OBC is dependent on the pre-selected air voids criterion. In fact, the influence of the air voids criteria on OBC can be simply interpreted as changes in OBC. These air voids content criteria differences are commonly reflected in the design of surface course and binder course mixes. The mixes for a binder course often use lower air voids criteria, as compared to a surface course.

The binder content variation during plant production is regulated by the quality assurance program of individual states. Since this variation should be well controlled by contractors and ought to stay in a small range, the binder content tolerances for quality acceptance set forth by states are also small. Agencies often prefer these smaller ranges; however, if the tolerance is too small, the contractor may have difficulty complying with it. On the other hand, if the tolerance is too wide, it may lose its effectiveness to incentivize contractors to do a good job. Therefore, setting up a reasonable tolerance is not an easy task; the decision should be based on how well a contractor can control the deviation when a rigorous quality control method is implemented.

The most distinct characteristic of binder content is that the tolerance specified by a QA program is a small range. NCHRP Project 409 stated that based on previous projects, the standard deviation for binder content determined by solvent extraction is 0.25% (Cominsky et al.,

1998). The standard deviation summarized by Monismith et al. on various projects showed a typical value of 0.3-0.4% (2004). However, previous research conducted using the binder content variation as the treatment factor had relatively large ranges. For instance, in the WesTrack project the binder content was set at ± 0.7% design binder content in an attempt to simulate the binder content variation due to construction. However, the true binder content due to construction cannot be allowed to be that high; the binder content treatment level does not represent the binder content variation. This larger range between the two treatment levels might not adequately examine the possible effect of a smaller binder content variation on mixture performance. In other words, the question pertaining to quality control is whether or not a small binder deviation from the target value will bring about significant mixture performance change. This is a question that cannot be answered by previous research. Furthermore, binder variations would unavoidably be involved in the construction of the road test pavement. Therefore, more research should be conducted in a realistically smaller range to investigate the effects of binder content variations.

MAT DENSITY

In-place mat density is a ratio of bulk specific gravity (BSG) of the asphalt concrete to the theoretical maximum specific gravity (MSG) measured immediately after new pavement is constructed. Because of the inverse relationship between mixture density and air voids content, throughout the paper AV is used as the alternative for in-place mat density.

The air voids content criteria in mix design usually is widely adopted at 4%, but in the field, the pavement is not always compacted to the mix design level, so the density is often much smaller compared to the corresponding 4% AV level. It is rationalized that two or three years

later after a asphalt concrete (AC) pavement has been open to traffic, the pavement will be brought to the design density (or AV) level from the initial as-constructed in-place density due to traffic densification. Prowell & Brown conducted research to monitor the field densification in 40 pavement projects. They found after two years of traffic, the traffic no longer has a significant effect on the pavement density, and the field densities appear to reach a stable state. The stable state density are approximated 1.5% less than the mix design density level (2007). If 4% AV is the corresponding density level for laboratory compacted specimens in the mix design process, it can be inferred that the stable-state field density is roughly about 94.5%.

In the literature, some researchers contended the threshold air void value of asphalt pavement is approximately 8% (Zube, 1962; Brown et al., 1989; Vivar & Haddock, 2007). This proposition was made from the standpoint of lowering permeability. Another research study showed that the loss in asphalt cement penetration increases significantly as the air voids exceed 8 percent, indicating rapid oxidation is avoided in the dense-graded asphalt mixtures with an air voids contents below about 8 percent (Sautucci et al., 1985). Most of the agencies in the US are using 92-93% as their baseline for as-constructed field density.

Several researchers showed that the fatigue life (time from original construction to substantial fatigue cracking of asphalt pavement) was reduced by 10 to 30 percent for every one percent increase in AV content over the normal field range (Fin & Epps, 1980; Epps & Monismith, 1971; Puangchit et al., 1982). From the pavement effective thickness, more air voids means less effective thickness, for example, for a 4-in. pavement, even one percent increase in AV from the 7% baseline value will lead to 0.5 inches of reduction in the effective pavement thickness. Linden et al. did research on the effect of compaction (Linden et al., 1989), which consisted of

three parts: literature review about pavement life reduction due to air voids content increase, a survey of state highway agencies (SHAs), and the Washington State Pavement Management System (WSPMS). Their results are tabulated in Table 2.1; clearly from every perspective, increasing the air voids content leads to a reduction in pavement life.

Table 2.1 Effect of Compaction of Pavement Performance (after R.N. Linden et al.)

Air Voids (%)	Pavement Life Reduction (%)		
	Literature[a]	SHA Survey[b]	WSPMS
7	0	7	0
8	10	13	2
9	20	21	6
10	30	27	17
11	40	38	--
12	50	46	36

[a] Lower bound of range; [b] Average.

Inadequate density of a pavement will leave an excessively high level of air content in it, and the void structure could be interconnected. On top of the poor performance of the pavement itself, the voids allow water and air to permeate into the pavement, causing water damage and binder aging (oxidation/hardening), which will exacerbate the process of pavement deterioration and lead to premature failure of the pavement. In a study about the performance of 18 test sections during 11 years of service, Tam et al. concluded that decreasing the void content from 10% to 5% could yield a 10 percent increase in retained penetration (an indication of age hardening) (1989). This reveals the relationship between air voids content and the rate of aging; increasing density will be beneficial to control age-hardening.

A roller pattern needs to be developed to achieve the field mat density. As shown in Figure 2.1, too much compactive effort does not necessarily render a denser pavement, as the HMA will move laterally due to insufficient confinement pressure. The establishment of a roller pattern depends on many factors, such as the use of proper compactors for different compaction phases (break-down, intermediate, and finish compaction), the proper pressure and passes for the compaction, etc. Some discussion about how to achieve field density can found in the literature (Kassem et al., 2008; Leiva & West, 2008). An evaluation of field measurement techniques for density and permeability was studied by Prowell and Dudley (2002).

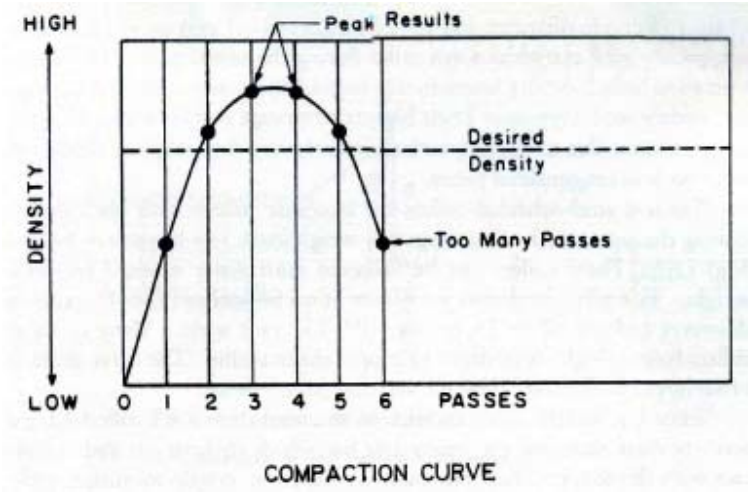

Figure 2.1 Establishing a Roller Pattern Using a Test Strip

From the above discussion, the consensus that can be reached is that the baseline for high end air voids content is 7-8%. How about the low end? Will a low level of air voids have a detrimental or beneficial effect on the properties of HMA materials? Answering these questions will help to determine whether or not constructing a higher density pavement should be encouraged by a QA program when the minimum density requirement is met.

The literature provides mixed accounts about rutting performance of high density pavement. A book on asphalt concrete states that "there is considerable evidence to show the initial in-place voids for dense-graded mixtures should…never fall below approximately 3 percent during the life of the pavement" (Roberts et al., 1996). The supporting evidence was given by others (Ford et al., 1989; Huber & Heiman, 1987). However, it was documented that two sections in the WesTrack project with low air voids content (just above 2.0%) were performing exceptionally well, having very low rut depth (Archilla & Madanat, 2001). Other asphalt concrete properties such as tensile cracking have not been fully documented. There is a need to evaluate the all-around performance of asphalt concrete with respect to mat density variations. One aspect of this research is mainly focused on the influences of the air voids content in the range of less than 7% on pavement performance.

As one may have noticed in the foregoing sections, discussing one of the individual parameters will involve the "intrusion" of other factors. The interactions or the interconnections of the three parameters are inevitable. Considering variations during the mix production and placement and compaction pattern and efforts, a pavement can end up with a number of combinations of values regarding these three factors. Because the three factors intertwine with each other, the effects of them on the pavement performance are confounding. It is very difficult to discern if the effect is attributable to which change in which factor, and it is not uncommon that the experimental results have been misinterpreted because only one factor is considered in their research and the effect observed is solely attributed to that factor, while other factors are confounding. The complexity of the interactions also lies in that the factor that is beneficial to one aspect of a mixture's properties yet may be detrimental to other properties.

PERMANENT DEFORMATION

Permanent deformation is the phenomenon when the surface of an asphalt concrete pavement depresses from the design position due to repetitive traffic loadings. The permanent deformation under the wheel path is called rutting. Most rutting problems occur in summer when the temperature of the pavement is extremely high and the binder stiffness is reduced. A small amount of deformation caused by heavy vehicles will not be recovered when the loads are removed. When the accumulated deformation grows to some extent, the rut poses a serious serviceability problem. Ruts tend to pull a vehicle towards the rut path; in rainy conditions they will be filled with water and cause vehicle hydroplaning, creating tremendous safety hazards to traffic. However, rutting normally is not viewed as a pavement structure failure.

There are two basic types of rutting: mix rutting and subgrade rutting. Subgrade rutting occurs when the subgrade exhibits wheel path depressions due to loading, while mix rutting is exhibited in the surface course and is due to HMA material properties. Rutting refers to mix rutting in this study.

Two mechanisms are involved in the formation of rutting: traffic densification and material lateral movement. Densification occurs in the first several summers after a pavement is open to traffic; the degree of densification depends on the initial compaction level. Material lateral movement is related to the shear resistance of a HMA material; aggregate angularity and mixture binder content are both crucial in the mixture shear property. An illustration of the shear failure zone is presented in Figure 2.2.

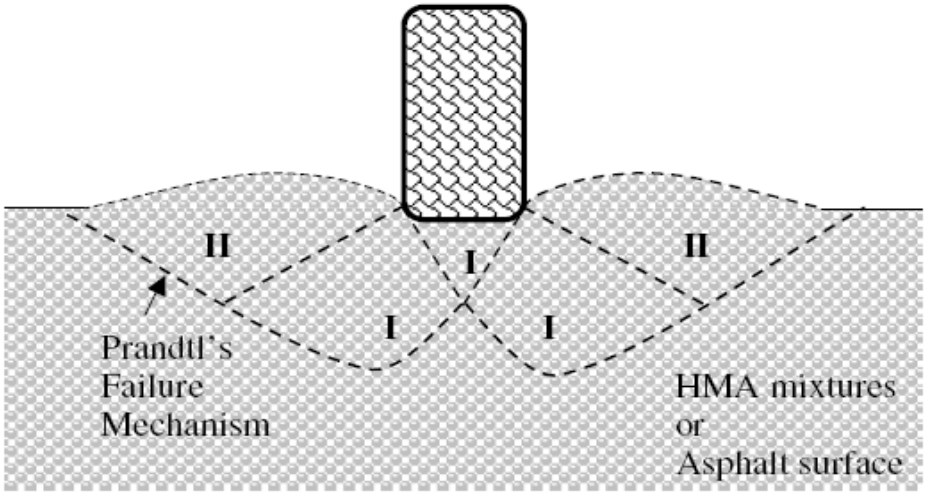

Figure 2.2 Failure (Flow) Zones under Tire Load (after Oh and Coree, 2004)

TENSILE CRACKING

Tensile cracking can be divided into three categories: fatigue cracking, top-down cracking and low temperature cracking (thermal cracking). Thermal cracking is a major concern in northern parts of the country, where the temperature can be extremely low in the winter, and it is effectively addressed by selecting a lower grade binder. This type of cracking is not the focus of this study. The other two are phenomena associated with the traffic loading in the intermediate temperature range, and need to be addressed by controlling the variability of construction of HMA pavement. In spite of the differences between them, the cracking failures depend on tensile performance of HMA, and fundamental cracking initiation and propagation laws can be applied.

Cracking is a major distress in asphalt pavement. Once the microcracks coalesce into macrocracks and reach the surface, the rate of deterioration of the pavement tends to accelerate because water can infiltrate into the pavement; water damage can truly shorten the service life of a pavement. After cracks are observed on the surface, preservation and rehabilitation methods,

such as crack sealing, are normally called for to extend the service life of the pavement. Undoubtedly, this will add strain to a transportation agency's resources, both financially and personnel-wise. Asphalt pavements made with higher tensile strength can withstand larger tensile stresses induced by traffic loads without exceeding the material tensile strength limit. Therefore, the initiation of microcracks can be delayed; and further, longer service life can be expected before the visible macrocracks propagate to the surface. Studying the asphaltic material's tensile performance is of practical significance for highway agencies and asphalt technologists.

Over the years, the energy-based study of cracking has gained interest by using the indirect tension test. Chatti and Mohtar developed the stored energy density criterion for cyclic IDT loading. Dissipated energy remains relatively constant until the crack initiation in the specimen and the number of cyclic loads (number of cycles to failure, N_f) is determined when the dissipated energy deviates from the plateau value (2004). A study by Zhang et al. showed that the dissipated creep strain energy limit, which can be determined from IDT strength test, is a good indicator to rank the cracking resistance of HMA material; it has a one-to-one correspondence to the measured dissipated energy in cyclic loading, indicating the threshold value is independent of loading mode. Moreover, if the critical value is not reached, the microcracks are healable (2001).

Top down cracking initiates at the surface of pavements and propagates downward and outward to form cracks within 0.3 to 1 m from the original cracks. It is one of the most significant distresses in pavements. For example, surface initiated cracking in Florida was found to represent 90 percent of the observed cracking in pavements scheduled for rehabilitation (Myers et al., 1998). Research indicated that top-down cracking is common in thicker pavements

(Uhlmeyer et al., 2000). Some researchers proposed two energy-based criteria to control top-down cracking of HMA: a minimum dissipated creep strain energy threshold and a minimum energy ratio for mixtures passing the minimum dissipated creep strain energy threshold (Roque et al., 2004). The material factors that can cause this type of cracking include low asphalt content, aggregate segregation, and moisture damage (Baladi et al., 2002; Harmelink et al., 2008).

Bottom-up cracking is often caused by loads which are too heavy for the pavement structure or the repeated loadings. Cracks initiate from the bottom of the pavement, since the bottom part of a pavement is subjected to the largest tensile stress and strain. From the material property standpoint rather than the structure (e.g., the thickness of a pavement), stiff mixtures have smaller strain under a given load. However, under repeated loadings mixture stiffness is an influential factor for fatigue performance (Monismith et al., 1985; Xiao et al., 2009; 2010). Shen and Carpenter used the dissipated energy approach to study mixture fatigue properties; they found the plateau value had a great inverse relationship with fatigue life (loading cycles) (Shen & Carpenter, 2006; 2007). The plateau value prediction model developed shows that flexural stiffness has a very strong relationship with the plateau value. Increase in flexural stiffness will increase the plateau value; as a result, the fatigue life will be reduced. On the other hand, using a thicker pavement is usually a structural means to increase the overall pavement stiffness, hence reducing the strain level in the "fibers" close to the bottom of a pavement.

Recently, Yoo and Al-Qadi proposed the concept of "near-surface" cracking after numerical analyses using finite element models (2008), and further argued that the near-surface cracking needs to be considered as a primary cause of pavement distress, namely fatigue cracking. The near-surface cracking is caused by significant vertical shear strain at a location near to the

surface, and is usually mistaken as top-down, bottom-up, and construction cracking, according to the authors.

Moreover, some researchers found that asphalt mixtures have some capacity to heal the microcracks, especially if a rest period is allowed before the next cycle of loading (Carpenter, Shen, 2006; Shen et al., 2010). Healing is hypothesized as the key reason to explain the existence of a fatigue endurance limit due to its ability to reverse the damage created by traffic loading and the environment.

MOISTURE SUSCEPTIBILITY

Asphalt mixtures are susceptible to moisture, which can lead to a problem commonly known as stripping. Stripping occurs when the bond or adhesion between aggregate and the asphalt binder becomes weaker; normally, the weakness is initiated by the intrusion of water into the pavement through interconnected voids or cracks. Manifestations of stripping on the pavement surface include various premature problems: fatigue cracking, rutting, raveling, shoving and potholes. It is one of the most serious problems with regard to pavement performance because the integrity of the pavement is greatly compromised.

The displacement of asphalt on the aggregate particle surface by water is a complex phenomenon, which involves the physicochemical interaction between aggregate, asphalt binder, and water. Mineralogy and chemical composition of the aggregate could be important contributing factors. In general, some aggregates have an affinity for water over asphalt (hydrophilic). These aggregates tend to be acidic and suffer from stripping after exposure to water. On the other hand, some aggregates have an affinity for asphalt over water (hydrophobic). However, the specific mechanism is not yet fully understood.

Kandhal summarized some production and construction problems that lead to stripping in asphalt pavements (1994). These external causes include inadequate pavement drainage, inadequate compaction, excessive dust coating on aggregate, use of open-graded asphalt friction course, inadequate drying of aggregate, weak and friable aggregate, etc. In addition, water can get into the pavement through the cracks developed when the pavement is in service; therefore, constructing a pavement with higher cracking resistance will delay the cracking occurrences, and further mitigate or delay the chances of water damage.

Measures to prevent stripping are to include anti-stripping agents in the asphalt concrete, such as hydrated lime, hydraulic cement, and liquid additives. Studies showed that lime is the most effective additive in reducing water damage compared to liquid additives, based on both long term and short term evaluation of asphaltic mixtures (Xiao et al., 2010; 2011).

CHAPTER III: EXPERIMENTAL METHODS AND MATERIALS

This research aimed to indentify the effects of three fundamental parameters on the performance of asphalt concrete, namely aggregate gradation, binder content variation, and air voids content. These parameters are integral parts of the characteristics of a pavement; leaving any one out of the equation will miss out on the true understanding of some fundamental influences of them. Previously, researchers have not put them into one picture. In this research the three parameters are treated as being independent of each other; the effects of the three parameters and the interaction factors will be partitioned out.

The aggregate gradation factor is the most independent variable in the experimental design, because neither the gradation selection in a mix design nor the gradation variation during the construction process is affected by variation in binder and air voids content. The design binder content will be viewed as a characteristic of the selected gradation, because the design binder content is partially dependent on the VMA, which is a distinct aggregate structure packing characteristic. The OBC difference between mixes could lead to a performance difference in the pavement. This effect will be viewed as part of the aggregate gradation effect, rather than a binder variation effect.

The binder content variation will be achieved by using higher and lower amounts of the binder content deviated from the design binder content. The effect of binder content on mix properties will reflect the effect of variability in binder content during plant production. Once the effects of binder content on mix properties are understood, the information may potentially be used to help with the binder selection for mix design, because with the compaction gyration

number varying in the possible range, the resulting binder content may change accordingly within roughly the same range as the construction variability of the binder content.

The factor of air voids content aims to provide the information about comparative performance of mixtures at a lower level to the baseline level, and further give some indication about whether or not constructing a higher density pavement should be encouraged. In lab compaction, the air voids content, which is the reverse of density, is mainly a function of compactive effort; the mixture is confined in a rigid mold, where more gyrations result in less voids in the mix. In the field, the density depends on the proper compaction pattern, such as the combination of rollers and the number of passes. Undoubtedly, variations in aggregate gradation and binder content can affect the mix compactability; if the compaction pattern is kept constant, the variations in those two factors will lead to different air voids levels in the final pavement product. However, this research assumes that the influences due to the variations in those two factors are limited, and the pavement can be constructed to the baseline density level (7-8% air void content), if the mix is properly designed and the mat temperature during placement is effectively maintained. Therefore, in spite of the compactability between mixtures, further constructing a pavement with less air voids mainly depends on the proper use of compaction patterns. Even though how much of increase in the mat density can be achieved is not well known, a 4% air voids content is used as the higher density level to represent the effect of appropriate construction methods or field control efforts. With the information about the mix performance at normal and lower density levels, policy makers can decide whether the effort that contractors take to construct a pavement of greater density should be encouraged or discouraged, rewarded or penalized.

The independence between the three experimental factors with respect to construction variability is quite on the contrary to the interrelationship of the factors during mix design. In a mix design, the three factors are intertwined; changing any of them will result in a change in the others. Once the mix design is done, in the construction process, the variability in these three parameters appear to be less intertwined, and it is the main reason why this research is trying to investigate the HMA material properties in the realm of construction variability.

Different experiments were carried out to evaluate the different characteristics of HMA performance: permanent deformation at high temperature, tensile cracking at intermediate temperature and moisture susceptibility. The structure of explaining the experimental methods will be arranged in accordance to these performance classifications.

EXPERIMENTAL PLAN FOR RUTTING ASSESSMENT

Experimental Factors and Treatment Levels

A full level, 4^{th} order factorial experiment was designed. The treatment factors were aggregate source, aggregate gradation, air void content, and binder content, with each factor having two treatment levels. Aggregates A and B were selected because they have a fair share of the South Carolina aggregate market; another reason is that their mineralogy and physical properties differ from each other a great deal, and can be used as ideal candidates to research the effect that aggregate materials can have on the mixture rutting resistance.

The two treatment levels for gradation factor are: coarse-graded and fine-graded. As defined in the AASHTO specification, the coarse-graded aggregate passes below the maximum density line at the primary control size (PCS). By contrast, the fine-graded aggregate passes above the

PCS for the defined sieve size. These two levels represent two situations of aggregate gradation variation in the field.

Air voids content levels were selected as 4% and 7%. The design air voids content is 4% and it also represents a higher density level to which a pavement could be possibly compacted. The typical as-constructed air void content value in the field is 7%. The air voids content for a pavement will be most likely anywhere in between these two values; it is so when considering the constant field traffic densification in the first several years of service. This set-up of treatment levels allows for evaluating the effect of air voids in the realistic range; the treatment levels for air void content will be representative of field pavement density levels. Further, this also provides a density context where other factors, such as binder content variation, will be evaluated.

Asphalt binder contents at the high and low levels represent the small-range binder content deviation from the target design binder content in the field. The higher level and lower level are set at approximately ±0.25% from the design binder content; the difference between the two levels is exactly 0.5%. Presented in Table 3.1 are the four treatment factors, their treatment levels and the code designations.

Table 3.1 Experiment Design Levels and Code Designation for Rutting Assessment

Aggregate	Gradation	AV (air voids)	BC (Binder Content)	Binder Content (%)	Code Designation
A	C (Coarse-Graded)	4%	L	5.4	AC4%L
			H	5.9	AC4%H
		7%	L	5.4	AC7%L
			H	5.9	AC7%H
	F (Fine-Graded)	4%	L	5.4	AF4%L
			H	5.9	AF4%H
		7%	L	5.4	AF7%L
			H	5.9	AF7%H
B	C (Coarse-Graded)	4%	L	4.45	BC4%L
			H	4.95	BC4%H
		7%	L	4.45	BC7%L
			H	4.95	BC7%H
	F (Fine-Graded)	4%	L	3.95	BF4%L
			H	4.45	BF4%H
		7%	L	3.95	BF7%L
			H	4.45	BF7%H

Experiment Flow Chart

Once the treatment factors and levels were decided, Superpave mix designs were carried out in the lab, and the optimum binder contents were determined for the four types of mixtures involved (the combinations of two aggregates and two gradations). The test samples were prepared according to the Superpave mixing and compaction protocol. The rutting test specimens were compacted to a height of 75mm, and diameter of 150mm. To achieve the target air void contents (4% and 7%); the batch weight for a specimen was calculated and strictly controlled during mixing and compaction. Bulk specific gravity (BSG) tests were conducted for every sample to determine the air voids content before conducting rutting tests. The flow chart of the experimental plan is illustrated in Figure 3.1.

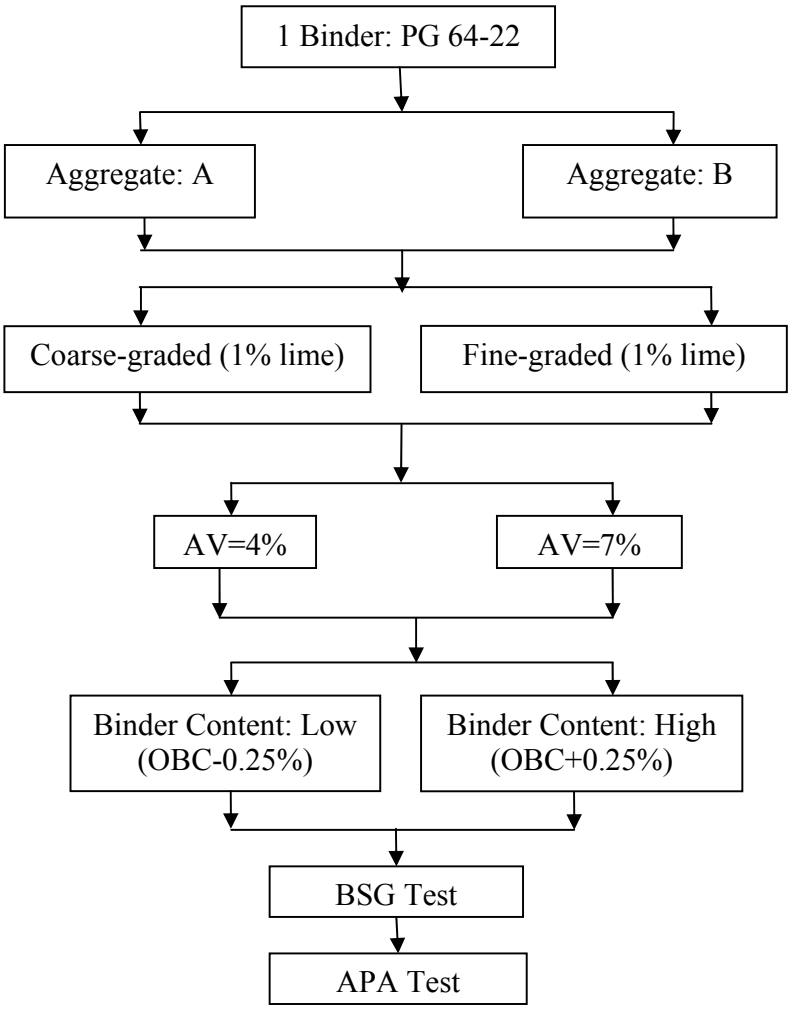

Figure 3.1 Experimental Plan Flow Chart for Rutting Evaluation

Rutting Test and Procedures

In this research, the Asphalt Pavement Analyzer (APA) was utilized to investigate the rutting susceptibility of the HMA mixtures. The standard test procedure is described in AASHTO TP 63-07, *Determining Rutting Susceptibility of Hot-Mix Asphalt (HMA) Using the Asphalt Pavement Analyzer (APA)*. The APA is a simulative test; the load on the samples applied by the rolling wheels through the pressurized hose simulates heavy vehicle tires passing on the

pavement. Research has been done, showing that APA test results have a good correlation with the rutting performance under the accelerated pavement testing with a heavy vehicle simulator (Choubane et al., 2006). Other researchers have shown that APA rut depths correlate well to field performance when loading and environmental conditions are appropriate (Kandhal & Cooley, 2008; Choubane et al., 2000; Williams & Prowell, 1999). In this study, the test temperature was set at 64°C (147°F), the same temperature as the binder high temperature grade, the hose pressure was set at 690±35 kPa (100 ±5 psi), the cylinder load on each wheel was set 445±22 N (100±5 lbf); after 8000 loading cycles the rut depths were measured manually.

EXPERIMENTAL PLAN FOR TENSILE CRACKING

Experimental Factors and Treatment Levels

For the pavement tensile cracking evaluation, the main experimental factors and treatment levels are generally the same as the rutting resistance evaluation. One difference is that three aggregate sources were utilized. In addition to aggregates A and B, aggregate C was introduced. The introduction of another aggregate source can provide a broader context to observe whether the effects (if any) of the other three treatment factors on the tensile cracking are consistent in all the aggregate sources.

Experiment Flow Chart

The specimen fabrication was the same as described in the rutting section. After the BSG test, the indirect tensile test was conducted. The flow chart is presented in Figure 3.2, and the experimental factors and treatment levels are presented in Figure 3.2.

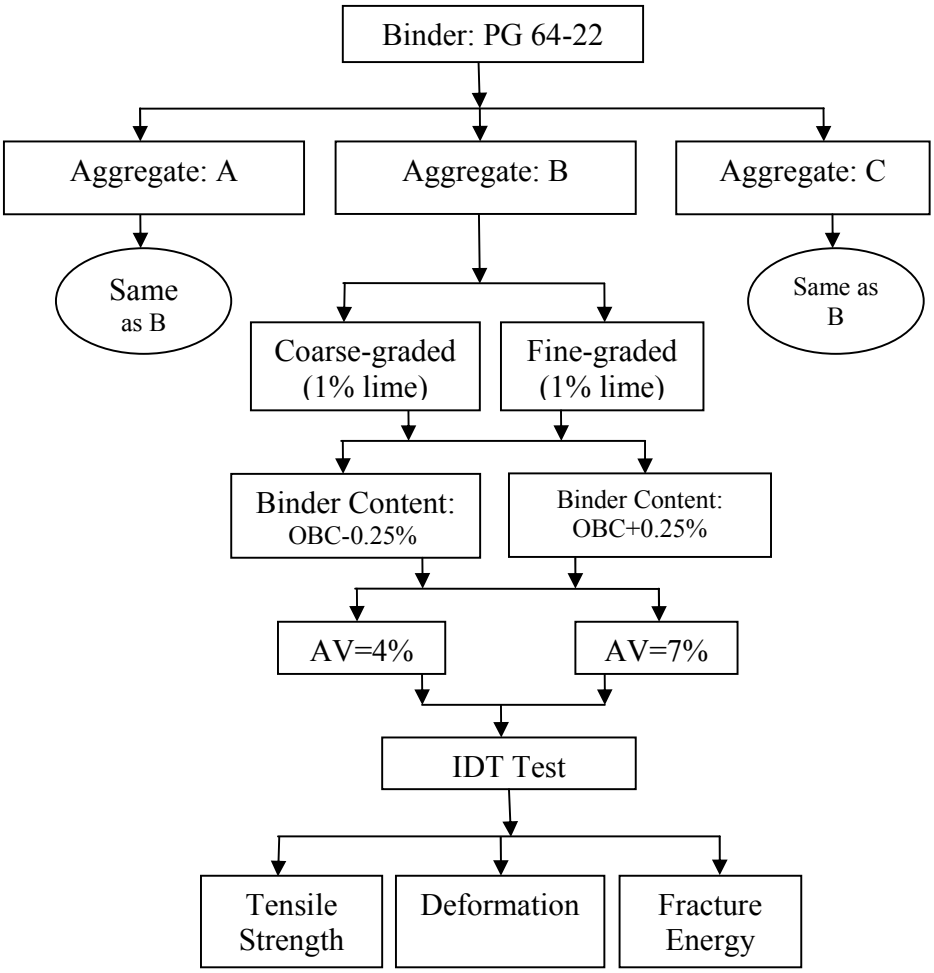

Figure 3.2 Experimental Plan Flow Chart for Tensile Cracking Evaluation

Table 3.2 Experiment Design Levels and Code Designation for Tensile Cracking

Aggregate	Gradation	AV (air voids)	BC (Binder Content)	Binder Content (%)	Code Designation
A	C (Coarse-Graded)	4%	L	5.75	AC4%L
			H	6.25	AC4%H
		7%	L	5.75	AC7%L
			H	6.25	AC7%H
	F (Fine-Graded)	4%	L	5.75	AF4%L
			H	6.25	AF4%H
		7%	L	5.75	AF7%L
			H	6.25	AF7%H
B	C (Coarse-Graded)	4%	L	4.45	BC4%L
			H	4.95	BC4%H
		7%	L	4.45	BC7%L
			H	4.95	BC7%H
	F (Fine-Graded)	4%	L	3.95	BF4%L
			H	4.45	BF4%H
		7%	L	3.95	BF7%L
			H	4.45	BF7%H
C	C (Coarse-Graded)	4%	L	5.55	CC4%L
			H	6.05	CC4%H
		7%	L	5.55	CC7%L
			H	6.05	CC7%H
	F (Fine-Graded)	4%	L	4.55	CF4%L
			H	5.05	CF4%H
		7%	L	4.55	CF7%L
			H	5.05	CF7%H

Test Method and Procedures

The indirect tensile (IDT) test was utilized in this research to study the tensile properties of the various asphalt mixtures. Besides the traditional water susceptibility evaluation and the correlation study between the cohesion part of shear strength and the indirect tensile strength, in recent years the IDT test has been used to measure various types of HMA cracking related performance: low temperature cracking, repeated fatigue cracking, top-down cracking, and the fundamental cracking mechanism and laws from an energy point of view (Zhang et al., 2001;

Chatti & Mohtar, 2004; Christensen & Bonaquist, 2004; Roque et al., 2004; Birgisson et al., 2006). In the test, a load is applied diametrically along the vertical plane of the test sample; the horizontal tensile stress is induced due to the loading, as illustrated in Figure 3.3. Once the tensile strength of the specimen is reached, the load starts to reduce because of the tensile failure mode; a typical IDT test curve is shown in Figure 3.4. Before the specimen fails, no visible cracking can be observed (Pellinen et al., 2005). The test temperature selected for this study is was 25°C (77°F), because it represents the average intermediate temperature where tensile failures, such as the fatigue cracking and top-down cracking occur. It is also the test temperature for dynamic shear rheometer (DSR) binder fatigue parameter, G*sinδ. A constant displacement rate of 50 mm/min was adopted, which represents the strain rate that a pavement will be subjected to under medium traffic speed (Pellinen et al., 2005). Three parameters were evaluated:

Indirect tensile strength (ITS) is calculated by using the maximum vertical loading:

$$ITS = \frac{P_{\max}}{2\pi dt} \qquad \text{(Eq 3.1)}$$

Where P_{max}= peak load (N); d= the diameter of the test sample; and t= the thickness of the test sample.

Deformation ($\delta_{\max}$) is the vertical displacement value when the vertical maximum loading is reached.

Fracture energy (FE) is the area under the force-displacement curve loading curve up to the deformation, area 1 as illustrated in Figure 3.4.

The equation for fracture energy is given by

$$FE = \frac{\int_0^{\delta_{max}} P d\delta}{dt} \qquad \text{(Eq 3.2)}$$

Where δ is the deformation; P is the load; d is the sample's diameter; and t is the sample's thickness.

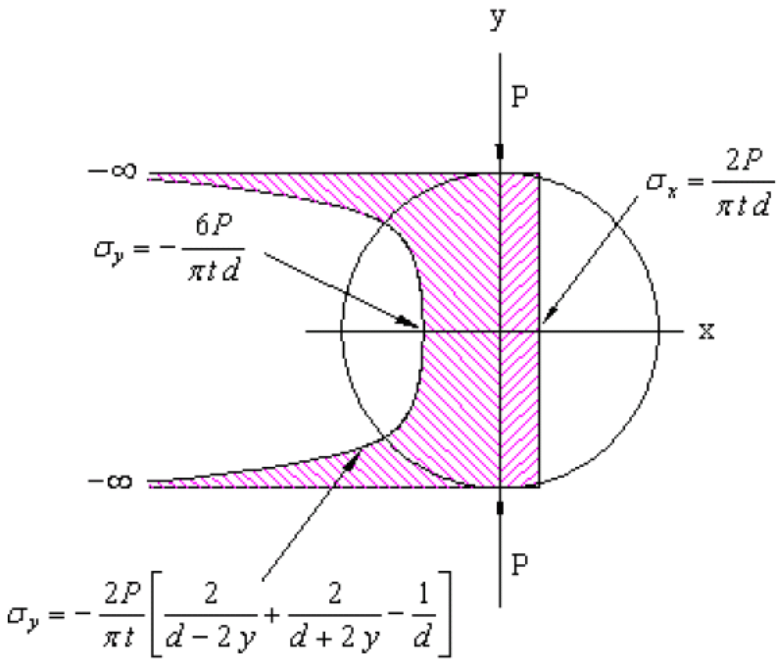

Figure 3.3 Theoretical Stress Distributions on the Vertical Diametrical Plane in IDT Test (After Yoder And Witczak, 1975)

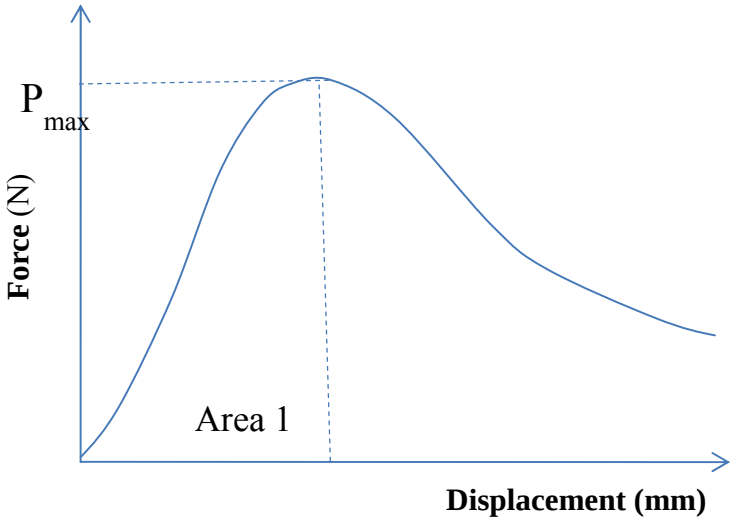

Figure 3.4 A Typical Load-Displacement Curve

EXPERIMENTAL PLAN FOR MOISTURE SUSCEPTIBILITY

Experimental Factors and Treatment Levels

In the evaluation of the mixtures' susceptibility to moisture induced damage, the air voids content was not a variable factor; it was targeted at 7% for the fabricated samples. The reason is that the voids structure must simulate the situations where water can be allowed to infiltrate into the pavement. Gradation and binder content treatment levels were the same as the indirect tensile cracking evaluation; and the aggregate sources were also the same as the cracking evaluation.

In the moisture susceptibility evaluation, additional samples are required to be wet-conditioned and conduct the IDT test on them. The experimental flow chart is given in Figure 3.5.

.

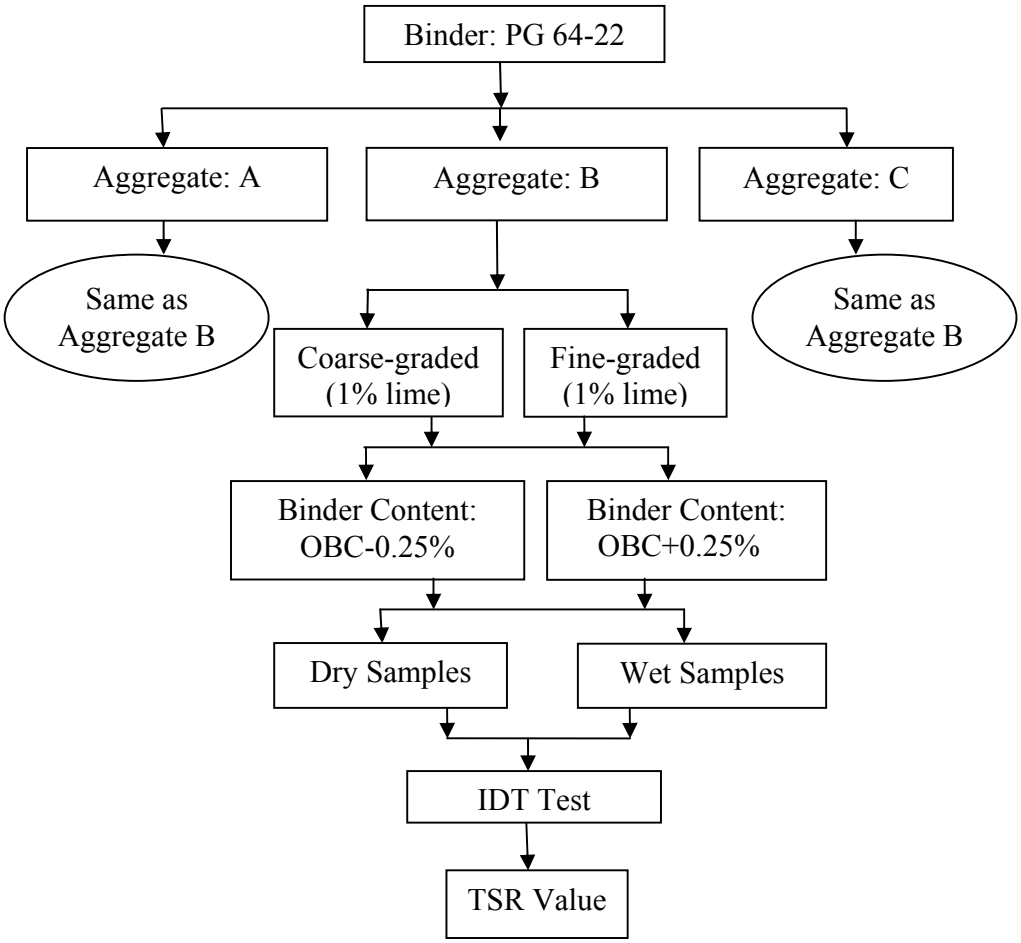

Figure 3.5 Experimental Flow Chart for Moisture Susceptibility Evaluation

Test Method and Procedures

Test procedure SC-T-70 (*Laboratory Determination of Moisture Susceptibility based on Retained Strength of Asphalt Concrete Mixture*) was followed to conduct the moisture susceptibility test (SCDOT, 2009). Four samples were fabricated and the BSG of these specimens was determined. Two of them were wet conditioned. The wet conditioning included sample saturation and hot water bath conditioning. In the saturation procedure, a wet specimen was submerged under water at 25 °C in a container, and then vacuum pressure was applied to the

air-tight space inside the container. As the air was removed from the system, water filled the air voids in the sample. This operation normally takes less than 30 seconds before the target saturation (70-80%) is reached. Immediately after the saturation, the sample was transferred into a pre-heated water bath. The temperature of the water bath was 60 °C; the sample was conditioned for 24 hours. During this conditioning period, water penetrates the thin film of the asphalt around aggregate particles through diffusion, and the adhesive bonding between aggregate and binder is compromised by moisture. After 24 hours, the sample was transferred into another water bath and allowed to cool off to the temperature of 25 °C for 2 hours.

Both the dry and wet specimens were tested using the IDT test. The indirect tensile strengths were used to calculate the tensile strength ratio (TSR), which is an indicator of moisture susceptibility of the mixture; the equation is given below. In addition, the deformation of the IDT test was recorded in this study, as well as the fracture energy.

$$TSR = 100 \times \frac{ITS_{wet}}{ITS_{dry}} \qquad \text{(Eq 3.3)}$$

Where TSR = tensile strength ratio in percent

ITS_{wet} = average indirect tensile strength of wet samples

ITS_{dry} = average indirect tensile strength of dry samples

MATERIALS PROPERTIES

Asphalt Binder

The binder utilized in this experiment was from one asphalt terminal with a performance grade of 64-22. PG 64-22 binder is widely used in highway pavements throughout the United States. The properties of the binder are summarized in Table 3.3.

Table 3.3 the Properties of PG 64-22 Asphalt Binder

Properties		values
Original		
Viscosity, *Pa·s*	*(135ºC)*	0.405
G*/sinδ, *kPa*	*(64ºC)*	1.207
RTFO Residue		
Mass Change, *%*	*(163ºC)*	-0.02
G*/sinδ, *kPa*	*(64ºC)*	2.815
PAV Residue		
G*sinδ, *kPa*	*(25ºC)*	2970
Stiffness (60s), *MPa*	*(-12ºC)*	183
m-value (60s)	*(-12ºC)*	0.311
Mixing temperature	*(ºC)*	150-155
Compaction temperature	*(ºC)*	139-144

Aggregate

Three aggregates, designated by A, B, and C were from three different quarries in South Carolina, which represent the SC aggregate market. Aggregate A is micaceous granite; aggregate B is marble schist, and aggregate C is also granite. Because of their origin and mineral composition, their physical properties (Table 3.4) vary a great deal. For example, in terms of L.A. abrasion, aggregate A has the highest value, while aggregate B and C are at a comparable lower level. Another noteworthy significant difference in the characteristics of the three aggregates, though not shown in Table 3.4, is their surface texture; by visual observation aggregate A has a rugged surface, whereas aggregates B and C have a much smoother surface. In addition, aggregate A has historically been prone to stripping, while aggregates B and C have not. The vast differences between the aggregates provide a broader context where the main experimental factors' effects are evaluated and examined.

Table 3.4 Physical Properties of Aggregates (after SC DOT, 2010; 2011)

Coarse Aggregate	L.A. Abrasion Loss (%)	Absorption (%)	Specific Gravity			Soundness % Loss at 5 Cycles			Sand Equivalent	Hardness
			Dry (BLK)	SSD (BLK)	Apparent	$1\frac{1}{2}$ to $\frac{3}{4}$	$\frac{3}{4}$ to $\frac{3}{8}$	$\frac{3}{8}$ to #4		
A	47	1.5	2.66	2.70	2.77	0.8	0.5	1.2	--	5
B	32	0.1	2.75	2.78	2.83	1.1	0.7	2.2	54	5
C	30	0.5	2.61	2.63	2.65	1.1	1.7	4.1	53	6
Fine Aggregate	Fineness Modulus	Absorption (%)		SSD (BLK)	Soundness % Loss					
A	2.46	0.2		2.81	3.5					
B	3.30	0.6		2.82	1.8					
C	2.98	0.6		2.64	0.1					

CHAPTER IV: STATISTICAL ANALYSIS

This research project involved many aspects of statistics, from the experimental design to the final data analysis. The experiment was carefully designed, where multiple factors were involved; the principle for designing a full-level 2^n factorial experiment was followed. In the execution of the lab experiments, the factors that might potentially influence the test results were carefully controlled and kept constant. For example, the oven temperatures were strictly controlled to maintain accuracy over the course of this experiment. The appropriate statistical analysis procedures were adapted to approach different tasks to better analyze and interpret the data.

The Minitab statistical software was used to facilitate the data analysis. Even though it makes the process much easier, it is necessary to have a basic knowledge of statistics. The reasons include, but are not limited to: (1) determining which statistical procedure to use that may be most appropriate for the specific task; (2) making appropriate assumptions that may be required for a particular statistical procedure; and (3) making correct inferences about the statistical analysis results.

This chapter will introduce the statistical procedures involved in this study. The intent is to provide brief information to help readers understand the related analysis, rather than provide a detailed explanation. To gain more detailed knowledge about statistics, books on this topic can be referenced.

ANALYSIS OF VARIANCE

The Analysis of Variance (ANOVA) is used to compare the means of multiple populations. It permits the hypothesis of "multiple means being equal" to be analyzed at a specified probability of a Type I error (0.05 for example). It can be used to examine the difference of treatment means

for various designed experiments, but the basic principles are almost the same. They include treatment effects models, test hypotheses, and the ANOVA table. The illustration of the ANOVA procedure will be put into the context of a Completely Randomized Design, where there is only one treatment factor.

The Treatment Effects Model

A treatment effects model is a linear model that can be constructed to describe responses for the observations, where the response can be represented as the grand mean plus a treatment effect and an effect of random disturbances within the treatment. It is given as:

$$y_{ij} = \mu + \tau_i + e_{ij} \qquad \text{(Eq 4.1)}$$

Where y_{ij} = the observation for the j^{th} replicate from the i^{th} treatment,

μ = the grand mean,

τ_i = the effect of the i^{th} treatment, and

e_{ij} = the experimental error for the j^{th} replicate from the i^{th} treatment.

Certain assumptions about the experimental errors (e_{ij}'s) are necessary for conducting a hypothesis test. They are:

(1) The e_{ij}'s for each treatment are independent.

(2) The expected value (mean) of the e_{ij}'s for each treatment is zero.

(3) The variance of the e_{ij}'s for each treatment is σ^2.

(4) The e_{ij}'s for each treatment are normally distributed.

A graphic illustration of the treatment effect model is given in Figure 4.1. The grand mean of the population and the means within each treatment are marked by the vertical lines. Meanwhile,

the variability of the treatment means about the grand mean and the variability of the responses within each treatment are delineated by the horizontal dashed and solid lines, respectively.

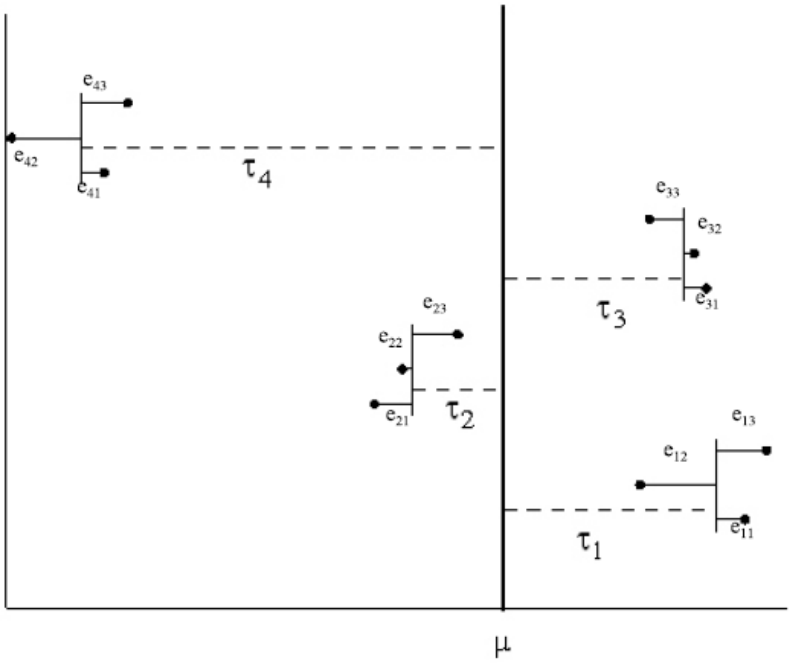

Figure 4.1 Graphic Illustration of the Treatment Effects Model (After Toler, 2008)

Estimating the Parameters for the Treatment Effects Model

Since the parameters in the Eq 4.1 are usually unknown, the Method of Least Squares is used to obtain the estimates for them. When there are an equal number of replicates per treatment, the estimates that can be obtained are given as follows,

$$\hat{\mu} = \overline{y}_{..}$$

$$\hat{\tau}_i = \overline{y}_{i.} - \overline{y}_{..} \quad \text{for i=1,…,t}$$

$$\hat{e}_{ij} = y_{ij} - \overline{y}_{i.} \quad \text{for i=1,…,t and j=1,…,r}$$

Where $y_{..}$=the grand mean of all the sample responses from the t treatments,

$y_{i.}$= the mean of the samples for the i^{th} treatment,

y_{ji}= the observation for the j^{th} replicate from the i^{th} treatment.

For an experiment where treatments have unequal replicates, the estimates of the model parameters (such as treatment effects) can be easily calculated using a computer program (Toler 2008).

Hypothesis Testing

In an ANOVA for *t* populations, the null and alternative hypothesis for the treatment means have the following specific form:

H_0: $\mu_1 = \mu_2 = \ldots = \mu$ or equivalently H_0: $\tau_1 = \tau_2 = \ldots = 0$

H_A: not all means are equal or equivalently H_A: not all $\tau_i = 0$

A level of significance (α) for the ANOVA test is pre-selected; it is widely accepted as 5%. This level of significance further defines a rejection region in the upper tail area of the F-distribution associated with a specific ANOVA test. An example of the F distribution is given in Figure 4.2, where the shaded area is the rejection region with a significance level of 0.05. The ANOVA procedure produces a test statistic (F_{obs}= MST/MSE). If the statistic falls within the rejection region, the null hypothesis will be rejected; otherwise, the test will fail to reject the null hypothesis.

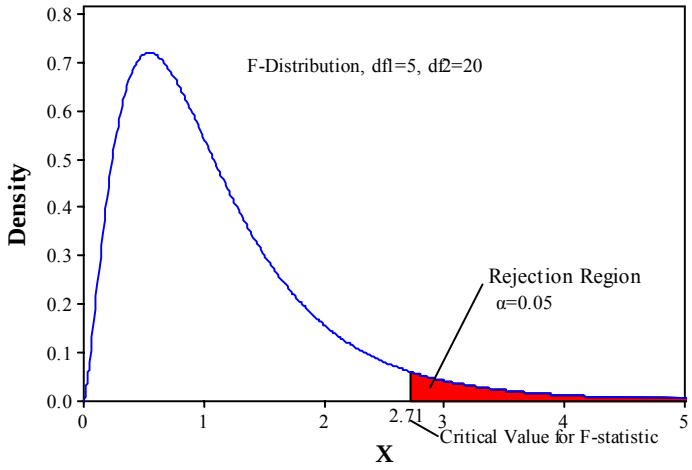

Figure 4.2 An Example of F Distribution with Rejection Region

The P-value is commonly used to compare with the preselected significance level, and then make a decision with regard to whether or not to reject the null hypothesis. Assuming the null hypothesis is correct in an ANOVA test, a P-value represents the probability for an F-statistic occurring in the region to be greater than the observed test F-value. It is a measure of how much evidence there is against the null hypothesis. When the P-value is smaller than the preselected significance level, the decision is to reject H_0. Further looking at the P-value will give the indication of the confidence level of making such a decision. The smaller the P-value is, the less likely it is that one will make a Type I error in making such a decision as to reject the null hypothesis.

ANOVA Table

To obtain the F-statistic, the ANOVA procedure uses an ANOVA table by calculating the terms from the sample observations. The format of an ANOVA table and calculation formulas are given in Table 4.1.

Table 4.1 the ANOVA (1-way) Table Format

ANOVA Table				
Source Due to	Sum of Squares	Degree of Freedom	Mean Square	F-statistic
Total	SSTotal	N_T-1		
Treatment	SST	t-1	MST=SST/(t-1)	MST/MSE
Error	SSE	N_T-t	MSE=SSE/(N_T-t)	

Where the terms are defined as follows:

N_T = total sample number

t = treatment number

SSTotal = total sum of squares = $\sum_{i=1}^{t}\sum_{j=1}^{r_i}(y_{ij}-\overline{y}_{..})^2$

SST = sum of squares of treatments = $\sum_{i=1}^{t} r_i(\overline{y}_{i.}-\overline{y}_{..})^2$

SSE = sum of squares for errors = $\sum_{i=1}^{t}\sum_{j=1}^{r_i}(y_{ij}-\overline{y}_{i.})^2$

MST = mean square for treatments

MSE = mean square for errors

The ANOVA for other experimental designs, such as complete block designs and factorial experiments (2 factors or more), will follow a similar procedure, and the ANOVA tables will have a similar construction. Hence, the inference to the test results would be the same as the foregoing discussions.

TUKEY'S METHOD FOR MULTIPLE COMPARISONS

ANOVA only tells whether there is a significant difference among the means of treatment factors—that is, whether at least one of the treatment means differs from the rest—but no information about which treatment level is different, or which is the best treatment. When multiple treatment levels are involved in an experiment, methods for multiple comparisons can be employed to discern which treatment(s) is different from the others.

The Minitab program provides several methods for the purpose of multiple comparisons. Tukey's method was used in this study. The procedure is outlined as follows (Ott and Longnecker, 2001; Mendenhall and Sincich, 1993).

(1) Rank the t treatment means;

(2) Two population means μ_i and μ_j are declared different if

$$\left|y_{i.} - y_{j.}\right| \geq W$$

$$W = q_{\alpha}(t,\upsilon)\sqrt{\frac{MSE}{n_t}} \qquad \text{(Eq 4.2)}$$

Where t = Number of treatments

υ = Number of degrees of freedom associated with MSE

MSE = the mean square error within treatments

n_t = Number of observations in each of the t treatments

$q_{\alpha}(t,\upsilon)$ = Upper-tail critical value of the Studentized range

The error rate that is controlled is an experiment-wise error rate.

ANALYSIS OF COVARIANCE

This research adopted the principle of analysis of covariance to process data before conducting ANOVA analysis for the involved factorial experiments. The purpose was to improve the efficiency and precision of the parameter estimates; and as a result, reach meaningful hypothesis test results.

The factor that is used as a covariate in the analysis must be quantitative. Meanwhile, the factor is viewed as a "nuisance"—that is, it is influential to the experiment results (or the properties of experimental units). There are several reasons for the nuisance factor to exist in a well controlled experiment. For example, it may be impractical or impossible to use the blocking technique, or the effect of a factor may not be realized until after the experiment has been initiated. To eliminate the effect of the nuisance factor, the analysis of covariance can be called for.

In this experiment, the air voids contents were set at 4% and 7%. A great effort was made to make sure the test specimens were fabricated to the target as close as possible. Because the HMA material is highly inhomogeneous, especially due to the arrangement and/or the orientation of the aggregate particles in the compaction process, sometimes it is very difficult to control a specimen's density, even though everything else is well controlled. Therefore, some samples had a larger deviation from the target value. Further, even for the samples that were within the tolerance, because the air voids content is such an influential factor to the mix properties, it is highly possible for them to have a deviated representation for the properties at the target values.

On the other hand, the ANOVA analysis employed in 2^n factorial experiments is a very powerful statistical tool, as many factor effects (main and interaction) are partitioned out from the residual errors. If the engineering properties are affected by the deviation of air voids content, even by a limited amount, the tests are likely to be affected, hence giving erroneous results. To eliminate this nuisance from affecting the hypothesis test results, the principle of Analysis of Covariance was employed to adjust the data to correspond with their target levels.

The analysis of covariance takes a feature from regression analysis. An influencing coefficient can be found for the nuisance factor. The "noise" in the treatment means due to the amount of deviation in the covariate from the target levels can be essentially adjusted out, by using the influencing coefficient to multiply the deviation.

FACTORIAL EXPERIMENT DESIGN

The full-level 2^4 factorial experimental design method was followed to carry out the study on the fundamental mix properties' influence on HMA material rutting performance. Since the fundamental factors were allowed to vary in small ranges by HMA specifications, two levels for each treatment factor can represent the possible values over these ranges; hence, this experimental design was an appropriate means to approach the research objectives.

One of the advantages to using this design is that it allows the various factor interaction effects to be evaluated. The 4^{th} order 2-level factorial experiment design will yield four main factor effects, six 2-way interaction effects, four 3-way interaction effects and one 4-way interaction effect. Each of them has two treatment levels; if there is a significant difference, no further comparative analysis would be needed.

The linear model for a 2^4 factorial design in a complete randomized design is given by as follows (Toler, 2008):

$$y_{ijklm} = \mu+\alpha_i+\beta_j+\gamma_k+\delta_l+(\alpha\beta)_{ij}+(\alpha\gamma)_{ik}+(\alpha\delta)_{il}+(\beta\gamma)_{jk}+(\beta\delta)_{jl}+(\gamma\delta)_{kl}+(\alpha\beta\gamma)_{ijk}$$

$$+(\alpha\gamma\delta)_{ikl}+(\beta\gamma\delta)_{jkl}+(\alpha\beta\gamma\delta)_{ijkl}+e_{ijklm} \qquad \text{(Eq 4.3)}$$

Where μ = the grand mean

$\alpha_i,\beta_j,\ldots, (\alpha\beta\gamma\delta)_{ijkl}$ = the effects of the main factors and the interaction factors

e_{ijklm} = the experimental error

The hypotheses of interest are:

H_0: Effect = 0 and H_A: Effect $\neq 0$

An ANOVA table will be constructed and F-tests will be conducted to test the hypotheses. The estimates of the effects in Eq 4.3 can be obtained by calculating the linear contrast of the observations. The method to construct linear contrast for each individual effect will not be given here; because a computer program can easily do all the calculations of the F-tests.

It is worth noting that while the ANOVA test gives equal power to examine the effects of the main factors and the interaction factors. The higher order interactions are less significant than the main factors or the 2-way interaction factors. Nonetheless, how to meaningfully interpret the F-test results requires practical understanding of the subject matter.

LINEAR REGRESSION ANALYSIS

Linear regression was used to develop a statistical model to fit the data sets in this study. Since many factors are significant to the response variable, as revealed by the ANOVA analysis, the models were multivariate.

The Purpose

One purpose of the regression analysis is to summarize the test results in this study by putting all the factors into one picture, and to precisely capture the factors that are most relevant to the specific HMA properties. For example, suppose binder content has an effect on the rutting performance of the HMA mixtures in this experiment. Normally, the total weight content would be used as a predictor; however, there may be other related factors that would be more accurate in predicting the response variable, such as effective binder content, total volume content of binder, or volume content of effective binder. In other words, one of these variables could provide the best description of the major feature of the data set. The same is true for HMA tensile properties. The regression analysis employs the trial and error technique, which could potentially identify the most relevant parameters. With this kind of information found, qualitative comparisons of the engineering properties between mixtures would be more accurately predicted by HMA material engineers. Additionally, when there is a need to develop a new model to predict the response variable using other materials—other sources of aggregate or binder—these identified relevant parameters can be readily adopted.

The second purpose of such regression analysis is to develop statistical models for the related properties, where the quantitative relationship between the independent variables (or the exploratory variables) and response variables will be established. Then, the models can potentially be further used for predicting the performance of materials made with the same or similar components, or sensitivity analysis can be performed by varying the values of the predicting parameters.

Such models sometimes can be very useful to predict response variables. Obtaining the response variables usually requires sophisticated test equipment, and other resources, such as time, money, and manpower, and sometimes there could be constraints on these resources. Under these circumstances, using reliable predictive models would be convenient and helpful. So, for this purpose, one of the characteristics for independent variables should be that obtaining the values of them should be simple—not taking a lot of time or financial resources.

A general expression of a multiple regression model is given as below (Ott & Longnecker, 2001),

$$y = \beta_0+\beta_1x_1+\beta_2x_2+\ldots+\beta_kx_k+\varepsilon \qquad \text{(Eq 4.4)}$$

Where y = response variable

$x_1, x_2, \ldots, x_k$ = independent variables (a set of k variables)

β_0 = constant intercept

$\beta_1, \beta_2, \ldots, \beta_k$ = coefficients (slopes) for the independent variables

ε = random error

The estimates of the intercept and coefficients are determined by the least-square method. Since nowadays a computer program can assist researchers in the regression analysis and make the process easier, the equations for how to calculate the estimates will not be elaborated on here.

Several techniques can be involved to come up with appropriate models. Normally, it takes practice to acquire the techniques. A few of these methods include: examining the data pattern of a scatter plot, conducting the Pearson's correlation analysis to find the relevant parameters, trying different parameters (including transformation of independent variables or response

variables), analyzing residual plots, paying close attention to R-square (the coefficient of determination) and identifying the high leverage points.

The Procedure

The coefficient of determination (R-square) is defined as "the proportion of the variation in the responses y that is explained by the model relating y to $x_1, x_2, \ldots, x_k$." (Ott & Longnecker, 2001). It could be viewed as a goodness of fit for the proposed model. For example, if a multiple regression has a R-square value of 0.892, it means 89.2% of the variability is accounted for by using the model relating y to $x_1, x_2, \ldots, x_k$. The formula is given in Eq 4.5.

$$R^2_{y \bullet x_1 \cdots x_k} = \frac{SS(Total) - SS(\mathrm{Re}idual)}{SS(Total)} \qquad \text{(Eq 4.5)}$$

Where SS(Total) = total sum of squares $\sum_{i=1}^{n} (y_i - \overline{y})^2$

Lastly, when a model is used to predict the response variable by using a new set of independent variables, one should be cautious about extrapolation. A model was developed within a data range or an experimentation region, and predicting outside of that scope could lead to incorrect results. It requires professional judgment or additional validation to give the confidence to do such an extrapolation.

CHAPTER V: PERMANENT DEFORMATION

GRADATION AND MIX DESIGN

The South Carolina DOT technical specification (2007) for Hot-Mix Asphalt material properties was followed to conduct the aggregate gradation and mix design. Four mix designs were completed for a Type B surface course, which is the designation for high volume primary roads in South Carolina. The nominal maximum aggregate size (NMAS) was 12.5 millimeter and the four mix designs were: aggregate A coarse-graded, aggregate A fine-graded, aggregate B coarse-graded, and aggregate B fine-graded. The fine and coarse gradation curves are given Figure 5.1. Along with them are the SCDOT gradation upper and lower spec limits, the maximum density line, AASHTO control points, and even the obsolete restricted zone line are plotted on the graph, so that the relative location can be interpreted by asphalt pavement technologists and compared to the gradation requirement in their own states.

The mix design for aggregate A was conducted first; the fine-graded mix was intended to meet the PCS requirement and ARZ as well. Since the SCDOT upper spec limit is barely above the ARZ, later in the selection of the aggregate B fine gradation, only the PCS requirement was met. The coarse-graded aggregate A tends to result in a much higher VMA. To minimize the VMA as a confounding factor on the rutting resistance effect, several coarse-graded aggregate gradations were made and tested by trial and error, and the gradations shown on Figure 5.1 were finally chosen. Two other issues worth mentioning here are: (1) 1% lime was used to minimize the moisture susceptibility of the mixes, which is a standard practice in many states for high volume roads; (2) the filler content in the gradation for all four mixtures was kept the same to avoid the variation of properties caused by filler content.

Optimum binder content was identified by setting the design air voids at 4% and the design gyration number at 75. Other volumetric parameters, such as VMA and VFA were determined at the corresponding OBC to conform to the SCDOT technical specification, and they are presented in Table 5.1. As evidenced during the mix design process, the gyratory compactability for the aggregate A fine-graded mix is very sensitive to binder content, evidenced by a deep slope on the AV vs. BC curve. This was also reflected by the difficulty in later compacting the fine-graded mixture samples with OBC-0.25%, which generally took more than 400 gyrations to finish the compaction process. This behavior led to speculation that the aggregate A fine-gradation rutting resistance performance would be better than coarse-gradation.

Aggregate B tends to have a lower binder content compared to aggregate A, thus the attempt to use the same gradation in aggregate B as aggregate A was unsuccessful. To meet the minimum binder content requirement, the gradation curve was adjusted further away from the maximum density line, either primarily on the coarse aggregate portion or on both fine and coarse portions. Because aggregate A has a rougher surface texture, more binder is absorbed into the surface pores, the OBC is higher by roughly 1% compared to aggregate B; however, their VMAs are at a comparable level, as shown in Table 5.1.

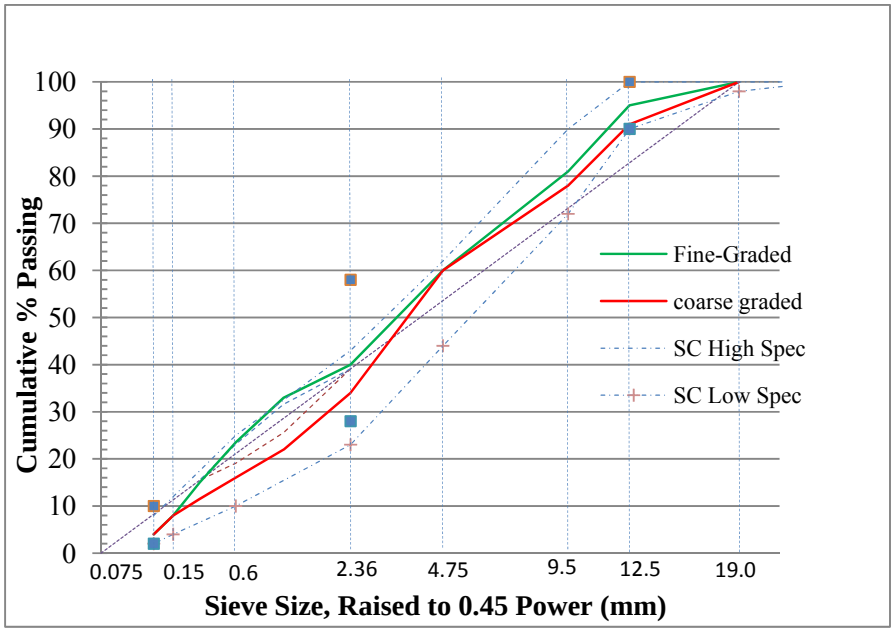

(a)

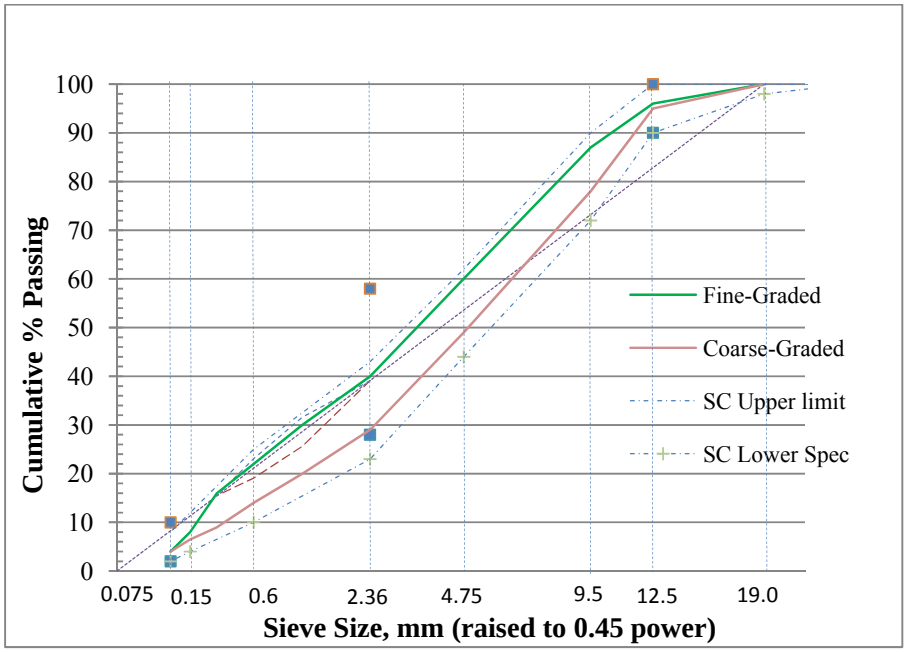

(b)

Figure 5.1 Gradation Charts: (a) Aggregate A; (b) Aggregate B

Table 5.1 Mix Design Parameters in Rutting Assessment

	Aggregate: A		Aggregate: B			
Gradation	Fine	Coarse	Fine	Coarse	Fine	Coarse
Gyration	75	75	75	75	100	100
Optimum Binder Content, P_b(%)	5.53	5.73	4.18	4.72	3.98	4.38
V_a (%)	4.0	4.0	4.0	4.0	4.0	4.0
VMA (%)	13.3	13.9	13.7	14.2	13.3	13.4
VFA (%)	70.0	71.2	70.9	71.8	70.0	70.2
Effective Binder Content, P_{be} (%)	3.92	4.23	4.07	4.24	3.87	3.90
Aggregate SSA (m^2/kg)	5.42	4.76	5.38	4.24	5.38	4.24
Film Thickness (micron)	7.39	9.06	7.58	10.09	7.19	9.24
D/A Ratio	0.72	0.70	0.96	0.85	1.01	0.91

Where V_a=Volume of air voids; VMA=Volume of voids in mineral aggregate; VFA=Volume of voids filled with asphalt; SSA=Specific Surface Area; D/A Ratio=Dust/Asphalt Ratio.

INTERPRETATION OF GRADATION AND AGGREGATE INTERACTION

A general linear model procedure was employed to conduct the statistical analysis of the APA test results. In the model, the rutting depth of a given sample was partitioned into 16 portions (refer to Eq 4.3): four main factor effects, six 2-way interaction effects, four 3-way interaction effects, one 4-way interaction effect and the experimental error. Both the individual factor effects and the factor combination effects can be examined and evaluated.

Preliminary statistical analysis shows that the gradation factor (treatment levels: coarse-graded and fine-graded) is not statistically significant; however the “aggregate source*gradation”

interaction effect is statistically significant (Appendix D). Further examination reveals that the rutting performance of fine-graded mixtures is different from coarse-graded mixtures within each aggregate source as illustrated in Figure 5.2: coarse-graded gradation performs better in aggregate A, while fine-graded gradation is better with aggregate B.

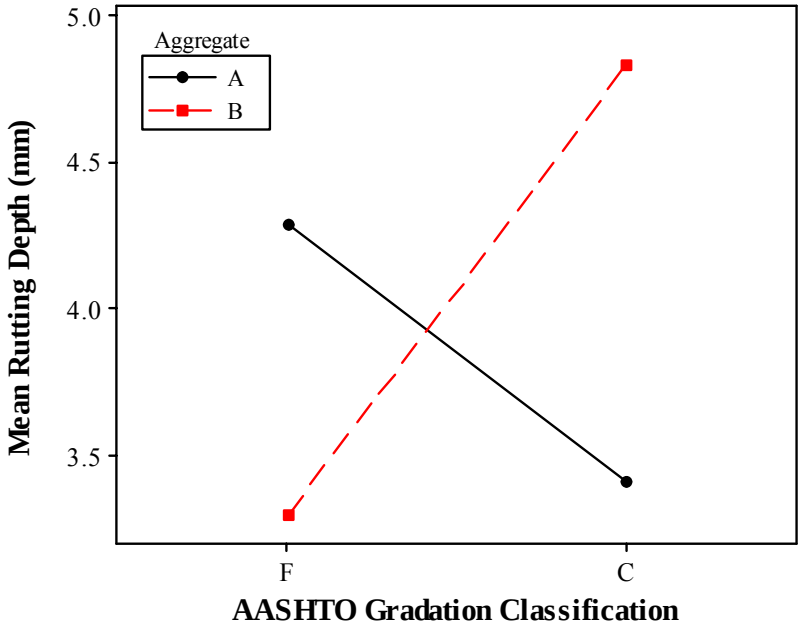

Figure 5.2 Interaction Plot between Aggregate Source and AASHTO Gradation

This phenomenon clearly demonstrates that the gradation effect is aggregate source specific. Previous research on the restricted zone of fine aggregate had similar conclusions; the gradation above the restricted zone (fine gradation) can perform better or as good as the gradation below the restricted zone (coarse gradation), indicating that a coarse gradation does not necessarily provide better internal friction between aggregate particles for some aggregate sources (Kandhal & Cooley, 2002; Zhang et al., 2004). On the other hand, this reveals that gradation classification

of coarse-graded and fine-graded according to ASSHTO criterion cannot potentially distinguish or predict the rutting performance of a mixture during design.

With the aggregate source-gradation interaction having been correctly interpreted, to further address the underlying reasons that may explain the performance of each aggregate source and increase the clarity of interpreting other statistical analysis results, the gradation treatment levels were re-assigned a new designation. The gradation with better rutting resistance performance from one source is designated as “good” (the lower level of gradation factor); while the lower performing gradation is designated as “bad” (the higher level of gradation factor). Namely, “Good” gradations are coarse-graded in aggregate A, fine-graded in aggregate B, and vice versa for “Bad”. Table 5.2 shows the performance-based designation and the corresponding AASHTO gradation classification. The interaction effect between the aggregate source and new gradation is illustrated in Figure 5.3. As observed in the figure, after classifying the aggregate gradation as “Good” and “Bad” the relationship between gradation and rut depth tend to be congruent for both aggregate sources; the slopes are negative and similar. Even though the trend lines intersect at one end, it is possible there is no interaction between aggregate source and new classified aggregate gradation.

Table 5.2 New Aggregate Gradation Classifications

Aggregate Source	AASHTO Gradation Classification	Performance Classification	New Gradation Designation
A	Coarse-Graded	Good	A-Good
	Fine-Graded	Bad	A-Bad
B	Coarse-Graded	Bad	B-Bad
	Fine-Graded	Good	B-Good

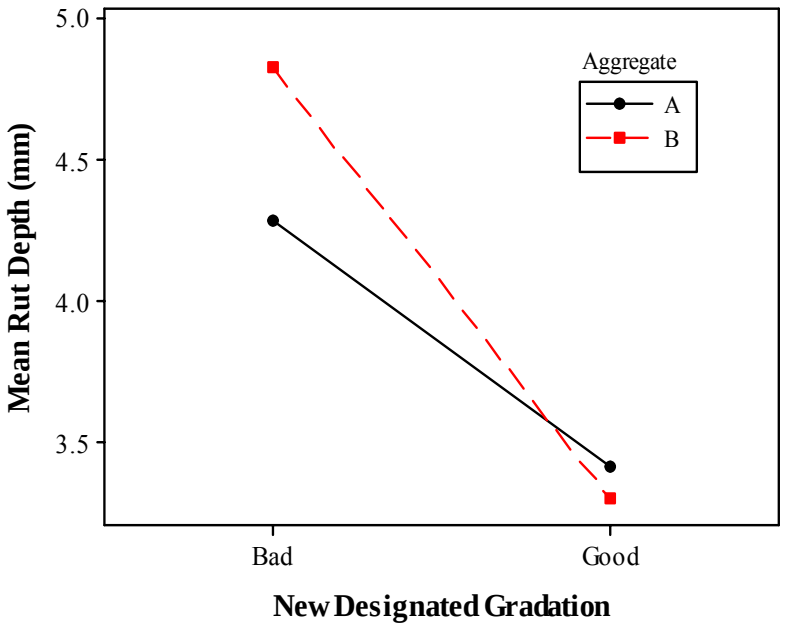

Figure 5.3 Interaction Plot between Aggregate Source and Performance Gradation

The subsequent statistical analysis reveals at a 5% level of significance, that aggregate source is not a significant factor; the other three main factors: aggregate gradation, AV and BC are statistically significant to rutting performance. One two-way interaction factor, aggregate*air voids, is significant; and one three-way interaction effect (gradation* air voids*binder content) is significant. The analysis of variance (ANOVA) table for the 4-factor full level experiment is

presented in Table 5.3. The statistical results are similar to those of an analysis with air voids content as the covariate. Further discussion is given to practically interpret the statistical results in the following section.

Table 5.3 ANOVA Table for Rutting Results

Source	DF	Seq SS	Adj SS	Adj MS	F-statistic	P-value	Significant?[2]
Aggregate source	1	0.824	0.740	0.740	1.050	0.311	No
Gradation[1](Gr.)	1	18.194	18.537	18.537	26.380	0.000	Yes[3]
AV	1	53.675	54.412	54.412	77.450	0.000	Yes
BC	1	10.818	11.299	11.299	16.080	0.000	Yes
Aggregate*Gr.	1	1.239	1.248	1.248	1.780	0.190	No
Aggregate*AV	1	4.059	3.779	3.779	5.380	0.026	Yes
Aggregate*BC	1	0.421	0.479	0.479	0.680	0.414	No
Gr.*AV	1	1.863	1.761	1.761	2.510	0.121	No
Gr.*BC	1	0.090	0.115	0.115	0.160	0.688	No
AV*BC	1	0.101	0.040	0.040	0.060	0.813	No
Aggregate* Gr. *AV	1	0.213	0.135	0.135	0.190	0.663	No
aggregate*Gradation*BC	1	0.047	0.014	0.014	0.020	0.890	No
aggregate*AV*BC	1	0.048	0.097	0.097	0.140	0.712	No
Gr.*AV*BC	1	8.936	8.856	8.856	12.610	0.001	Yes
Aggregate* Gr. *AV*BC	1	0.033	0.033	0.033	0.050	0.829	No
Error	39	27.400	27.400	0.703			
Total	54	127.961					

Note 1: two levels of gradation used in the analysis are re-designated as “Good” and “Bad”.
Note 2: significance level is set at 5% to contrast with P-value.
Note 3: the gradation effect is aggregate source specific: within each source, two gradations are statistically different; the way of difference depends on each aggregate source.

AGGREGATE SOURCE EFFECT

In this study, the aggregate sources (A and B) do not distinguish from each other, even though their physical properties are substantially different. Aggregate A has a much rougher surface texture compared to aggregate B; however, this characteristic does not give aggregate A more advantage than aggregate B in rutting performance. Overall, their rutting performance is good and about at the same level. This may be attributed to their rigorous compliance with the aggregate angularity requirement. Coarse aggregate angularity is expressed by the percentage of particles having one or two crushed surfaces; fine aggregate angularity is expressed by the percent air voids present in loosely compacted fine aggregates. Both angularities are crucial to provide better internal friction within the aggregate structure. If two aggregates' rutting performance is significantly different, the primary contributor to the difference might lie in aggregate angularity properties.

GRADATION EFFECT

Aggregate gradation selection is one of the most important issues in the mix design process. As mentioned before, to improve the mix performance, the gradation issue can obviously be addressed more effectively in the mix design phase than during the production process. Different gradations provide a different aggregate skeleton and packing characteristic; gradation affects the VMA (voids in mineral aggregate) and further dictates the OBC determined through mix design. Thus, within one aggregate source, VMA and OBC (at the same gyration level) are dependent upon gradation selection.

The gradation effect is statically significant in this study, and the gradation classification based on rutting performance was identified for each of the aggregate sources. As mentioned in

the previous sections, simply using the AASHTO classification (fine and coarse-graded) cannot provide a consistent indication to the rutting potential of the mixtures. This may be because the AASHTO classification is too simplistic to encompass the complexity of aggregate gradation. Thus, knowing the gradation classification of an aggregate gives little or no indication as to whether the mixture will perform better or not. It is necessary to find a performance-based predicting parameter that can reflect the gradation effect on the permanent deformation, regardless of the gradation's AASHTO classification. Such a parameter should be able to be identified in the design process, and it is also preferable that the parameter is a quantifiable variable, instead of categorical (e.g. the AASHTO gradation classification is categorical), so that the comparison between gradations on rutting resistance will be easier for mix design technologists.

In this study, the four aggregate gradations are A-Good, A-Bad, B-Good, and B-Bad (Table 5.2). Their rutting performances at the 4% and 7% AV level are illustrated in Figure 5.4. The error bars represent $\pm 1\sigma$ (standard deviation) in the graph. The rut depth limit set forth by the SCDOT specification for a Type B surface course is no more than 5 millimeters where test samples should be fabricated at the 4% AV level. As shown in Figure 5.4, all 4 gradations meet the standard requirement, so for the gradations included in this study, there is really no absolute "bad" gradation. Meeting the standard volumetric requirements in this case satisfies the

"performance-based" specification.

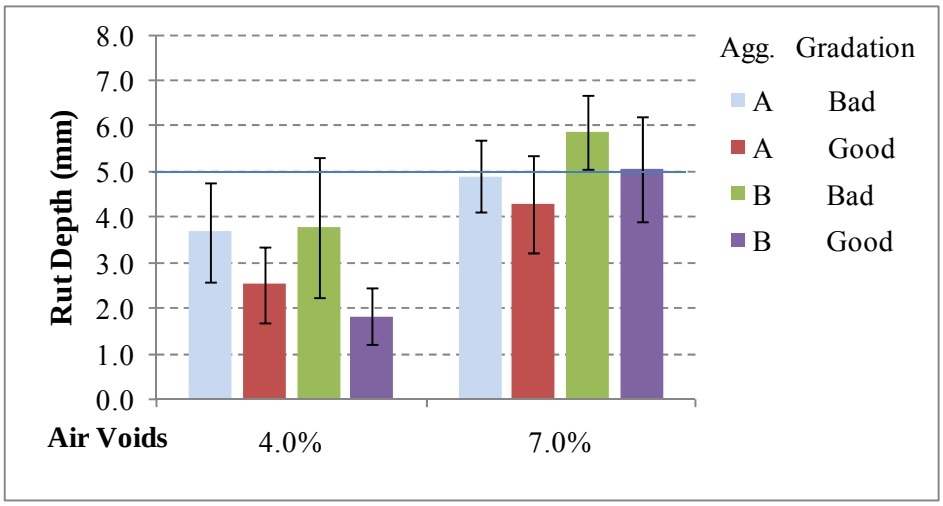

Figure 5.4 Four Gradation Rutting Performances at 4% and 7% AV Level

The aggregate gradation's rutting resistance has little correlation with the gyration number needed to compact the samples to the target air void level. It was observed that during the lab compaction, the fine-graded mixtures of aggregate A required a distinctively higher gyration number to complete the compaction than the coarse-graded mixtures. The longer compaction time was speculatively interpreted as a reflection of better shear resistance. However, the APA test results showed the performance of the fine-graded mixtures is contrary to the expectation; overall, the coarse-graded samples were better in the rutting results for aggregate A. This indicates that there is no correlation between the number of compaction gyrations and the rutting resistance based on these results.

The next step is to identify a new parameter that can best correlate the rutting performance to reflect the gradation effect as discussed early so that the new parameter can be used to predict the rutting performance of a mixture when selecting the proper gradation during mix design. First,

the initial idea was to try to relate the rutting performance of the different gradations to the percentage of aggregate passing certain sieve sizes. However, the attempt was not successful; it turned out the correlation between the rutting performance and the aggregate gradation is very poor, and no meaningful relationship could be established.

The second method tried was to conduct a Pearson correlation analysis. The parameters selected in the correlation analysis are somewhat dependent upon (or related to) aggregate gradation. For example, as gradation changes, the packing characteristic changes accordingly, thus VMA changes, as well as effective binder content (P_{be}). Similarly, as gradation changes, the specific surface area (SSA) also changes. The correlation analysis results are presented in Table 5.4. Two standards can be used to identify the degree to which two variables are correlated: the Pearson correlation coefficient and P-value. The closer the Pearson coefficient is to 1 or -1, the stronger the correlation is; the P-value shows the likelihood of making a type I error in determining the Pearson coefficient.

Table 5.4 Design Parameters vs. Gradation Rut depth Correlation Analysis

Parameters Examined	Rut Depth (4% &7% combined)		Rut Depth (at 4% AV level)		Rut Depth (at 7% AV level)	
	Pearson Coefficient	P-Value	Pearson Coefficient	P-Value	Pearson Coefficient	P-Value
VMA	0.197	0.803	-0.010	0.990	0.437	0.563
VFA	0.202	0.798	-0.008	0.992	0.448	0.552
Effective Binder	0.035	0.965	-0.080	0.920	0.149	0.851
Film Thickness	0.471	0.529	0.366	0.634	0.416	0.584
Specific Surface Area (SSA*)	-0.524	0.476	-0.414	0.586	-0.461	0.539
Normalized Absorbed Asphalt ($P_{ba,n}$)	0.878	0.122	0.872	0.128	0.527	0.473
SSA*$P_{ba,n}$	0.888	0.112	0.947	0.053	0.425	0.575

* The formula followed to calculate SSA c is given in a reference book (Roberts et al., 1996).

As shown in Table 5.4, VMA, VFA, effective binder content and film thickness failed to reflect the gradation effect on rutting, as their Pearson coefficients are too low. SSA has a negative correlation with gradation effect, but the correlation is not strong enough for SSA to be used as a single indicator to differentiate the gradation effects. The variable showing the strongest relationship to gradation effect is Normalized Absorbed Asphalt ($P_{ba,n}$).

Normalized absorbed asphalt is a new term used in this study to correlate the gradation effect. The absorbed asphalt content (P_{ba}) is expressed by the percentage of aggregate mass. In this study it was found that absorbed asphalt content has a strong relationship with the gradation performance within each of aggregate sources. Since the aggregate A surface texture is much rougher than aggregate B, the level of absorbed asphalt content in aggregate A is significantly higher than aggregate B (Table 5.5). The difference in absorption level is a reflection of the surface texture between aggregate sources, rather than the gradation effect. To better expose the gradation effect, the normalization concept was employed so that the aggregate source effect on the absorbed asphalt content can be eliminated. The normalized absorbed asphalt content accounts for the gradation difference. The baseline for normalization is set as the average of the P_{ba} of the fine- and coarse-gradation within each aggregate source. Further combining the SSA and $P_{ba,n}$, the correlation coefficient can improve, especially at the 4% AV level, showing that the product of SSA and $P_{ba,n}$ could be identified as the parameter to compare the mixture rutting performance in the mix design process. The gradation effect correlation parameter values are presented in

Table 5.5; the gradation effects manifested by the parameters $P_{ba,n}$ and SSA*$P_{ba,n}$, are presented in Figure 5.5 and Figure 5.6, respectively. The following two paragraphs will explain why these factors stand out as gradation effect indicators. The equations used to calculate P_{ba} are given as follows:

$$P_{ba} = 100 \times \frac{G_{se} - G_{sb}}{G_{sb} G_{se}} \times G_b \qquad \text{(Eq 5.1)}$$

Where P_{ba} = absorbed asphalt, percent by mass of aggregate

G_{se} = effective specific gravity of aggregate

G_{sb} = bulk specific gravity of aggregate

G_b = specific gravity of asphalt

$$G_{se} = \frac{P_{mm} - P_b}{\frac{P_{mm}}{G_{mm}} - \frac{P_b}{G_b}} \qquad \text{(Eq 5.2)}$$

Where G_{mm} = maximum specific gravity (AASHTO T209) of paving mixture (no air voids)

P_{mm} = percent by mass of total loose mixture=100

P_b = asphalt content at which AASHTO T209 test was performed, percent by total mass of mixture

G_b = specific gravity of asphalt

To calculate $P_{ba,n}$, the reference value of absorbed binder content is obtained by averaging the P_{ba} of the fine- and coarse-gradation for each aggregate source. Each $P_{ba,n}$ is calculated by dividing the P_{ba} of the gradation by the reference P_{ba} value of corresponding aggregate source.

Table 5.5 The Values for Parameters in the Correlation Analysis

Gradation	Rut depth (mm) (4% & 7% AV combined)	Rut depth (mm) (4%AV)	Rut depth (mm) (7%AV)	SSA (m^2/kg)	P_{ba} (%)	$P_{ba,n}$ (%)	SSA* $P_{ba,n}$
A-Good	3.4	2.5	4.3	4.76	1.59	0.97	4.62
A-Bad	4.3	3.7	4.9	5.42	1.69	1.03	5.58
B-Good	3.3	1.8	5.1	5.38	0.12	0.37	1.99
B-Bad	4.8	3.8	5.9	4.24	0.50	1.63	6.91

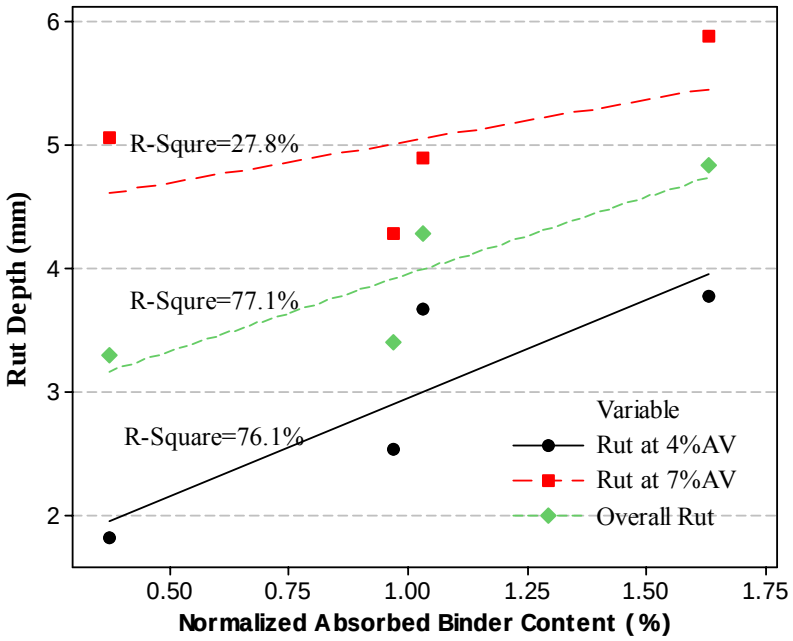

Figure 5.5 The gradation rutting effect reflected by $P_{ba,n}$

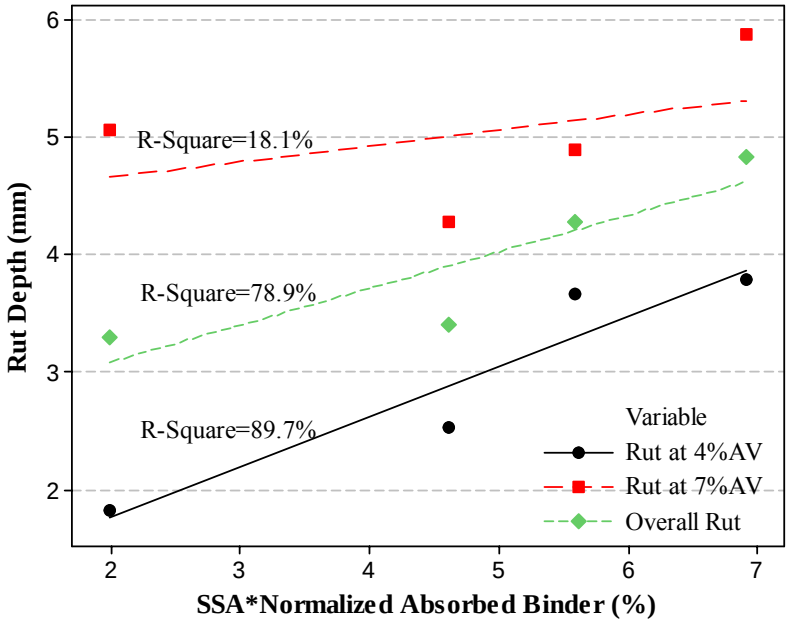

Figure 5.6 The gradation rutting effect reflected by SSA*$P_{ba,n}$

Surface area was found to have a negative correlation to rut depth, meaning the higher the surface area, the lower the rut depth. The hypothesis of this relationship is that the higher specific surface area, the more chance the aggregate will come into contact with each other and the more internal friction will occur between aggregate particles. The fine portion of an aggregate gradation has a large impact on the aggregate SSA, it is normal to see fine-graded gradations have a higher SSA value. However, the correlation coefficient is so low that the SSA alone cannot be used as a gradation effect indicator.

Why does the absorbed asphalt content matter? Due to geologic origin in the aggregate quarries, the two aggregates used in this experiment have a noticeable difference in surface texture. Rougher surfaces were expected to have better rutting resistance. However, as revealed by the statistical analysis, aggregate A does not substantially differentiate itself from aggregate B;

instead, their rutting performances are generally equal, which is counterintuitive. Through further examination it was determined that aggregate A also has higher absorbed asphalt content, as it has rougher surface texture. These observations raise the question: could the higher binder content counteract the advantage of a rougher surface texture with regard to rutting resistance? Though the mechanism of the influence is not fully understood, it is speculated that the difference in the normalized absorbed asphalt content reflects the gradation's overall ultimate surface texture characteristic after the aggregate is coated with asphalt. The aggregate with rougher surface texture (like aggregate A) theoretically should have a larger internal friction angle and better shear resistance. However, an aggregate with rough surface tends to have high absorbed asphalt binder content because the absorbed binder fills the pores on the aggregate surface, thus the roughness of the surface is smoothed, and the shear resistance provided by the rough aggregate surface is offset by the high absorbed binder content. The more asphalt the aggregate absorbs into its surface structure, the larger the degree to which the roughness of the surface is subdued, and less shear resistance will develop between aggregate particles.

In this study, the surface of aggregate A was rougher than aggregate B, and it absorbed more binder, which counteracts this absolute aggregate texture effect, leaving the same level of ultimate aggregate surface texture characteristics. Caution should be used when two aggregate gradations are compared using normalized absorbed asphalt. The normalization in this study works well because there is no statistical difference observed between the rutting performances of the two aggregates. When two aggregates' angularity properties are significantly different, the aggregate source effect may confound the gradation effect. Moreover, there is a need to find a realistic method to establish the baseline as the reference point to "normalize" the absorbed

asphalt content level. Nevertheless, when working with one aggregate, the normalized absorbed asphalt, or in conjunction with the "SSA", could be a quantitative parameter as a gradation indicator during mix design to select the aggregate gradation which will have good permanent deformation resistance.

Finally, the advantage of using the "gradation" indicator is that it is simple, no mechanical tests and expensive equipment are involved and both the "absorbed asphalt" and "SSA" are required to be determined by most of the agencies during the mix design anyway. The merit of this indicator can lend itself as a good tool for gradation optimization and quality control as well. The finding of this "gradation" indicator was based on a limited study. Even though it appears convincing and promising for future implementation, more research is required to validate this proposition and develop a more accurate indicator to correlate the gradation effect.

AIR VOIDS LEVEL EFFECT

The statistical analysis shows that the rut depths at different air void content levels are significantly different. Mixtures with higher air voids content have higher rut depth than the lower air voids content mixture (Table 5.5); thus, low air voids content in this study is the favorable rutting resistance end. Therefore, increasing the density of the pavement can reduce the air voids content in the pavement, and further increase rutting performance.

A rut is the result of a combination of material consolidation and shear displacement. Two mechanisms may be involved in this air voids level effect: densification and aggregate particles interlocking. The specimens at the 7% AV level may be subjected to densification more during the APA test than those at the 4% AV level. Meanwhile, at the low AV level, the aggregate

particles may be compacted in a way where they are interlocked to each other; therefore, a higher shear resistance is provided by the aggregate skeleton.

BINDER CONTENT EFFECT

The effect of variation in binder content on rutting performance under the APA test is statistically significant (Table 5.3). The graphical illustration is presented in Figure 5.7. Mixtures with higher binder content are more susceptible to permanent deformation than the ones with lower binder content. Therefore, the lower binder content is favorable with regard to rutting resistance.

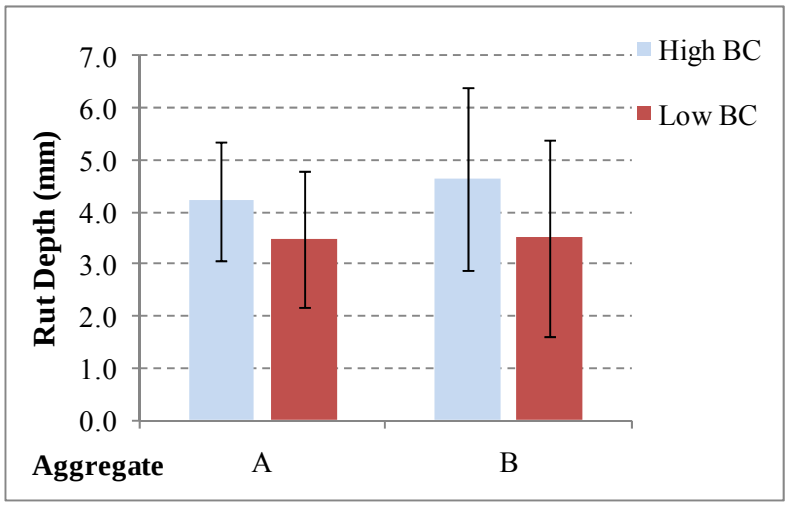

Figure 5.7 Binder Content Treatment Effect

The statistical results (Table 5.3) show there are no 2-way interaction effects between the binder content and other factors, such as aggregate source, gradation and air voids content. This indicates that the effect of binder content on the pavement rutting performance is not affected by the presence of other factors at a 2-way level in this study.

The effect of binder content on the rutting performance has significant practical implication from a quality control point of view. Quality control programs allow the binder content to vary over a small range. This research shows that binder content changes even within a small range can have a statistically significant effect on rutting performance; an increase in the binder content even by a small amount will increase pavement's susceptibility rutting.

The significance of this effect of binder content on rutting performance lies in the small and realistic deviation range of binder content. In that range, the practical effect on rutting may not be significant; however, when the binder content deviates from the design binder content by 0.5%, the effect on rutting could be significant. Further, this finding is applicable to the effect of larger binder content change for a particular aggregate gradation since the binder content treatment level is relatively small. It can be used to explain why sometimes a pavement is observed with rutting failure even though the field air voids content is low. When the mix design is poorly conducted, the designed binder content can be much higher than it should be for that particular aggregate gradation, creating a mixture with excessive binder content. The excessive binder content makes it easier to construct the pavement with lower air voids content, and it can also lead to a premature failure of rutting. Therefore, the excessive binder content is the reason for this rutting failure, which "overrides" the low field air voids content. This finding shows how important it is to avoid a mix with an excessive binder content in the mix design process.

The mixes with the lower binder content (BC = optimum-0.25%) are of particular interest, because they represent the binder content level of the interstate surface course mixtures (Type A: the binder content at 100 gyrations). As illustrated in Figure 5.8, all mixtures meet the rutting test requirement set forth by SCDOT (3mm) for Type A mixtures, regardless of aggregate source.

The “good” gradation mixes have better performance compared to the “Bad” gradation mixes. This means that in combination to good gradation selection, lower binder content can increase the possibility of meeting the interstate traffic level rutting requirement. Note that in this study, that the binder used is PG 64-22, instead of the stiffer PG 76-22 polymer modified binder specified for Type A surface courses. As discussed by Davis (2001), softer binders can be beneficial to the healing characteristic and reduce the cracking potentials, reducing not only the initial construction cost but lifetime costs as well, so if it is possible to keep the rutting problems in check by selecting the right gradation and lower binder content while using a low binder grade, it will be promising both economically and from a cracking reduction perspective.

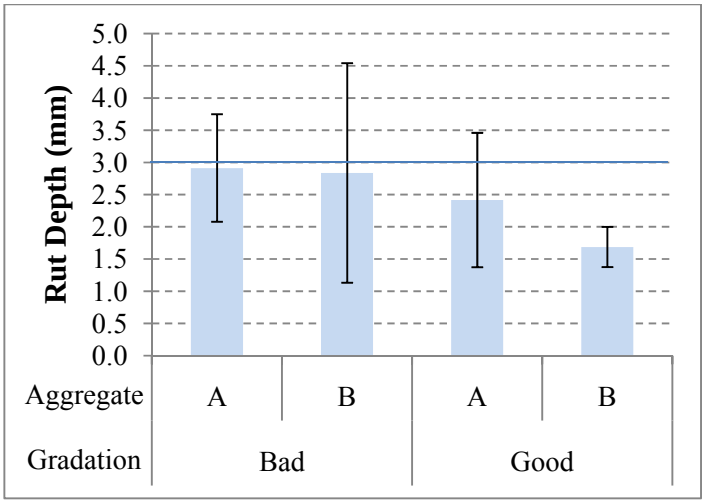

Figure 5.8 Rut Depths at 4% Air Voids with Lower Binder Content

MAIN PARAMETER SENSITIVITY ANALYSIS

Up to this point, effects of the main treatment factors on the rutting performance have been evaluated. It is important to compare the sensitivity of them to pavement permanent deformation. The mean values of the factors in this study are given in Table 5.6. The rut depth change due to

one unit change for a given main treatment factor is simply calculated by dividing the difference in rut depth between two treatment levels of the factor by the unit change in the factor. The main factor influencing rank can be used for factor sensitivity analysis in rutting performance. In the "Rut depth/Unit change" column, the information can be inferred that the increase in the rut depth due to a 1% AV increase is approximately equivalent to the effect of 0.37% increase in binder content. Further, the gradation is more influential compared to the effect on rut depth due to unit change in air voids content or 0.37% change in binder content.

Table 5.6 Treatment Level Means and Sensitivity Analysis for the Main Factors

Main Factors	Treatment Level	Mean Rut depth (mm)	Δ in Mean between Treatment Level	Rut depth/Unit change
Aggregate	A	3.848	0.236	N/A
	B	4.084		
Gradation	Good	3.375	1.183	N/A
	Bad	4.558		
AV	4%	2.953	2.027	0.676[1]
	7%	4.980		
BC	L	3.504	0.924	1.848[2]
	H	4.428		

Note: 1: the change of rut depth due to 1% change in air voids content.
2: the change of rut depth due to 1% change in binder content.

2-WAY INTERACTION EFFECT

The most important finding regarding 2-way interaction is that between any of the three parameters, the interaction effects are not significant. This means the individual effect on the rutting property due to the construction variation in each of the parameters is additive, when two of them are present. In other words, the effect of one factor on rutting would not be different at

the different treatment levels of either of the other factors. For example, when the binder content deviates to the lower side of the evaluated range, and mat density is reduced at the same time, an additive positive effect of these changes can be expected, given the gradation is kept unchanged.

Further, statistical analysis results showed that at the 3-way interaction level, where the aggregate source is the third factor, there is no interaction, whatsoever. That means the 2-way interaction effects are the same with both the aggregates.

The only 2-way interaction effect that was observed to be statistically significant in this experiment was the aggregate source and AV interaction. Further analysis revealed that at the 4% AV level, aggregate A and aggregate B have the same rutting resistance conformance; however, at the 7% AV level, aggregate A shows better rutting resistance. Graphic illustration of the 2-way interaction is presented in Figure 5.9. This means that changing the APA test specification on AV requirement from 4% to 7% sometimes can potentially differentiate two aggregates, even though they may have the same performance at the 4% AV level. Interpretation of this should be very careful because the difference between two aggregates may not be practically significant; the difference under the APA test is only in a margin of less than 1 millimeter. The statistical difference only displays the power of statistical analysis that was used.

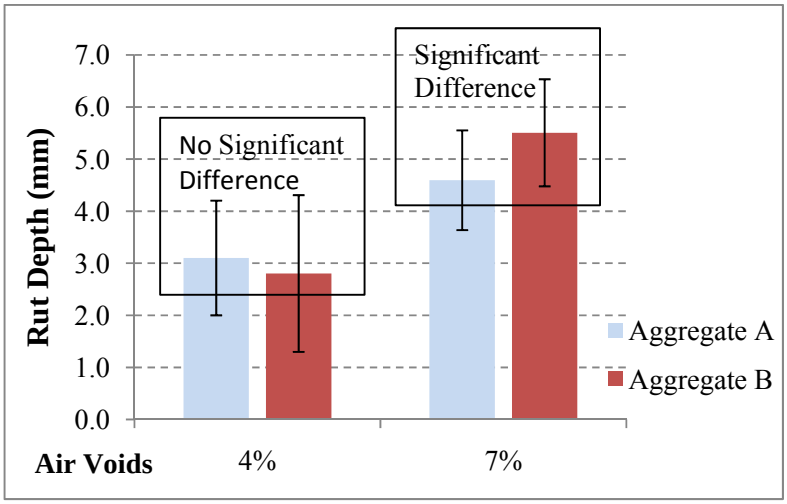

Figure 5.9 Aggregate Source and AV Interaction Effect

A very important interaction between gradation and binder content needs to be examined when gradation variation occurs during the construction process, rather than the gradation selection during a mix design. Most of the mix designs using a coarse gradation end up having higher asphalt binder contents than those using a fine gradation, because coarse gradation tends to have more voids in the mineral aggregate, thus more binder content is needed to fill the VMA to maintain the air voids content at 4% in the designed mix. In this study, the coarse and fine gradations for aggregate A were deliberately selected to keep the VMA at a comparable level, even though a slightly higher binder content is produced. In the case of aggregate B, the difference in binder content between the coarse and fine gradation is more than 0.5%. The interactions between aggregate gradation deviation and binder content on rutting are presented in Table 5.7. An example using the aggregate A coarse gradation is provided to follow the logic of this interaction.

Table 5.7 Hypothetical Gradation and Binder Content Interaction due to Gradation Deviation in the Construction Process

	Aggregate: A		Aggregate: B	
Design Gradation	Fine (Bad)	Coarse (Good)	Fine (Good)	Coarse (Bad)
Design Optimum Binder Content, P_b (%)	5.53	5.73	4.18	4.72
Gradation deviation to (During Construction)	Coarse	Fine	Coarse	Fine
BC (%) supposed to be (Based on the new deviated gradation)	5.73	5.53	4.72	4.18
Relative BC Variation (%)	-0.20	0.20	-0.54	0.54
Gradation Variation Effect	+	-	-	+
Binder Variation Effect	+	-	+	-
Overall Effect	2 positive	2 negative	Offset	Offset

Suppose the coarse gradation using aggregate A is selected in the job mix formula (in Table 5.7). During construction, it is possible for the coarse gradation to deviate into a fine gradation. This gradation deviation can occur, for a number of reasons. One example is that a high concentration of fine content can occur at the top of an aggregate stockpile, and may be added into the production process leading to a surge in the fine portion of the gradation, and a mixture having a fine gradation will be produced. However, the binder content added during the production process is the same as intended for a coarse gradation; the mixture will end up with a slightly higher binder content (by +0.2%) based on the new deviated aggregate gradation. The pavement constructed using the flawed mixture deviates from the job mix formula twofold in

terms of rutting performance: the gradation deviates from coarse to fine, and the excessive binder content compared to the new deviated aggregate gradation. A double negative effect can be expected for the segment of pavement using material due to the unfavorable change in the aggregate gradation.

The situations listed in Table 5.7 are hypothetical scenarios, but many other possible aggregate gradation deviations are likely to happen in the construction process that can cause similar interaction with relative binder content variation. The results show that depending on the aggregate gradation selected in the mix design and the gradation change during production, the possible outcome varies. In the case of aggregate A, either two positive or two negative effects can be expected; in aggregate B, the change in the gradation and the relative binder content variation can offset each other, regardless of the designed gradation. The quantitative overall effect remains to be evaluated.

3-WAY INTERACTION EFFECT

The 3-way interaction effect for the three fundamental parameters is statistically significant in this study. Normally, 3-way interactions are less important, practically speaking. However, it is worthwhile to further examine whether there is a common pattern or any pattern at all in terms of the presentation of this interaction, especially in light of the fact that there is no 4-way interaction effect when the aggregate factor joins this 3-way interaction effect, which means this 3-way effect is applicable for both of the aggregates. Therefore, further examination seems to be a task worth taking.

Regardless of the aggregate source, the combination of gradation and binder content can divide the mixtures into 4 groups: Good-H (good gradation, high binder), Good-L (good

gradation, low binder), Bad-H (bad gradation, high binder), Bad-L (bad gradation, low binder). Tukey's method for multiple comparisons was conducted to further investigate the 3-way interaction (Appendix D). The results are presented in Table 5.8 and in Figure 5.10. Table 5.8 shows that at the 4% air voids level mixture, only mixture Bad-H's performance is fair, while the other three mixtures have excellent performance; at the 7% air voids level only mixture Good-L has good rutting performance, while the others perform fair.

Table 5.8 Tukey's Multiple Comparisons Results

Mix Designation	Good-L	Good-H	Bad-L	Bad-H
At 4% AV level				
Statistical Group	A	A	A	B
Numbers of factors on favorable rutting resistance end	3	2	2	1
Overall Performance Rating	excellent	excellent	excellent	fair
At 7% AV level				
Statistical Group	A	B	B	B
Numbers of factors on favorable rutting resistance end	2	1	1	0
Overall Performance Rating	good	fair	fair	fair

Note: 1.A, B are statistically different at 5% significant level; A is less in rut depth than B; 2. Rating is defined as: excellent (rut depth<3mm), Good (3mm<rut depth<4.5mm), fair (rut depth>4.5mm)

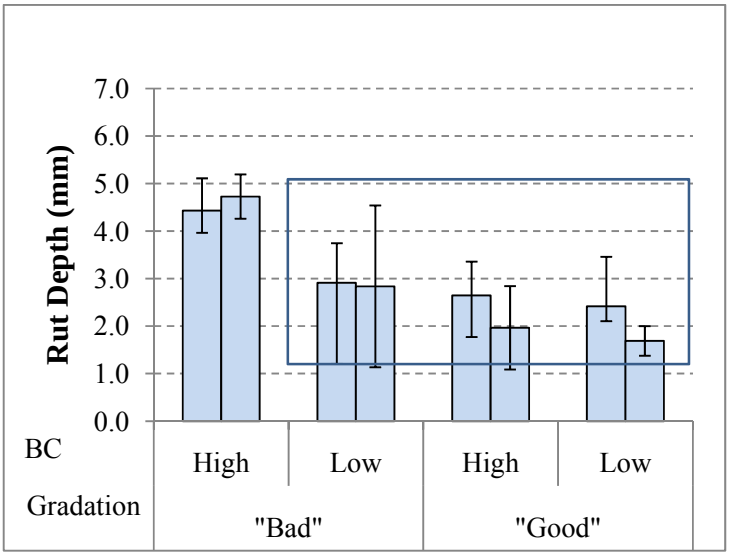

(a)

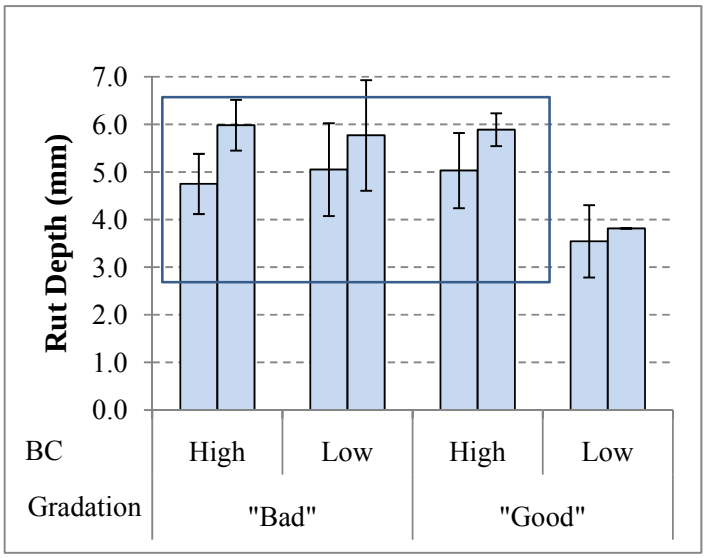

(b)

Figure 5.10 Gradation And Binder Content Combination Effect: (a) at 4% AV; (b) at 7% AV. (Note: the side-by-side bars are aggregate A and B.)

In the ANOVA table (Table 5.3), there are no two-way factor interaction effects between the three parameters, indicating that the individual effect is additive in the presence of any of the two

factors (the third factor is held constant). The three-way interaction effect shows that the effect of the third factor is additive only for some of the combinations of the other two factors. It is evidenced from Table 5.8 that, to expect the HMA pavement to have a good rutting performance, the mixture should have at least two factors in its favorable ends, out of the three factors. On the other hand, if the mixtures have two parameters that may lead to the adverse end, their performance could be expected to be as poor as the ones where all three parameters are at the adverse end.

This finding about 3-way interaction could have an application in increasing the robustness of the HMA quality. One of the robust design ideas is trying to reduce the sensitivity of noise factors to a product's quality, rather than eliminating it. The variability of the fundamental factors of HMA pavement affects the rutting performance. If two of the factors can be well controlled to the end where a mixture's rutting property is favorably affected, the third factor— which would be the most "uncontrollable" factor— will be insensitive to the material's rutting performance. That is, whether the third factor is in the good or poor performance end, the quality of the mixture will not be significantly affected and remain of good quality.

STATISTICAL MODELS

Based on the experiments, multiple regression statistical models were developed. The purpose of developing the models was to establish a simple and reasonable predictive relationship between parameters obtained in design/construction quality control and the lab APA test performance. This could be an indication of future field performance of the constructed asphalt pavement.

The critical procedure in developing a predictive model is to select the independent variables. It is desirable to find a quantifiable variable to represent the treatment factor instead of a categorical variable. In this case, the dependent variable is the rut depth in millimeters. Air voids content has a significant impact on the rut depth; therefore, it is not questionable to adopt the air voids content in the model. VMA is also a very important volumetric parameter that governs the rutting performance. Because VMA is the sum of the volume of air voids and volume of effective binder, the effective binder volume (V_{be}) was selected to represent the binder content in the experimental treatment. Moreover, effective binder volume is a percentage of total volume, just like air voids content; each individual sample has a unique effective binder volume, giving a spectrum of values for this independent variable. After trial and error, the effective asphalt binder volume was proven to be better than the binder weight content in the model development. To account for the gradation effect, it was observed that using the normalized absorbed asphalt content ($P_{ab,n}$) was better than using the AASHTO gradation classification as the independent variable. The reason is well discussed in the previous section (refer to "Gradation Effect"). However, it should be noted that when the gradation variable is used in one aggregate source, it acts the same as a categorical variable, as only two levels are involved. The models and the corresponding R-square values are listed in Table 5.9.

Table 5.9 Statistical Rutting Model Using Volumetric Variables

	Model	R-square	Equation Number
Individual aggregate A	Rut = -26.0+0.546AV+ $0.792V_{be}$+$19.4P_{ba,n}$	0.70	Eq 5.3
Individual aggregate B	Rut = -11.7+0.954AV +$0.980V_{be}$+$0.887P_{ba,n}$	0.75	Eq 5.4
Aggregate Combined	Rut = -7.25+0.757AV +$0.619V_{be}$+$1.01P_{ba,n}$	0.66	Eq 5.5
Aggregate Combined (another set of variables)	Rut = -6.10+1.58Ln(AV-2.8)+$0.779V_{be}$+ 0.277SSA*$P_{ba,n}$	0.71	Eq 5.6

Where AV =Volume of air voids in the mix (%)

V_{be} = Effective binder volume (%)

$P_{ba,n}$ = Normalized absorbed asphalt content

SSA = Specific surface area (m^2/kg)

The R-square value in a multiple regression analysis represents the amount of experimental errors in the response variable that can be reduced by fitting an equation with multiple independent variables. The models built for an individual aggregate source (Eq 5.3 and Eq 5.4) can establish a baseline about how high of an R-square value can be achieved. As can be seen in Eq 5.5, the R-square value drops by approximately 0.05, the reduction is due to the introduction of one more aggregate source; the disparity in the two aggregate properties increases the variability (scatter of data points). The ability to use the same set of variables to predict the rut depths is reduced correspondingly. To address the variability brought about by incorporating one more aggregate source, other independent variables were tried. In Eq 5.6, for the combined aggregate sources, the natural logarithm function (ln(AV-2.8)) was used to substitute for the air

voids content; it puts a curbing limit on the low side of AV (AV must be greater than 2.8). Additionally, SSA*$P_{ba,n}$ was used to substitute for the $P_{ba,n}$ as the gradation term in the equation. Equation 5.6 raises the R-square value up to the comparable level as the individual aggregate model (Eq 5.3 and Eq 5.4).

Even though Equation 5.6 has a better R-square value, it is presented only as an alternative to equation 5.5 to compare its effectiveness. Equation 5.5 is still the one recommended to use because of its simplicity. Equation 5.6 requires more input variables; and because the logarithm function is used, it cannot be used to extrapolate the rut depth where the AV content is larger than 9%. It should also be noted there is no term in any of these equations to address the binder grade on rut depth. The binder grade for these equations is PG 64-22. The equation can be used to estimate the rut depth by changing the gradation, binder content and in-place mat density.

Two particular things need to be emphasized about the regression equations. Firstly, the volume of effective binder content is adopted to represent the effects contributed by the constituent of asphalt binder on the rutting results. There are other similar parameters that can possibly represent the binder component, including the volume of binder content, and weight content of total binder or effective binder. All the parameters were tried during the process of modeling. The final selected parameter, volume of effective binder, was proven to give the best description on the rutting results due to binder characteristics of the mixtures.

Secondly, note that the difference between the coefficients of AV and V_{be} is small and one might be tempted to think that it is fine for a mix to have a high binder content to reduce the voids content. This is simply not true. The models were developed for the mixes that were designed using accepted mix design procedures. The binder contents are in the range of the

design binder contents for each aggregate and gradation. That means the binder content is within a reasonable range for the aggregate gradations. Also, for a well designed mixture with reasonable binder content, the air voids content is not likely to reach a very low level; otherwise, the mix must have excessively high binder content. Therefore, the equations are only applicable to similarly designed mixes. Some degree of extrapolation outside the experimental range may be allowed, but extreme extrapolations are not recommended and may lead to erroneous results.

Finally, the measured and predicted rut depths are plotted in Figure 5.11. A noteworthy observation is that while the data sets evenly scatter on both sides of the equality line where the rut depth is relatively higher, at the low rut depth end the predicted values tend to be slightly higher than the actual measured depths, indicating that overall that the equations are conservative when they are used to predict the rutting behavior for HMA specimens with low air voids level.

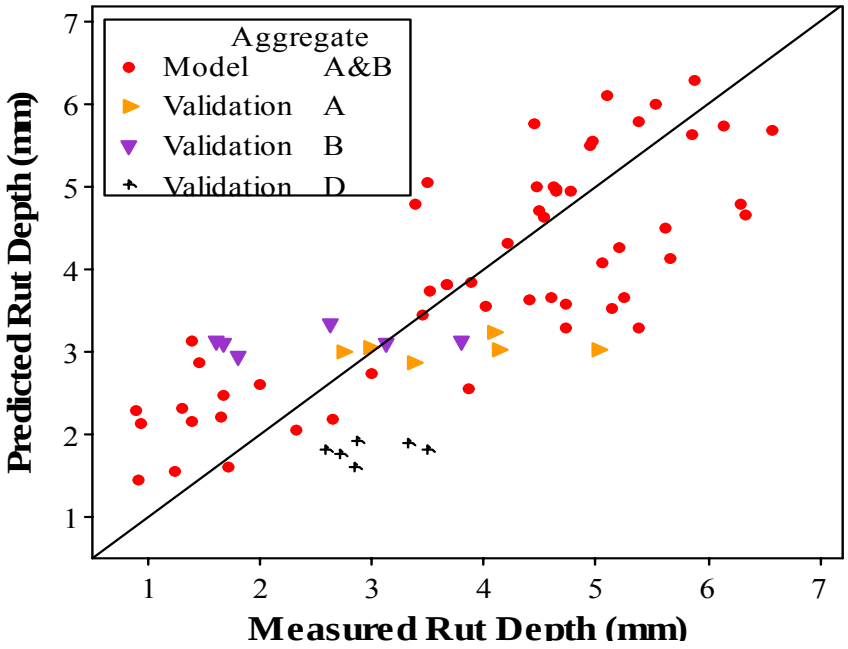

Figure 5.11 Measured and Predicted Rut Depths by Eq 5.5

Figure 5.12 is a plot of the rut depth values (from Eq 5.5) with air voids content as the variable while the volume content of effective binder (V_{be}) and the normalized absorbed binder content ($P_{ba,n}$) are kept constant at 10.0% and 1.0, respectively. A 95% confidence interval and the prediction interval are also shown in the figure. The confidence interval gives a range of the mean value of the predicted rut depth with 95% confidence for a particular air void content. The confidence interval is narrow, which indicates the estimation of the response variable is stable. The prediction interval shows the range that an observation can possibly fall in; it is broader than the confidence interval.

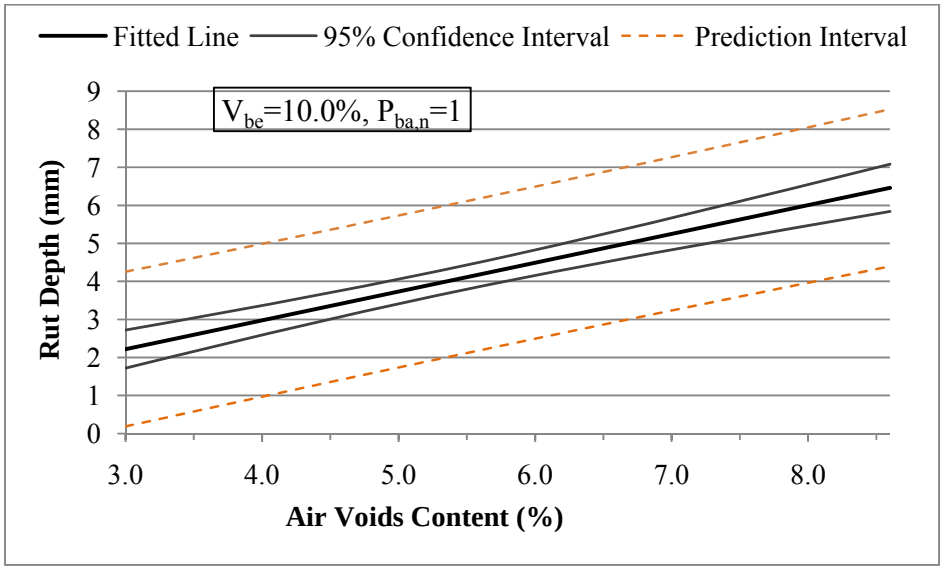

Figure 5.12 Rut Depth vs. Air Voids Content by Using Eq 5.5

The model (Eq 5.5) can also serve as a useful tool to mediate the requirements for rutting characteristics of a mixture in a mix design process. The following explanation intends to introduce the basic procedure, not a specification, because the selection of many input parameters involved is subject to the mix designer's judgment or requires further validation. In Figure 5.13, the relationships between the predicted rut depth and the volume content of effective

binder by Eq 5.5 are given for the HMA mixtures with an air voids content of 4.0% and 7.0%. The normalized absorbed binder content ($P_{ba,n}$), which accounts the possible gradation effect on rutting for the particular aggregate source in a mix design, is set at 1.2; a value larger than 1.0 is used to be conservative to some extent. Based on Figure 5.13, an upper binder content limit can be determined to satisfy the rutting requirement. For example, many states may have a requirement of the maximum rut depth for a mix design to screen out the mixtures that may experience premature rutting failure. In the SCDOT specification, the maximum rut depth is set forth at 5 mm for mixtures that are compacted to an AV level of 4% (SCDOT, 2009). To calculate the upper binder content limit, a mix design starts with the APA rut depth requirement, and then the corresponding volume of effective binder can be determined using Figure 5.13. The volume content of effective binder content can be converted to the weight content by using the chart in Appendix A. Then, the absorbed binder content is added to the effective binder content to get a total binder content. A mix with a binder content lower than that upper limit will satisfy the rutting requirement according to the used prediction equation. This binder content upper limit will be compared with the proposed binder content window (Chapter VI), and further to work out a desirable aggregate gradation to accommodate a binder content that is in a range, where both the rutting and cracking requirements can be met.

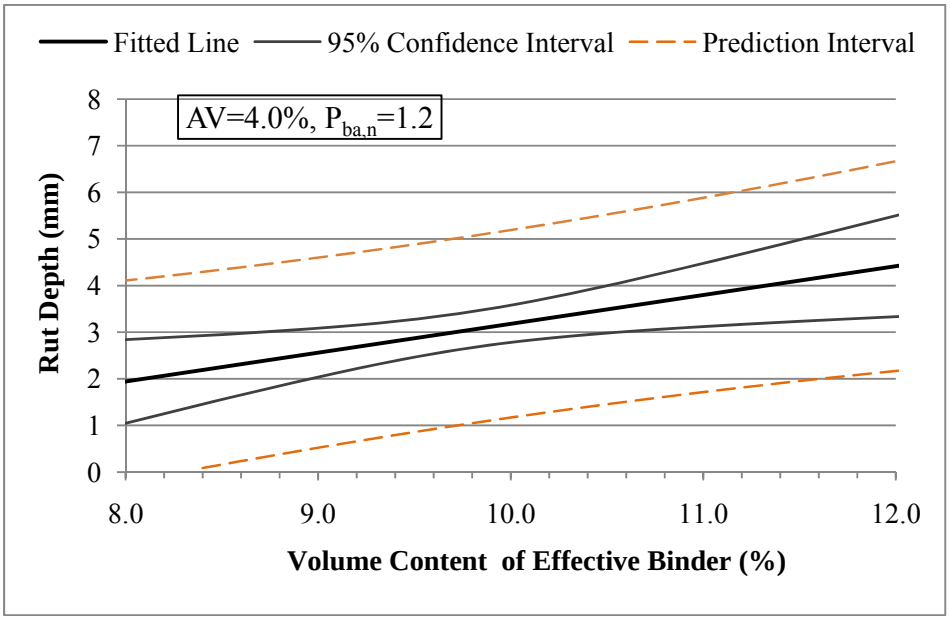

(a)

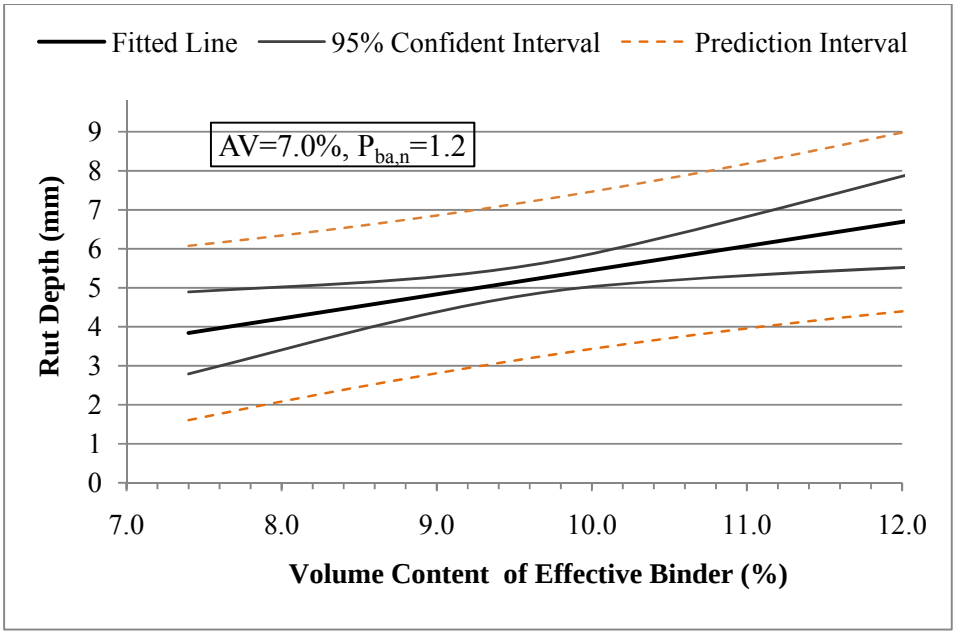

(b)

Figure 5.13 Relationship between Rut Depth and Volume Content of Effective Binder: (a) AV=4.0%; (b) AV=7.0%

The model (Eq 5.5) was validated by using the APA test data from a separate data set provided by another researcher. In addition to aggregates A and B, another source (D) was also used. All of the mixtures used for model validation were Type B mixtures with the same asphalt binder grade (PG 64-22); however, the binder used in the validation mixtures was from a different source than the binder used to develop the model and the aggregate gradations were different as well.

The rut depths of the validation mixtures were plotted in Figure 5.11. As can be observed, the validation data points of aggregates A and B fit well within the data scatter of the model. For aggregate D, the data points also fall in the variation band of the model. The fact that a different binder source and gradations were used in the validation mixtures, demonstrates that the model can be used for materials having similar properties to those used in the study.

CHAPTER VI: TENSILE CRACKING RESULTS AND DISSCUSIONS

GRADATION AND MIX DESIGN

The South Carolina DOT technical specification for Hot-Mix Asphalt material properties (SCDOT, 2009) was followed to conduct the aggregate gradation and mix design to evaluate the influence of binder content, air voids, and gradation on tensile properties. Six mix designs were carried out for a Type B surface course (high volume primary roads). In addition to aggregate source A and B, aggregate C was included in this tensile cracking study. The six mix designs are the combinations of three aggregate sources and two gradation types, and all mixes have a nominal maximum aggregate size (NMAS) of 12.5 millimeters. The fine and coarse gradation curves are given in Figure 6.1(c).

The gradations for aggregate B are the same as the ones used for the rutting performance assessment. Along with the gradation curves, other restrictive boundary curves are plotted, such as the SCDOT gradation upper and lower spec limits, the maximum density line, AASHTO control points, and even the obsolete fine aggregate restricted zone, so that the mix gradations can be compared by their relative location to the restrictive curves. Hydrated lime was added to each mixture at a rate of 1% by the mineral aggregate weight (including lime) as a standard practice in many states to minimize moisture susceptibility. As perceived in the graphs, the SCDOT aggregate gradation band has an S-shaped curve, and the upper specification limit nearly coincides with the upper boundary of the restricted zone (only for fine aggregate portions). Trying to design a fine-graded aggregate gradation passing between these two curves is very difficult. All of the adopted fine-graded gradation curves pass through the restricted zone.

Nevertheless, they meet the definition of a fine-graded aggregate gradation as defined in AASHTO M 323—above the corresponding point at the primary control sieve size.

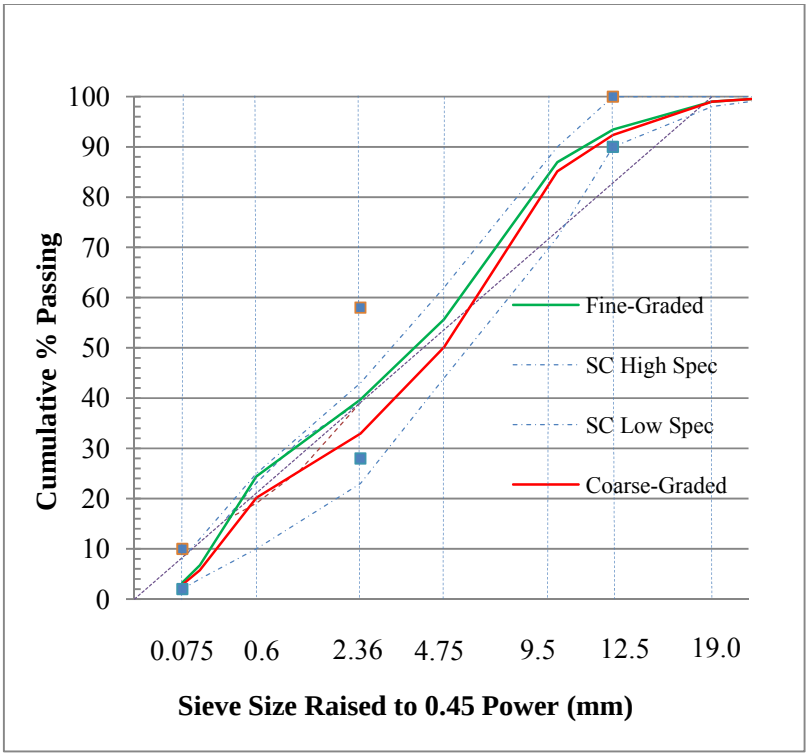

(a)

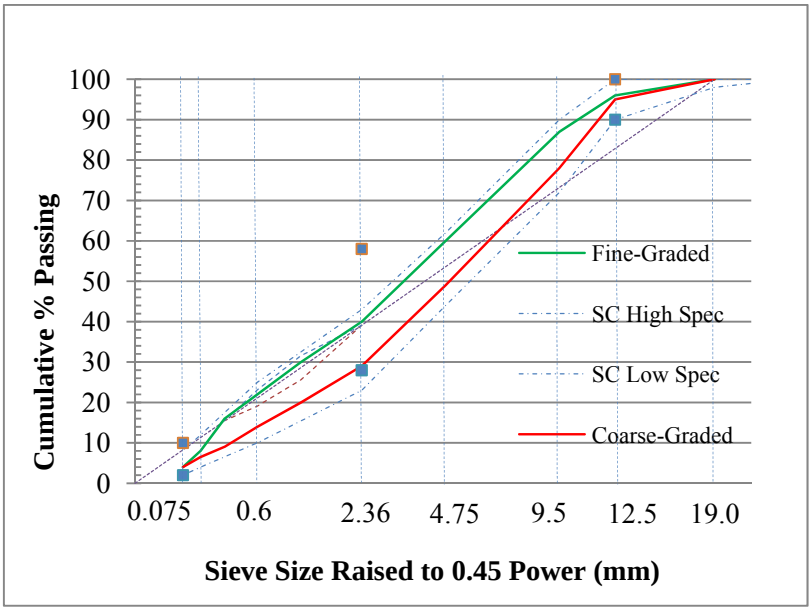

(b)

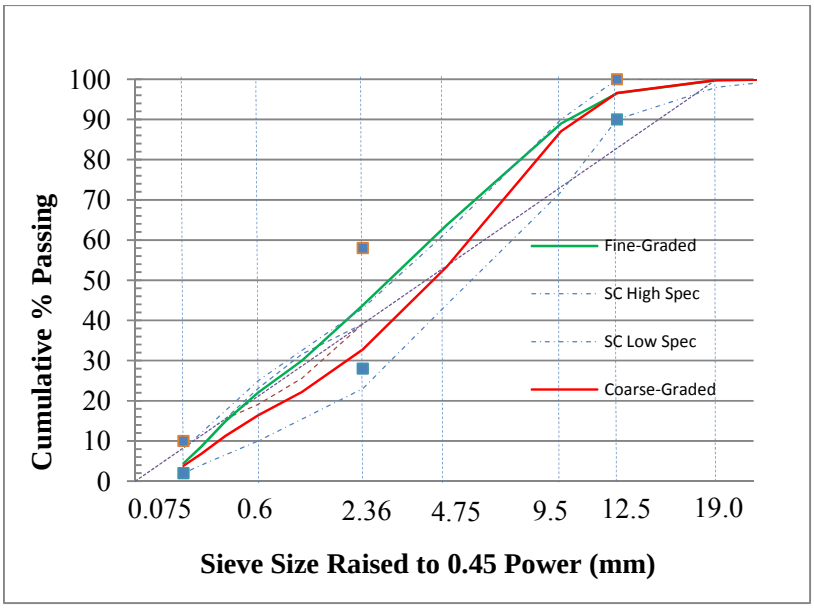

(c)

Figure 6.1 Gradation Charts in Cracking Evaluation: (a) aggregate A; (b) aggregate B; (c) aggregate C

Optimum binder content was determined for the six mixes in the laboratory using a design gyration number of 75 and corresponding AV of 4% per Superpave mix design procedures; other volumetric parameters, such as VMA (volume of voids in mineral aggregate) and VFA (voids filled with asphalt) were determined, and are summarized in Table 6.1. As evidenced in the table, the fine-graded mixtures generally have a lower binder content compared to coarse-graded mixes. This is primarily because the gradation curves are closer to the maximum density line; therefore, they have more compact aggregate packing characteristics. Consequently the VMAs are smaller, requiring less binder to fill the voids to end up at 4% air voids in the total mix.

Table 6.1 Mix Design Volumetric Parameters in Cracking Evaluation

	Aggregate: A		Aggregate: B		Aggregate: C	
Gradation	Fine	Coarse	Fine	Coarse	Fine	Coarse
Gyration	75	75	75	75	75	75
Optimum Binder Content, P_b(%)	6.00	6.00	4.18	4.72	4.80	5.80
Va (%)	4.0	4.0	4.0	4.0	4.0	4.0
VMA(%)	15.2	15.6	13.7	14.2	14.8	16.9
VFA(%)	77.5	73.8	70.9	71.8	73.0	76.3
Effective Binder Content, $P_{be,}$(%)	5.03	4.87	4.07	4.24	4.62	5.56
Aggregate SSA (m2/kg)	5.26	4.48	5.38	4.24	5.17	4.51
Film Thickness (micron)	9.77	11.10	7.58	10.09	9.02	12.57
D/A Ratio	0.66	0.60	0.96	0.85	0.97	0.68

To study the three parameters' effects on the asphalt concrete tensile performance, Analysis of Variance (ANOVA) with blocks, was utilized to discern the effects of treatment on the tensile performance parameters (ITS, Deformation, and Fracture Energy). The null hypothesis was that

all the treatment means are the same; the alternative hypothesis was that not all the treatment means are the same. The level of significance (α) was set at 5%. For the factors with more than two treatment levels, a multiple comparison analysis was conducted to distinguish the effects, and the effects were grouped into different statistical groups. The statistical analysis results regarding the production/construction variability factors and the aggregate sources are presented in Table 6.2 and Table 6.3, respectively.

Table 6.2 ANOVA Results of Main Factors and Treatment Levels

Test Parameters	Gradation Coarse~Fine	Binder Content OBC-0.25%~OBC+0.25%	Air Voids 4%~7%
ITS	B~A (0.028)	A~B (0.023)	A~B (0.000)
Deformation	NS (0.057)	B~A (0.010)	B~A (0.000)
FE	NS (0.183)	NS (0.180)	A~B (0.040)

Note: 1. test level of significance (α) is set at 5%
2. A and B represents two statistically different groups, with group A having a greater value than group B; NS: not significant.
3. The numbers in parenthesis are the test P-values.

Table 6.3 ANOVA Results of Aggregate Effect

Test Parameters	Aggregate Sources		
	A	B	C
ITS	B	A	A
Deformation	A	B	AB
FE	B	A	AB

Note: 1. test level of significance (α) is set at 5%
2. A and B represents two statistically different groups, with A having a greater value than group B; AB represents the group that is in between group A and B, and can not statistically distinguish from either A or B.

AGGREGATE GRADATION EFFECT ANALYSIS

Plotted in Figure 6.2(a) are the mean ITS values with the ±1σ (standard deviation) illustrated as the error bars. The overall ITS values of fine-graded mixtures are higher than the coarse-graded gradation, regardless of the aggregate sources. Aggregate C possesses the most striking difference between the two gradations, compared to aggregates A and B, partly because the difference in OBC level of the two gradations is the largest (1%). Different aggregate sources and gradations will lead to various aggregate packing characteristics; a specific VMA value is produced for a given combination of aggregate source and gradation type. During the mix design process, the VMA should be filled by asphalt binder to the extent where 4% air voids are left in the total; the corresponding binder contents could vary dramatically as a result of the gradation selection. In other words, OBC is a function of the aggregate source and gradation.

To separate the compounding effect due to binder content from the gradation effect and to increase the test precision, the statistical analysis was performed with the combination factor of aggregate and binder content treatment as a block factor. The specific statistical results are presented in Appendix E.

As seen in Table 6.2, there is a significant difference with respect to the ITS value due to the gradation treatment; the ITS values of the fine-graded mixes are higher than the values of the coarse gradations, which means fine mixtures are stronger in this study. This difference may be attributed to the fact the fine gradations generally have a lower binder content compared to the coarse-graded mixtures.

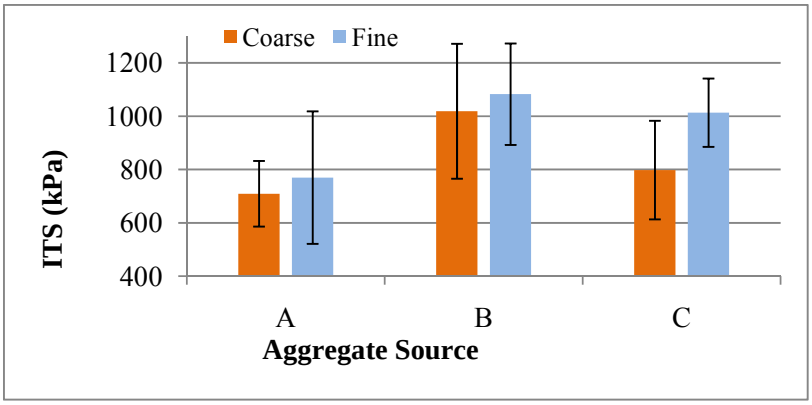

(a)

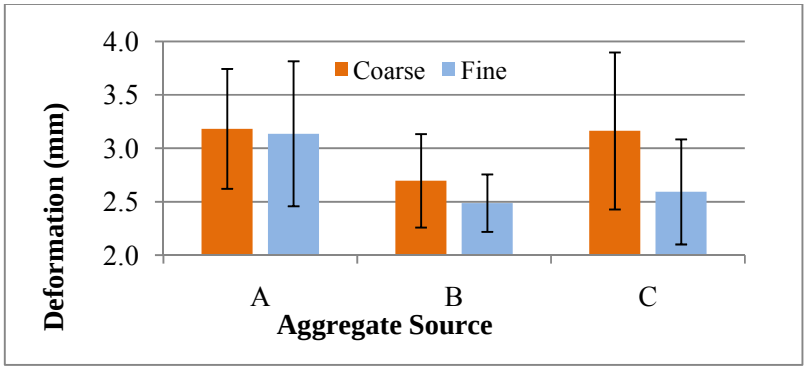

(b)

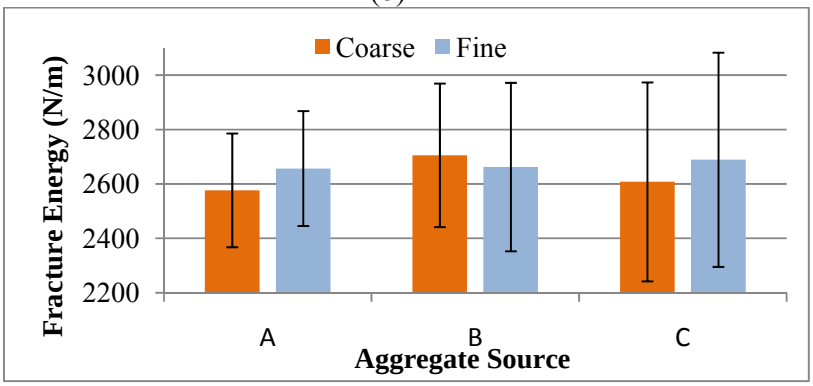

(c)

Figure 6.2 Aggregate and Gradation Effect on IDT Test: (a) ITS Values; (b) Deformation; (c) Fracture Energy

When all six gradations are compared in this study, it is found that the ITS values are correlated very well with the design binder content, as illustrated in Figure 6.3. The smaller the design binder content, the greater the ITS test result will be. As discussed earlier, a combination of aggregate and gradation selection will lead to a specific binder content by virtue of a mix design. However, this relationship indicates that the design binder content can be used as an indicator for the ITS prediction. In other words, the effect of a gradation and/or aggregate source of a mix on ITS is manifested through the binder content of the mix—the design binder contents of the mixes gave an indication of the mixes' ITS performance.

This finding may be used to further interpret the effect of production variability in gradation on the mix ITS property. As long as a binder content is well controlled and kept constant at the design value, a limited deviation of gradation from the target value seemingly will not affect this tensile property.

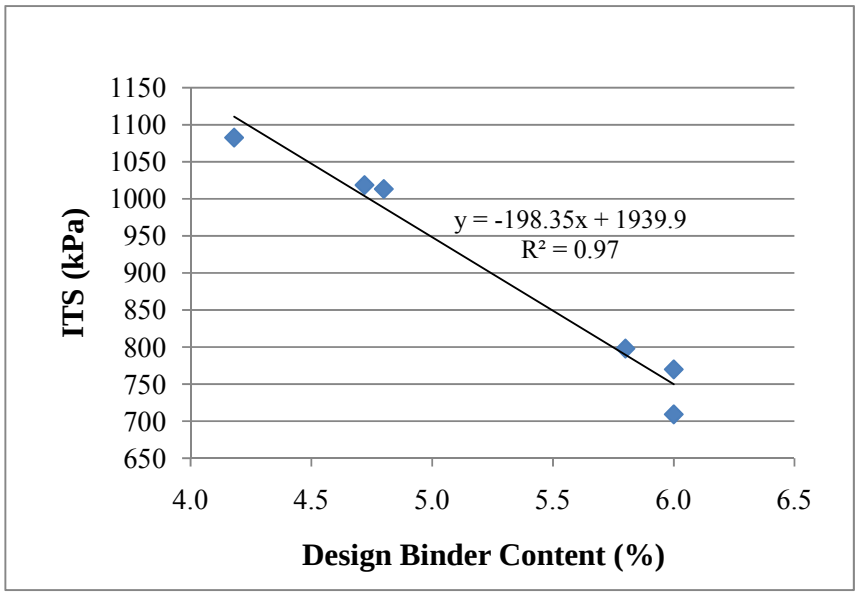

Figure 6.3 Correlation of the ITS with Design Binder Content for the Six Gradations

Deformation corresponds to the vertical displacement of a test specimen sample when it is subjected to the maximum force. During the upswing of a loading period, the tensile strain in the horizontal direction at the center of the specimen is increasing with the increase in load until the limit is reached at the failure point. Therefore, it is reasonable to assume the deformation is in an approximate proportional relationship with the tensile strain at the center point. The larger the deformation a specimen undergoes, the greater stain capability the specimen would have.

In Figure 6.2(b), the deformation values of the different mixtures are plotted. Overall, deformation values of fine-graded gradations are lower than those of coarse gradations. The deformation differences between coarse and fine gradations for aggregates B and C are noticeably larger, as compared to aggregate A. The statistical analysis (Appendix E) utilized the same blocking factor as conducted for ITS values. It is worthwhile to mention that the test P-value is 5.7% (Table 6.2), which makes the test barely fail to reject the null hypothesis.

A close relationship can be observed between the deformation and design binder content in Figure 6.4. The trend is that as the design binder content increases in the mixes, the deformation increases accordingly.

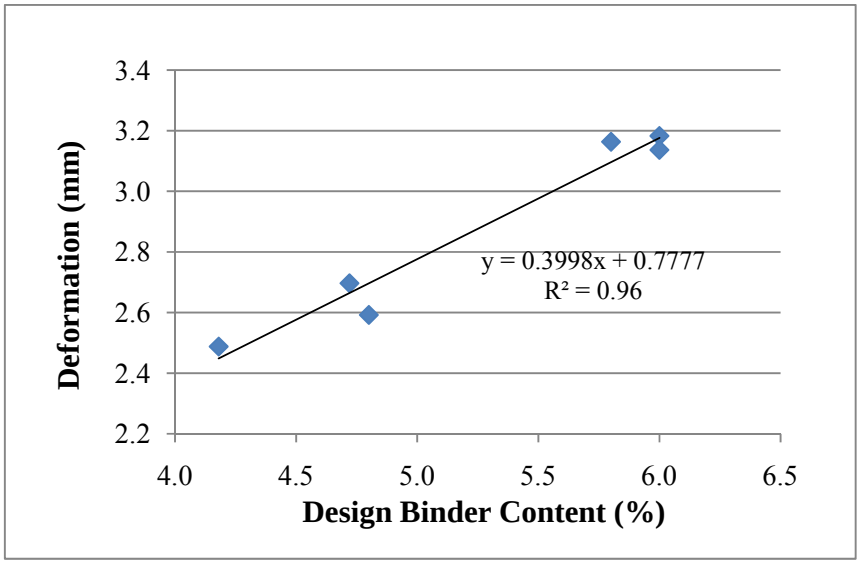

Figure 6.4 Correlation of the Deformation with Design Binder Content for the Six Gradations

Fracture energy is the total energy absorbed by a test specimen before it reaches the failure point over a unit diametrical cross area of the specimen. The force and vertical displacement are proportional to the ITS and horizontal tensile strain in the center, respectively; therefore, the fracture energy is proportional to the fracture energy density limit (the area under the stress-strain curve up to the peak stress) (Chatti & Mohtar, 2004). A study by Wen and Kim showed facture energy is an excellent indicator of the resistance of a mixture to fatigue cracking (2002). In Zhang et al.'s study, the dissipated creep strain energy limit was identified as an indicator to rank the cracking resistance of HMA mixes, and the pattern followed by certain mixtures ranked by the dissipated creep strain energy was in agreement with the one ranked by facture energy density (2001).

In Figure 6.2(c), it can be observed that except for aggregate B, the fracture energy values for the fine-graded gradations are slightly higher than the coarse-graded. However, statistical analysis results (Table 6.2) shows the gradation treatment does not show a significant difference.

The FE pattern of the six mixtures is different from the ITS pattern. This is because the deformation, another factor in determining the fracture energy, has an opposite pattern to the ITS values, as indicated in Figure 6.2(b).

BINDER CONTENT VARIATION EFFECT ANALYSIS

Binder content variation is an inevitable phenomenon in asphalt concrete production. Typically, a small range is allowed in the variation of binder content. It is necessary to investigate the effect of binder content variation on cracking related mix parameters, because the results can potentially provide the information needed for mix design optimization.

ITS values with regard to the binder content variation are shown in Figure 6.5(a). The side-by-side comparisons between the binder content at the low level and the high level show that the lower binder contents have higher ITS values. The statistical analysis shown in Table 6.2 indicates that this effect is statistically significant, and a lower binder content has a positive impact on the ITS value (higher value).

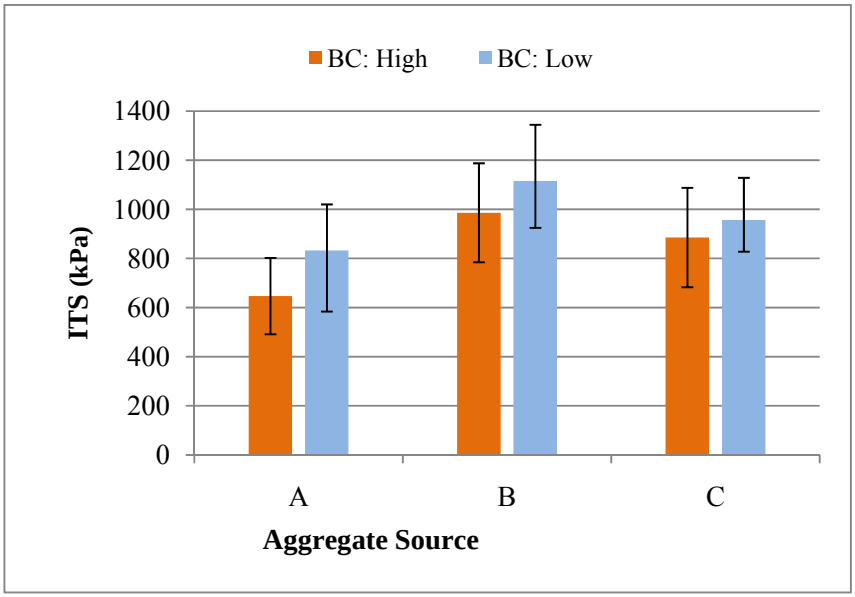
BC: High
BC: Low
1400
1200
1000
800
600
400
200
0
ITS (kPa)
A
B
C
Aggregate Source

(a)

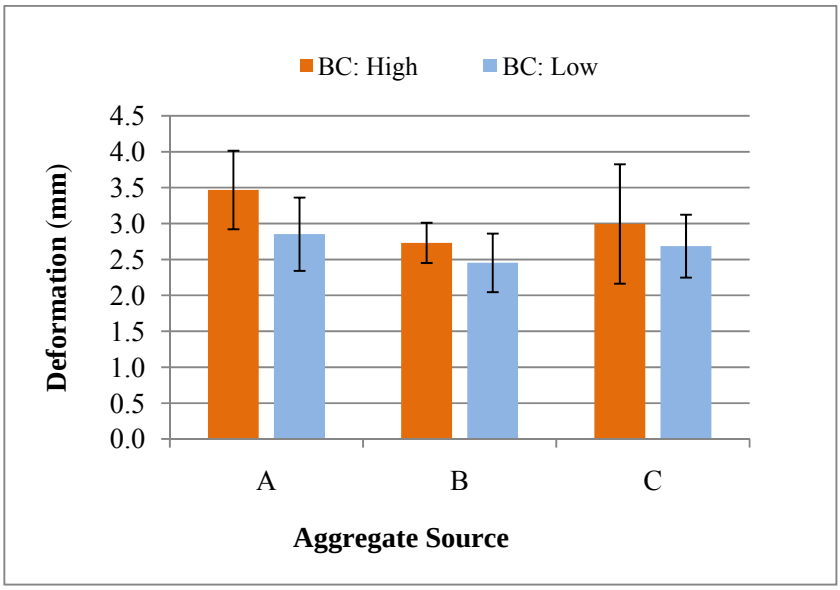
BC: High
BC: Low
4.5
4.0
3.5
3.0
2.5
2.0
1.5
1.0
0.5
0.0
Deformation (mm)
A
B
C
Aggregate Source

(b)

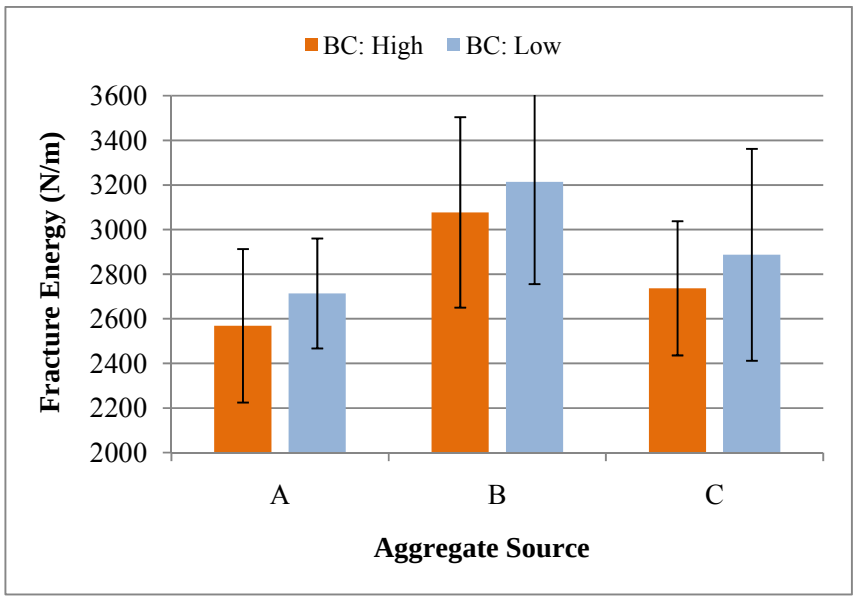

(c)

Figure 6.5 Binder Content Effects on IDT Test: (a) ITS Values; (b) Deformation; (c) Fracture. Note: (High: OBC+0.25%; Low: OBC-0.25%)

From Figure 6.5(b), an apparent difference in deformation can be observed between the two treatment levels: the deformations of the mixes with higher binder content are larger compared to mixes with lower binder content. The P-value in the statistical analysis is 0.01; strongly indicating the OBC+0.25% binder content is favorable to the deformation performance.

Fracture energy results are illustrated in Figure 6.5(c). Even though mixtures with lower binder content have slightly higher fracture energy than the higher binder content mixtures, statistical analysis showed that there is no sufficient evidence that there is a significant difference between the two binder content levels with respect to fracture energy (Table 6.2).

AIR VOIDS CONTENT EFFECT ANALYSIS

Air voids content is a measure of the density of a pavement. In Figure 6.6 (a) the contrast between the ITS values for the two AV levels is remarkable; the mixes with the low AV content

exhibit higher ITS values than the high AV mixes. The statistical results (Table 6.2) revealed the same effect.

In terms of deformation, the graphic illustration (Figure 6.6) shows the 7% air voids mixes have higher values; the statistical analysis reached the same conclusion (Table 6.2). For the fracture energy, the mixes with 4% air voids are superior to the higher air voids content mixes; the statistical analysis results (P-value = 4%, Table 6.2) positively corroborate that the increase in fracture energy is significant when the air voids level is reduced from 7% to 4%. Among the three fundamental parameters, this is also the only factor that is statistically significant in relation to the fracture energy.

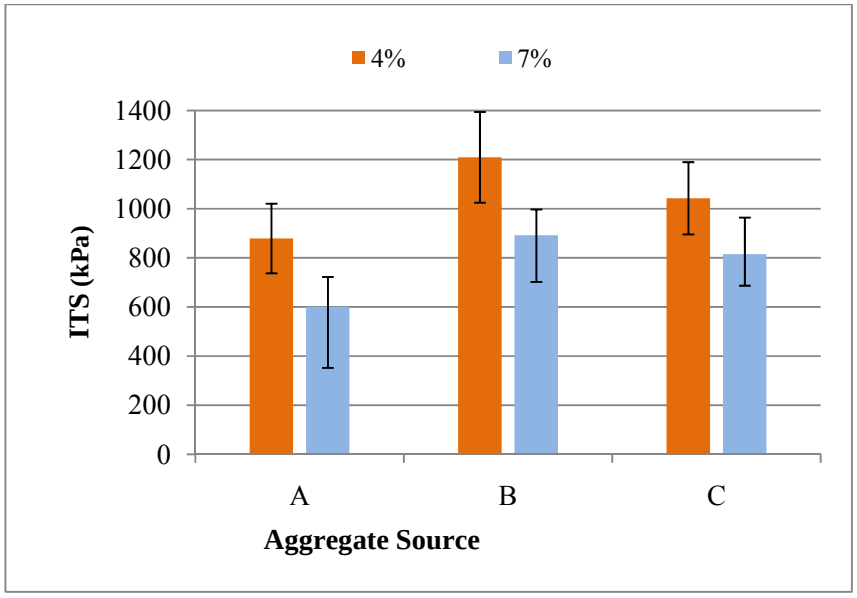

(a)

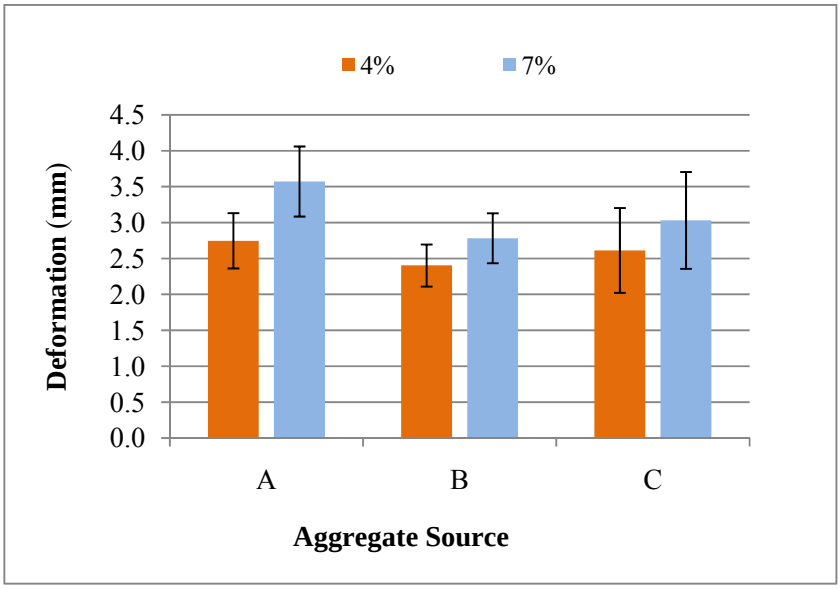

(b)

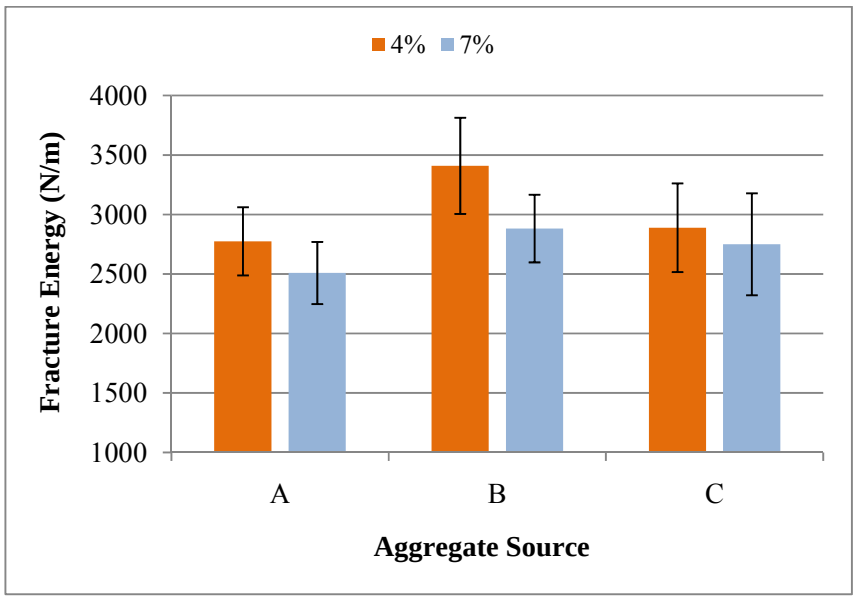

(c)

Figure 6.6 Air Voids Effect on IDT Test: (a) ITS Values; (b) Deformation; (c) Fracture Energy

2-WAY AND 3-WAY INTERACTION EFFECTS

Statistical analysis showed there were no interaction effects between the three mixture parameters either at the two-way level or at the three-way level. Further, the results also showed that the three mixture parameters do not interact with each other in any of the IDT test properties. This finding indicates it is adequate to evaluate a mixture's IDT tensile properties only by looking at the effects that individual mixture parameters have, and the effects caused by multiple parameters are additive. The statistical analysis results are given in Appendix E.

AGGREGATE SOURCE EFFECT ANALYSIS

Aggregate source makes a difference in the tensile cracking performance of the mixtures in this study. In Figure 6.7, the ITS value, deformation, and fracture energy were plotted. The data (aggregate A, B and C in each of the clusters) were compared side-by-side for each of the treatment combination levels. As seen in the ITS graph, the performance patterns among the three aggregates are highly consistent at all levels. Regarding the deformation and fracture energy, at certain treatment levels the pattern shows some degree of inconsistency; however, a general ranking pattern of the three aggregates can still be observed.

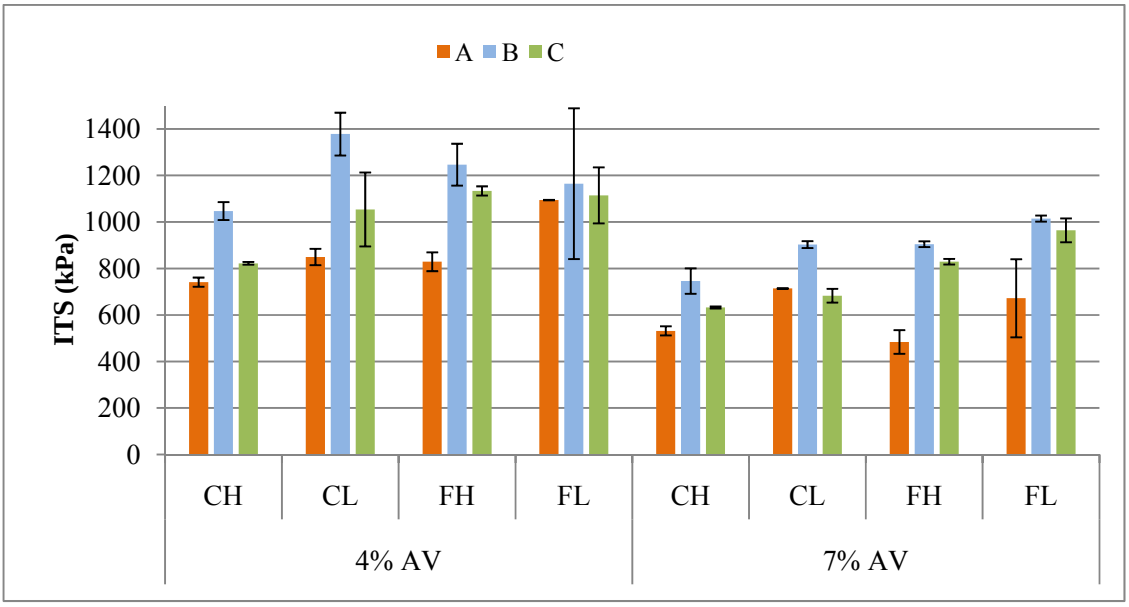
A B C
ITS (kPa)
1400
1200
1000
800
600
400
200
0
CH CL FH FL CH CL FH FL
4% AV
7% AV

(a)

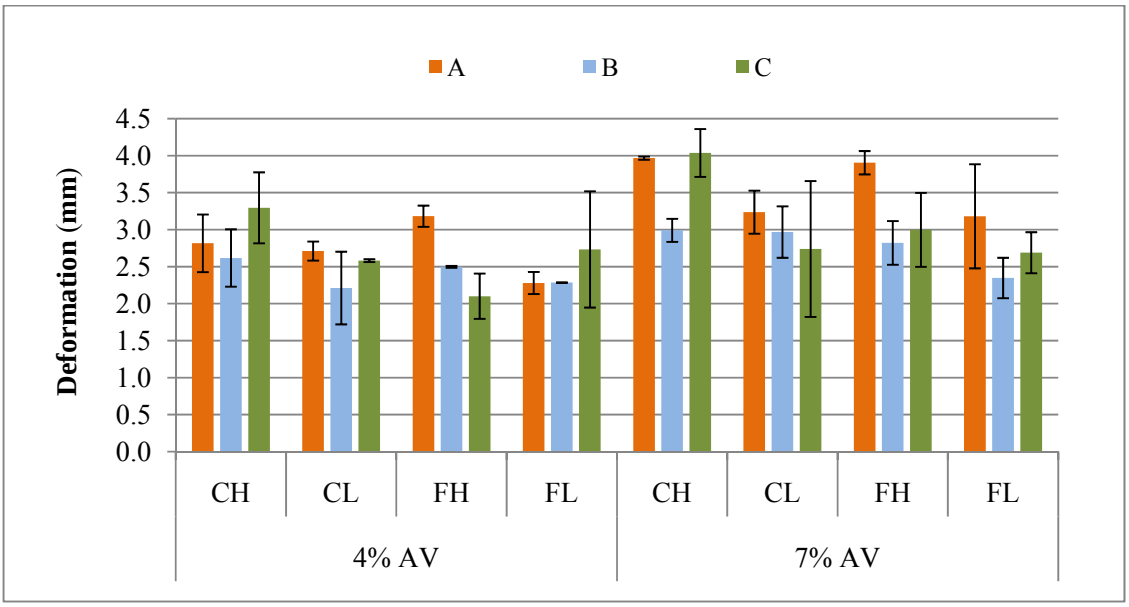
A B C
Deformation (mm)
4.5
4.0
3.5
3.0
2.5
2.0
1.5
1.0
0.5
0.0
CH CL FH FL CH CL FH FL
4% AV
7% AV

(b)

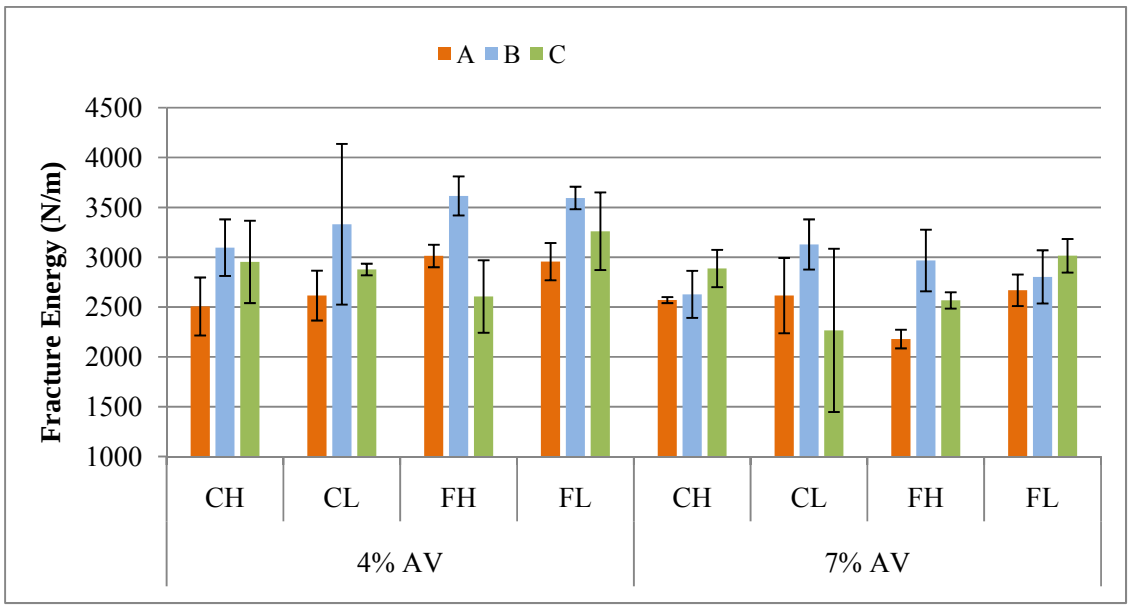

(c)

Figure 6.7 Aggregate Effect on IDT Test parameters: (a) ITS Values; (b) Deformation; (c) Fracture Energy

The ANOVA results are presented in Appendix E. For all the performance properties (namely ITS, deformation, and FE), the results showed that not all the means of the aggregate sources are statistically similar, since the P-values are smaller than the pre-selected level of significance (0.05). The significance mandates a further statistical analysis to compare the mean difference between the aggregate sources. Multiple comparison analysis by Tukey's method was conducted to compare the mean difference and group the aggregate IDT test properties. Presented in Table 6.3, the Tukey's multiple comparison results showed that for ITS values, aggregate B and C are in the same statistical group and their performance is better than aggregate A. In terms of deformation values, aggregate A has larger values, and is distinctly different from aggregate B; aggregate C has an intermediate performance. Regarding fracture energy, aggregate

B exhibits the highest performance, followed by aggregate C, and then by aggregate A; aggregate A is grouped statistically from aggregate B. The results of ITS and fracture energy groupings appear to be closer across the aggregates, as compared to the deformation.

ITS MODEL DEVELOPMENT

When time or financial resources are limited, it is convenient for pavement technologists to refer to some predictive models to compare the properties of mixes that are of interest. An effort was carried out to find statistical models to best fit the experimental data in this study.

Linear regression analysis is one of the most frequently used methods to develop statistical models, where a dependent variable (or response variable) and independent variables are assumed to have a linear relationship. A response variable is the one that needs to be predicted. It is normally not easy to obtain the values of the response variable for a number of reasons. For example, to obtain the dependent variable requires expensive equipment; sometimes the equipment is not readily available, or the test takes a long time to conduct. In this case, the dependent variables are the direct tensile cracking parameters, namely indirect tensile strength, deformation and fracture energy. Independent variables are used to express the dependent variable. Compared to the dependent variable, obtaining the values of independent variables should be easier and less expensive. In this study, the independent variables are the fundamental parameters or other mix volumetric parameters.

The individual effects of the fundamental factors on ITS were separated and illustrated in the previous sections, and they are all proven to be significant to a mixture's ITS properties in this study. However, the gradation (or aggregate source) effects can be reflected by the design binder content, while the effects of binder content variation around design binder content can also be

reflected by the actual binder content during production. Therefore, it is possible to combine the effects of these two factors into one variable: binder content. The ITS regression equation is given in Eq 6.1, where the adjusted R-square value is 0.882.

$$ITS\ (kPa) = 2549 - 223\ P_b - 86.4\ AV \qquad \text{(Eq 6.1)}$$

Where, ITS = Indirect Tensile Strength, in kPa;

P_b = Binder Content by weight, in percent;

AV = Air Voids content, in percent.

There are two things that might be worth noting in the process of regression analysis. First, the effective binder content was tried, the R-square value of the regression dropped by 0.16; therefore, in relating the binder volumetric parameters to the tensile strength property, the effective binder content does appear to be less relevant than the total binder content. Secondly, gradation was tried as another parameter (a categorical/qualitative parameter) in the regression analysis. However, it gives almost the same R-square value (drop by 0.1) as the proposed one. For a predicting equation development, it is always preferable to use fewer independent variables, especially when the data set has limited observations. Thus, the proposed equation is adequate to encompass the effects rendered by the aggregate sources and/or gradations in this study.

The predicted ITS values from the proposed equation are plotted against the measured/experimental ITS values in Figure 6.8. Overall, the data are scattered on both sides of the line of equality.

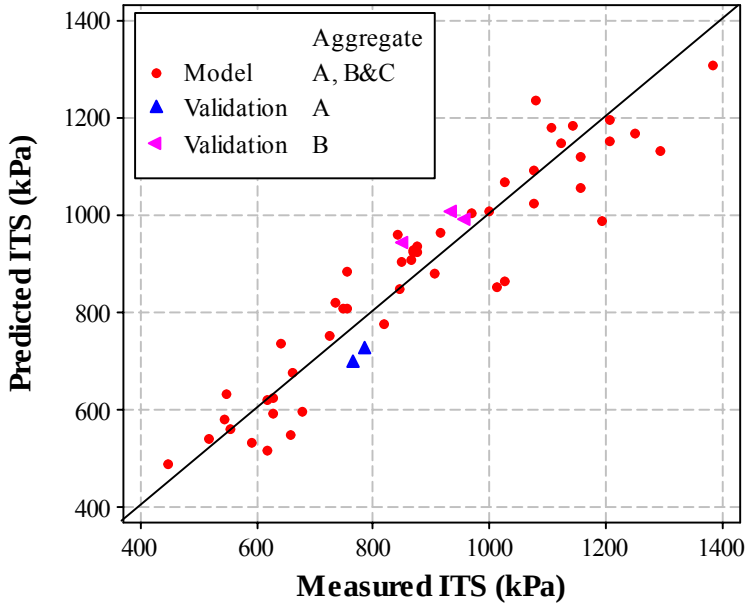

Figure 6.8 Measured Vs. Predicted ITS

In Figure 6.9, Equation 6.1 was used to predict the ITS values for different scenarios. The 95% confidence intervals and the prediction intervals are plotted in the figures, so that the variability level of the response variable can be perceived. In Figure 6.9 (a), the binder content is 5.3% and the air voids content is the independent variable for the response variable. In Figure 6.9 (b) and (c), the binder content is the independent variable and the air voids contents are 4% and 7%, respectively.

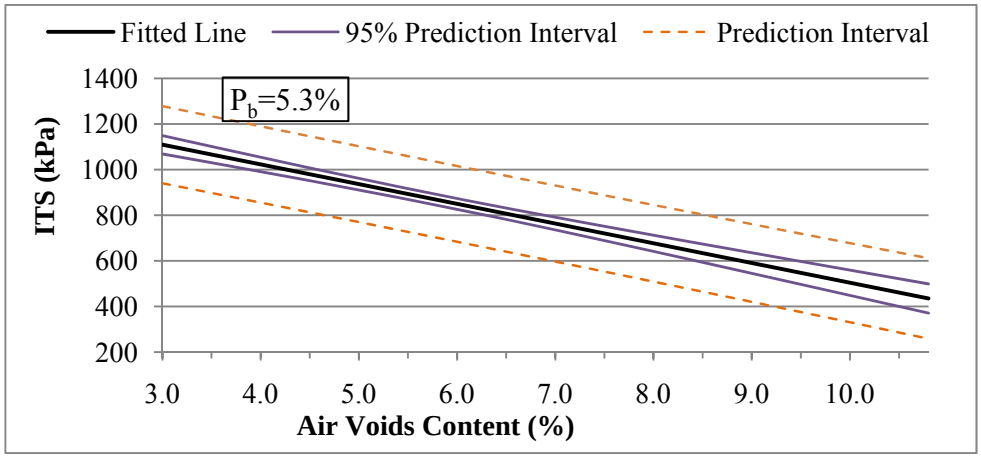

(a)

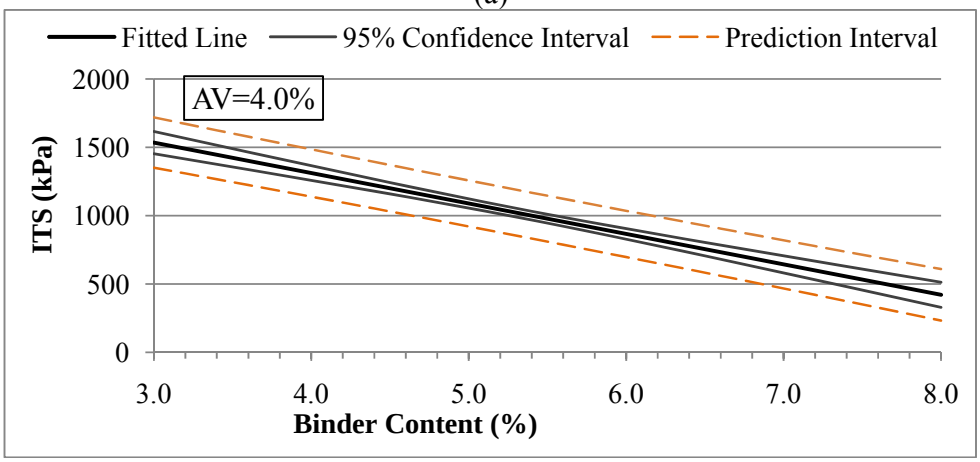

(b)

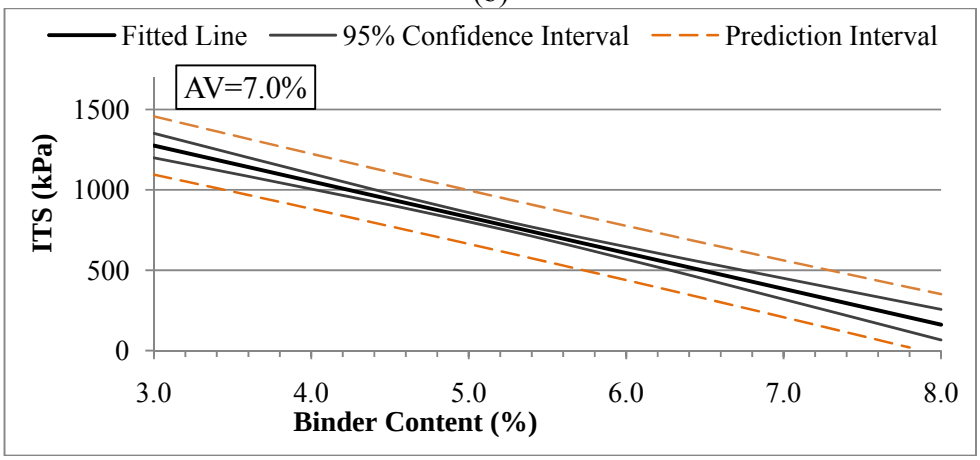

(c)

Figure 6.9 Rut depth Prediction Using Eq 6.1: (a) BC=5.3%, AV=Independent Variable; (b) AV=4%, BC=Independent Variable; (c) AV=7%, BC=Independent Variable

For the purpose of validating the dry ITS model (Eq. 6.1), data from another researcher were used. The validation mixtures were Type B mixtures with the same binder grade as the mixtures used to develop the model, but from a different crude source. The aggregate sources of the validation mixtures were aggregates A and B, but the gradations were slightly different. The dry ITS results of the validation mixes were plotted in Figure 6.8 along with the model data set. The validation data points were distributed evenly along the equality line and within the variation range of the model data, which indicates that the model can be applied to other mixtures with similar gradations and binder properties.

DEFORMATION MODEL

The same regression analysis was conducted on deformation values. As discussed in the previous section, a set of parameters was tried and introduced to the equation to relate the effects of asphalt binder and the aggregate gradations to the deformation performance. For the component of asphalt binder, effective binder content and binder content by volume were tried. None of them could further maximize the adjusted R-square value for the data set. The proposed deformation regression equation is shown below in Eq 6.2. The scatter plot of measured and predicted deformation is presented in Figure 6.10.

$$\text{Deformation} = -0.515 + 0.462P_b + 0.175AV \qquad \text{(Eq 6.2)}$$

Where Deformation, in millimeters;

P_b = Binder Content by weight, in percent;

AV= Air Voids content, in percent.

The R-square value for Eq 6.2 is 0.545; it suggests a fair predictive relationship between the response variable and independent variables. Nonetheless, such a relationship may reveal the nature of this matter: their quantitative relationship is not as reliable as for ITS. On the other hand, it provides insight into the qualitative influence of the fundamental parameters on deformation.

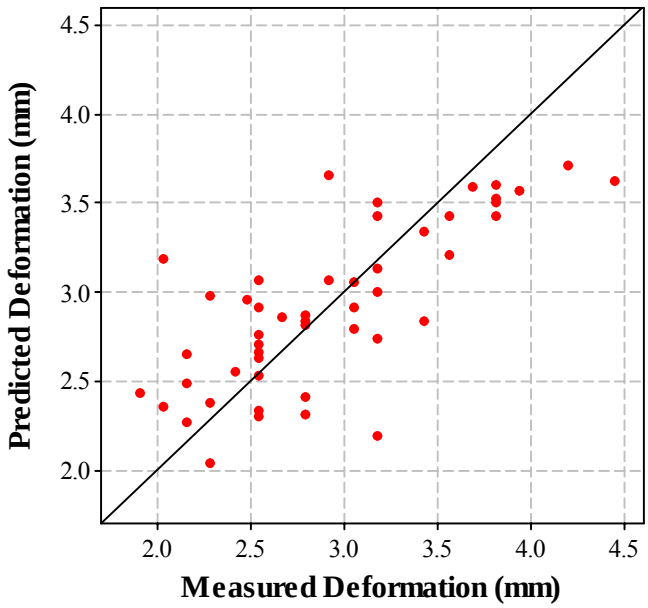

Figure 6.10 Scatter Plot of Predicted vs. Measured Deformation

Given Equations 6.1 and 6.2, one unique relationship between ITS and deformation can be concluded. In Eq 6.1 the coefficient for binder content has a negative value. That is, as the binder content increases for the asphaltic mixtures, the ITS value will decrease accordingly. In Eq 6.2 the coefficient for binder content has a positive value—as the binder content increases for the asphaltic mixtures, the deformation value will increase accordingly. Both properties of a mixture are closely associated with the mixture's unique binder content. An approximate inverse

relationship can be expected with respect to binder content as a varying parameter for HMA mixtures.

The scatter plot of the data in this study is presented in Figure 6.11. Not only can the inverse relationship be perceived, but also a wide range of data scatter can be observed. The data scatter might be due to the various combinations of binder content and air voids content in the samples; the complex interaction effects between them lead to a high level of complexity in the presentation of ITS and deformation relationships.

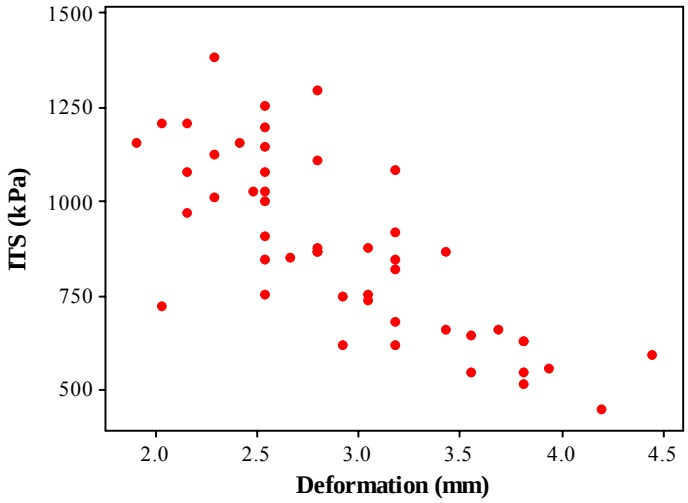

Figure 6.11 Scatter Plot of ITS vs. Deformation

If the data are simply fit with a linear line, the regression equation is presented in Eq 6.3, with an adjusted R-square value of 0.586. A curvilinear regression, such as logarithmic transformation of the ITS values, would produce a slightly higher R-square value. However, identifying the general inverse relationship between ITS and deformation is much more meaningful than trying to define the precise relationship between them. In other words, without addressing the relationship from the perspective of mix fundamental properties, any better

regression equations would not suggest better solutions, even though the R-square value is improved; hence, a quantitative relationship is not necessary. Therefore, with such wide data scatter, the presented linear regression equation (Eq 6.3) is intended only for reference.

Deformation (mm) = 4.67 - 0.00198 ITS (kPa) (Eq 6.3)

FRACTURE ENERGY MODEL

According to Eq 3.2, the area under the ITS-deformation curve up to the peak ITS is needed to calculate the fracture energy. Hence, both ITS and deformation will be two integral parts in determining a sample's FE value. The modeling process of FE was conducted at two levels: (1) using IDT test results, namely ITS and deformation and (2) the fundamental mix properties, namely binder content and air voids content. The regression equations for these two methods are presented below as Eq 6.4 and Eq 6.5, with the adjusted R-square of 0.825 and 0.353, respectively.

$$FE = - 1545 + 2.57\ ITS + 721\ Deformation \quad \text{(Eq. 6.4)}$$

$$FE = 4847 - 279\ P_b - 96.0\ AV \quad \text{(Eq. 6.5)}$$

Where FE = Fracture Energy, N/m

In Eq 6.4, the fracture energy is highly correlated to ITS and deformation, as evidenced by the high R-square value. Because the ITS and deformation can be affected by a number of factors, including the fundamental mix properties, such as binder content and air voids content of a mix, they can be viewed as "secondary" parameters. The determination of their values requires mechanical testing, where additional investment in equipment is needed, as well as the time and other resources associated with the test itself.

By contrast, the parameters in Eq 6.5 are "primary"; when it comes to engineering property prediction, they are good choices for predicting response variables. However, the reliability of the equation is very low, as indicated by the low R-square value. Given the fact that the deformation is a very important component in calculating fracture energy, this low reliability is partially because the relationship between these two independent variables and deformation is very complicated; a simple linear regression predicting equation is not reliable enough, as evidenced by Eq 6.2.

To address the complexity of the relationship between fracture energy and these two fundamental (or "primary") parameters, higher orders of the parameters (such as P_b^2, AV^2, or AV^3) and interaction terms would be introduced into the predicting equation. This will undoubtedly address the relationship better theoretically, or in other words, the residual errors in the regression analysis will be greatly reduced. However, it may be not be practically viable, because when the experimental observations are limited, the effectiveness of the equation would not increase as more variables are introduced into the equations.

CONTOUR PLOT OF FE

An alternative solution to get the quantitative relationship between fracture energy and the "primary" parameters through regression analysis was tried using a contour plot method. Within the capacity of the computerized statistical analysis program (Minitab), a contour plot can be easily drawn. It is presented in Figure 6.12.

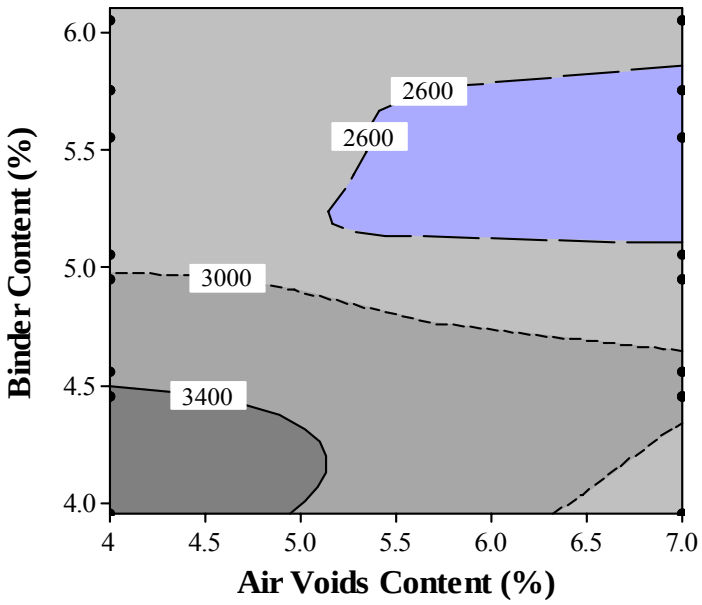

Figure 6.12 Contour Plot of Fracture Energy

Figure 6.12 shows a very complex pattern for binder and air voids to express fracture energy, thereby no reliable quantitative regression models could effectively capture the unique characteristics in their relationship. For air voids content, the general trend is that as air voids content increases with an increase in binder content, the fracture energy decreases.

In the range of AV from about 5.0 to 7.0 percent, there is a low value "island" area where the fracture energy is less than 2600 N/m. In that AV range, when the binder content increases, the fracture energy decreases. In the binder content range from about 5.0 to 6.0 percent, the FE reaches the "island". After that, with the binder content further increasing, the FE increases from the low value "island".

The middle range of binder content (5.0-6.0%) could define a "transition zone" in terms of the asphalt mixture's property. Lower binder content would result in a higher ITS value, being much stiffer. From the dissipated energy standpoint, the stiffer mixes may be susceptible to fatigue cracking under repeated loading because of their low capacity for deformation. The mixture stiffness relationship with fatigue performance was discussed in Chapter II. In addition, lower binder content means lower healing capability; hence, healing microcracks caused by other mechanisms would be negatively affected. In the higher binder content range, the deformations tend to be greater and play a large role in determining the FE outcomes. However, the mixtures will have lower stability as manifested by the lower ITS values, and might be more susceptible to rutting. The transition zone binder content could be established as a "binder content window" for mixture optimization in the mix design process, where the "trade-off" on the binder content would be made in that window.

From the perspective of robust design for HMA material, this finding could open a door to effectively engineer a HMA mixture with better engineering properties. For example, the proposed "binder content window" could be a starting point for a mix design. From there, the VMA value could be back calculated so as to be able to accommodate the binder content; the final step is to find an aggregate gradation which will yield a desired VMA value. With the application of the principles of robust design, this could be a "novel" but sound method to "revolutionize" the current mix design logic, where too many factors can be affecting the final binder content, including the compaction gyration number, the design air voids content, etc.

CHAPTER VII: MOSITURE SUSCEPTIBILITY RESULTS AND DISSCUSIONS

This chapter summarizes the results of the investigation into the effects of construction variability in binder variation and gradation change on the moisture susceptibility of HMA mixes by means of the ITS and TSR of the wet-conditioned samples.

TENSILE STRENGTH FOR WET-CONDITIONED SAMPLES

The ITS test results of wet-conditioned samples are presented in Figure 7.1. First, even though there is varied performance among the treatment combinations, all the treatments pass the threshold value, 448kPa, as specified by the SCDOT and other state DOT specifications, regardless of the binder content or the aggregate gradation. Secondly, from the figure, it can be observed that overall, the wet ITS values of aggregate B are the highest, followed by aggregate C with the second highest ITS values while aggregate A had the lowest ITS values. The pattern is similar to the ITS values of dry samples among the three aggregates as discussed in Chapter VI (Figure 6.2(a)).

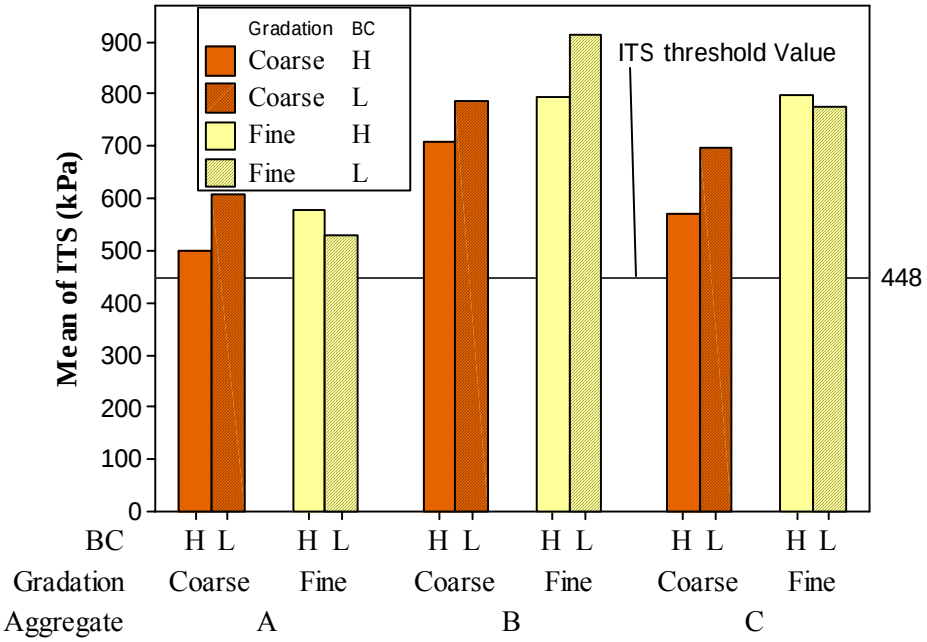

Figure 7.1 ITS Values of Wet-conditioned Samples

ITS STRENGTH MODEL FOR WET CONDITIONED SAMPLES

The statistical regression model for wet ITS is given in Eq 7.1. The R-square value for this regression analysis is 0.904. The scatter plot with measured and predicted values of wet ITS is presented in Figure 7.2. This ITS model can be used in conjunction with Eq 6.1 developed for dry ITS samples to predict the TSR value of similar HMA material without physically conducting the moisture susceptibility test.

$$ITS_{wet} = 1030 - 155\ P_b + 67.3\ AV \qquad \text{(Eq 7.1)}$$

Where ITS_{wet} = Wet Indirect Tensile Strength, in kPa;

P_b = Binder Content by weight, in percent;

AV = Air Voids content, in percent.

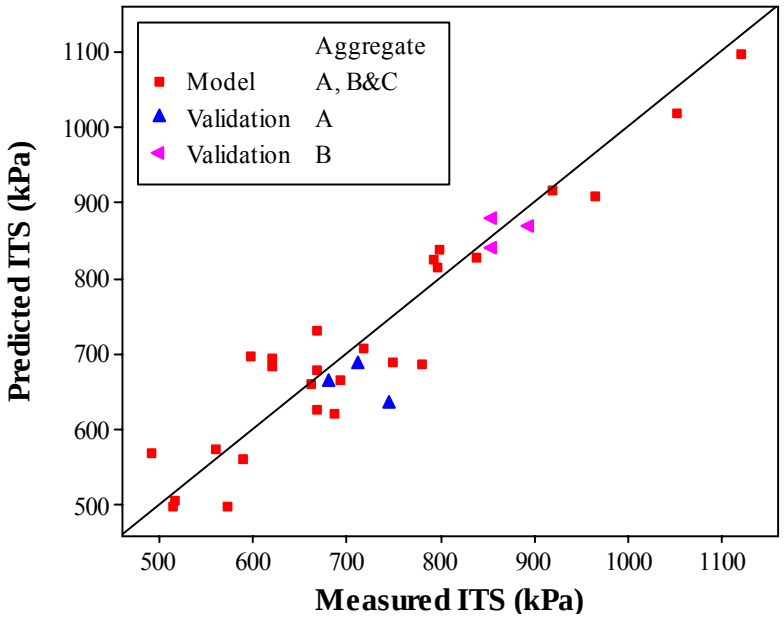

Figure 7.2 Predicted vs. Measured ITS for Wet Samples

To validate the ITS model for the wet samples, an additional data were used as mentioned in the dry ITS model validation. The validation data set was plotted in Figure 7.2 and it also shows that the new data fit well within the variation band of the data used to develop the model.

TSR RESULTS

The TSR results are presented in the Table 7.1, and Figure 7.2. The threshold value for TSR to differentiate a HMA material's moisture susceptibility is set at 0.85 according to the SCDOT specification. Out of the twelve mixtures, two do not meet the requirement; both of them have a fine gradation with lower binder content level (aggregates A and C). This indicates that when these two factors (fine gradation and low binder content) coincide; the chances the sample will fail increase.

Table 7.1 TSR Results

Aggregate Sources	Coarse-Graded		Fine-Graded	
	OBC+0.25%	OBC-0.25%	OBC+0.25%	OBC-0.25%
A	0.94	0.85	1.19	0.79
B	0.95	0.87	0.88	0.90
C	0.90	1.02	0.96	0.80

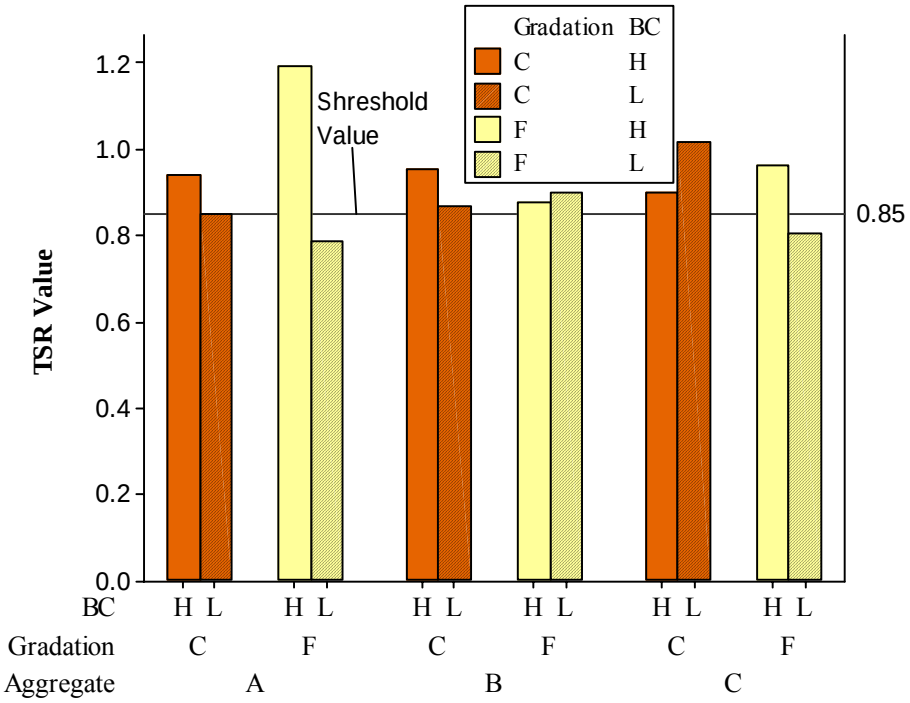

Figure 7.3 Graphic Illustration of TSR Results

Single sample ANOVA analysis was conducted to identify which factors, when varied slightly, can significantly affect TSR values. The results showed that the effect due to binder content difference between the two levels is statistically significant. By contrast, the effects of aggregate source and gradation treatment are not significant. The ANOVA table is given in

Table 7.2. It should be noted that single sample ANOVA analysis is a very subjective statistical analysis and the interpretation of the results is often subject to the interpreter's judgment.

Table 7.2 Single Sample ANOVA Analysis Table for TSR

Factor	DF	Seq SS	Adj SS	Adj MS	F value	P value	Significant?
Aggregate	2	0.004	0.004	0.002	**		No
Gradation	1	0.000	0.000	0.000	**		No
BC	1	0.030	0.030	0.030	22.871	0.017	Yes
Aggregate*Gradation	2	0.015	0.015	0.007	5.685	0.095	No
Aggregate*BC	2	0.034	0.034	0.017	13.032	0.033	Yes
Gradation*BC	1	0.020	0.020	0.020	15.515	0.029	Yes
Aggregate*Gradation*BC	2	0.028	0.028	0.014	10.655	0.043	Yes
Error	3	0.004	0.004	0.001			
Total	11	0.004					

The TRS values for a mixture can be predicted by using the ITS predictive models mentioned early in this study. The dry ITS value of the samples were predicted by using the dry ITS model (Eq 6.1), and the ITS values for the wet conditioned samples were predicted by using Eq. 7.1. The predicted TSR was then calculated by dividing Eq 7.1 by Eq 6.1. The results are presented in Table 7.3 and Figure 7.4. All of the predicted TSR values are lower than 1.0, which is reasnable, because theoritically the HMA mixtures will lose some strength capacity after wet conditioning. However, the experimentally obtained TSR for two mixtures were higher than 1.0 (Table 7.3). In Figure 7.4, the predicted TSR values are equally distributed along the two sides of the equality line. Also plotted in Figure 7.4 are the TSR results of the validation samples that

were predicted with Eqs 6.1 and 7.1. This validation data set also scatters along the equality line within the variability of the data used to develop the model.

Table 7.3 Comparison between Experimental and Predicted TSRs

Aggregate	Binder Content	Experimental TSR	Predicted Dry ITS (kPa)	Predicted Wet ITS (kPa)	Predicted TSR
B	3.95	0.90	1063	889	0.84
B	4.45	0.88	952	811	0.85
B	4.45	0.87	952	811	0.85
B	4.95	0.95	840	734	0.87
A	6.25	0.94	550	532	0.97
A	5.75	0.85	662	610	0.92
A	6.25	1.19	550	532	0.97
A	5.75	0.79	662	610	0.92
C	6.05	0.90	595	563	0.95
C	5.55	1.02	707	641	0.91
C	5.05	0.96	818	718	0.88
C	4.55	0.80	930	796	0.86

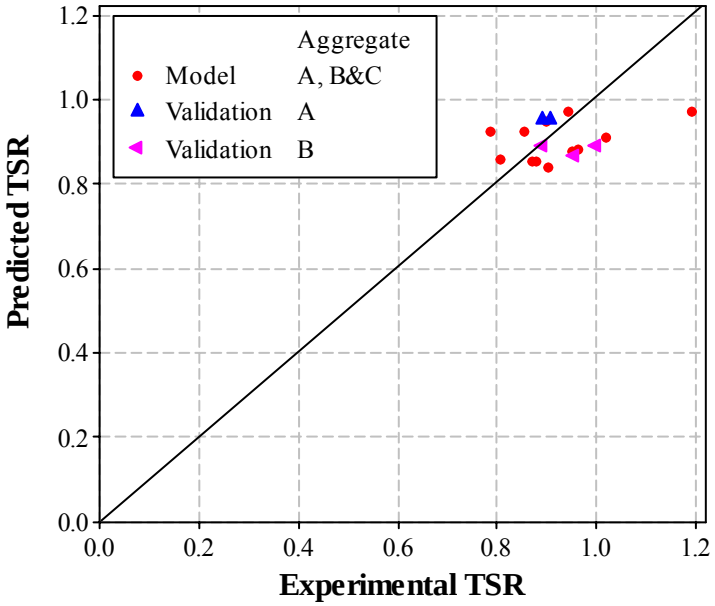

Figure 7.4 Predicted vs. Experimental TSR Values

DEFORMATION AND FRACTURE ENERGY RESULTS

The results of deformation and fracture energy are presented in Figure 7.5 and Figure 7.6, respectively. Since the intention of the experiment is to obtain the strengths of the wet-conditioned samples, the performance of these samples for deformation and fracture energy are not the focus. Moreover, in this case no apparent pattern with respect to the gradation and binder content treatment can be observed.

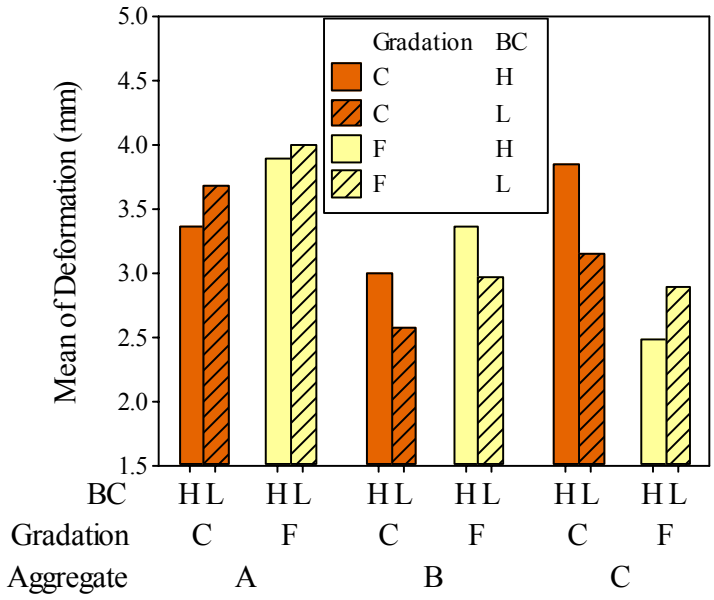

Figure 7.5 Deformation Results for Wet-conditioned Samples

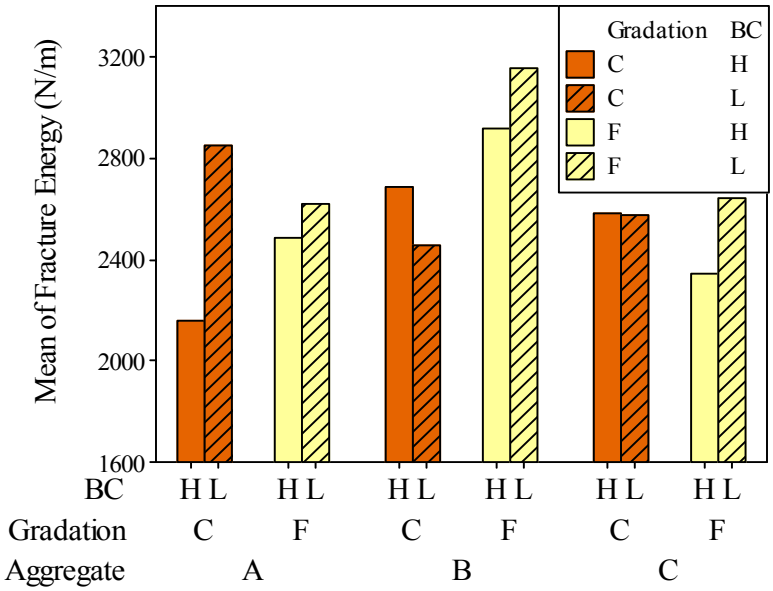

Figure 7.6 Fracture Energy Results for Wet-conditioned Samples

CHAPTER VIII: SUMMARY, CONCLUSIONS AND RECOMMENDATIONS

This research identified aggregate gradation, binder content and air voids content as three fundamental mixture parameters to underpin a HMA material's performance properties. Even though highway agencies might be using a different set of parameters (such as VMA) to calculate pay factors, what these parameters are trying to capture is the variation in the fundamental mixture properties to control the construction quality. In the Introduction chapter, an example was given to illustrate that the assigned PFs for a pavement are different between the two states, or the same PF could be assigned to two pavements with different density. Without input from HMA material performance properties, especially the influence of the variations in the three fundamental parameters, it is difficult to answer "which one, if any is better?" Therefore, the purpose of this research was to investigate the effects of the fundamental parameters on asphalt concrete properties in the context of construction variations.

Three aggregate sources and one PG64-22 asphalt binder were utilized in the study. The evaluation of influences of the fundamental parameters on the HMA performance properties covers three important facets of HMA mixtures, specifically permanent deformation (or rutting), IDT tensile properties (cracking), and moisture susceptibility (stripping). Lab investigation was carried out because not only can the factors of interest be controlled precisely, but also other factors that might introduce variability in a field study would be eliminated or maintained to a certain level in the lab setting.

The fundamental parameters' effects on the HMA material performance were successfully separated for rutting and indirect tensile cracking characteristics. Additionally, the possible

factor interaction effects were also evaluated. Further, the factors that can influence the HMA mixture performance were combined into one picture; multivariate linear models were developed to summarize the prediction relationship between the test properties and the fundamental parameters. The conclusions and findings reached based on the scope of this study are divided into three pavement performance aspects in the following section.

CONCLUSIONS/ FINDINGS FOR RUTTING PERFORMANCE

The conclusions/findings that were reached in the rutting performance evaluation are given as follows:

1) Of the four experimental treatment factors in this study, the aggregate source was found to have no significant effect on the rutting performance. By comparison, the other three factors (gradation, BC, AV) are significant to the HMA rutting performance. Moreover, the main and interaction effects between the three factors are remarkably consistent for the two aggregates in the study.

2) The air voids content effect on rutting performance is statistically significant. Rut depths at 4% air voids content are less than those at 7% air voids. This indicates that higher mat density is beneficial for rutting performance.

3) The experiment showed that the binder content variation evaluated in this study has a significant effect on the rutting performance of the mixtures. The mixes with lower binder content showed better rutting performance, indicating that even deviations within a small range (±0.25%) of binder content could significantly have an effect on rutting performance.

4) Gradation has a critical yet complex effect in regard to rutting: gradation effect is aggregate-specific if simply using “coarse-”or “fine-” gradation to classify the gradation. The

AASHTO classification is not adequate in capturing the effect brought about by the gradation types. An effort to find a new quantitative easy-to-use gradation effect indicator was made, and the term “normalized absorbed asphalt” or “normalized absorbed asphalt*SSA” is proven adequate to evaluate the gradation effect on rutting performance. It is suggested that these parameters could be used to predict and compare an aggregate rutting performance for gradation optimization.

5) The 2-way interaction effects between the three parameters were proven to not be statistically significant, which indicates that when two of the parameters are changing, the effect of each of the individual factor is additive.

6) The 3-way interaction effect is statistically significant in this study. This means that while 2-way interaction effects are additive, adding the change in another factor will not necessarily have an effect on rutting. However, there is a pattern on the 3-way interaction. When a sample has 2 factors that lead to increased or decreased rutting resistance, the introduction of the variation in the third factor would not be statistically significant; the rutting result will maintain at the same excellent or poor level. When a sample has one factor that leads to increased rutting resistance and one factor that leads to decreased rutting resistance, the introduction of the variation in the third factor would statistically have an effect on the result; if the third factor is on the favorable rutting resistance end, rutting resistance can be expected to improve, and vice versa. This observation could have a practical implication: for mixes to have good rutting performance, at least two factors should be in their favorable ends, and mixes with a combination of two or more factors at the adverse ends should be avoided.

7) A series of predictive statistical models were developed and validated to provide a tool for asphalt technologists to help understand and compare the HMA pavement rutting performance by using simple volumetric parameters. The model development process revealed that the volumes of effective binder content have a better correlation to rutting performance than the volumes of total binder content, or any of the binder contents by weight.

CONCLUSIONS/ FINDINGS FOR INDIRECT TENSILE CRACKING

1) Fine-graded mixtures, in general, are better than coarse-graded in ITS and fracture energy performance, but have smaller deformation values. However, only the ITS is statistically proven to be significantly different, the effects of deformation and fracture energy are not significant.

2) The 0.5% decrease in binder content treatment can increase ITS and fracture energy value, and decrease the deformation; statistical analysis shows that the variation by 0.5% in binder content is enough to produce significant effects on the ITS and deformation value, but no significant effect on fracture energy.

3) Air voids content is an important factor. Increasing density by 3% (AV from 7% to 4%) can make a significant difference in the tensile properties: ITS and fracture energy will increase, while the deformation will decrease.

4) No 2-way or 3-way interaction effects between the three mixture parameters were found in this study, indicating the individual parameter effects are additive when multiple parameters are coexisting.

5) The modeling process revealed that the binder content (% by weight) is a comprehensive parameter for predicting the ITS value; it encompasses all the effects on the ITS value coming

from the combinations of gradations and aggregate sources, and the binder content variation due to production variability.

6) From the contour plot of the fracture energy value, a binder content window of about 5% to 6% is proposed to produce a HMA mixture that is not too stiff or too unstable.

CONCLUSIONS/ FINDINGS FOR MOISTURE SUSCEPTIBILITY

1) Binder content is the only main factor that was found to be statistically significant on the TSR value, an increase in binder content can lead to an increase in the TSR value.

2) The statistical models have a strong fit for the ITS values for the wet-conditioned samples. In combination with the model developed for dry ITS sample, the TSR value of a HMA sample could be predicted.

RECOMMENDATIONS

Based on the findings from this study in the rutting, indirect tensile cracking, and moisture susceptibility assessment, the following recommendations are warranted to further build upon these related topics:

- More attention should be given to the "absorbed asphalt content" and "specific surface area" by agencies. This data should be included in the contractors' mix design report for further collective study.
- Field trial pavement segments could be constructed to evaluate the influences of the three studied parameters (gradation, air voids, and binder content) on HMA pavement, where field compactability can be also studied at the same time.

- The fatigue cracking characteristic under repeated loading should be further evaluated to investigate the fundamental parameters' effects on fatigue cracking, and possibly establish the cracking characteristic between the indirect tensile test and fatigue test under repeated loading.
- Binder rheological parameters could be added to increase the applicability of the rutting or ITS predicting models by incorporating various asphalt binders in an extended study. Also, the aggregates or binders from other states can be studied and integrated into the models.

CONTRIBUTIONS AND APPLICATIONS

To summarize, this dissertation is a study of asphalt mixture properties on performance properties, conducted uniquely from the perspective of construction variation. The three mixture properties included aggregate gradation, binder content, and air voids content, which are three of the most important considerations in engineering and producing quality mixture and pavement products. The properties that were evaluated spanned three critical performance properties of HMA materials: rutting, tensile cracking, and moisture susceptibility. All aspects were examined with the three mixture parameters in a holistic way. Previous studies have not provided such a wide scope in one study. Therefore, the arguments made in a narrow scope may be valid, but they may not be warranted when considered in a boarder scope, hence limiting its applicability. Readers of this study will gain comprehensive understanding on the effects of mixture properties on performance properties. The methods used in this study to develop quantitative equations could be very useful tools for HMA technologists to understand HMA material behavior and properties, and they can be used directly or as a framework to develop more robust models, where other parameters such as asphalt binder rheological properties are incorporated.

Some of the findings and conclusions that were reached from this study had not been found in previous studies, while some are in agreement with other studies. Take binder content as an example. In this study, the binder content variation was set within a small range (± 0.25% from the OBC) to bring the study in line with the level of construction variation in the field. Still, meaningful conclusions were reached within the small binder variation range. For rutting, the effective binder content should be looked at rather than the total binder content and the volume content is more relevant in predicting rutting performance than the weight content. The absorbed binder content was found to affect the ultimate aggregate surface characteristic, which further affects the shear resistance of the mix due to the internal friction of an aggregate structure. For tensile cracking, the total binder content can describe the ITS values well, without the need to further break down into effective binder content and absorbed binder content. For rutting, an excessive binder content could be created by variations in gradation, as a mix with a different gradation will also have a different VMA thus the capacity for accommodating the binder content is changed. In cracking, gradation deviation did not have a significant effect. This difference between rutting and tensile cracking indicates the difference in the influence of gradation variation in HMA production. Moreover, in the tensile cracking analysis, a "binder content window" is recommended based on this study, which may shed new light on the methodology of optimizing a mixture design.

Some of the highlights from this study, in conjunction with relevant knowledge from previous studies are summarized in the following table. The influences of the fundamental mixture parameters are differentiated at a mix design level and at a construction variation level, in which

the binder content deviation is assumed to be a small range. It is the author's hope that this summary will be helpful to asphalt practitioners and policy makers.

Table 8.1 A Summary of the Influence of Fundamental Mixture Parameters

	Shear Resistance (Rutting)	Tensile Strength (ITS)	Fracture Energy
Gradation (in design)	Through Normalized absorbed Binder Content	Through OBC	-
Gradation (variation in construction)*	Varied effects	No effect	No effect
BC (variation in construction) ↑	↓	↓	No significant
BC (OBC, in design) ↑	Content is related to VMA, careful about excessive BC, ↓	↓	A level of BC defines transition zone
AV (variation in construction) ↓	↑	↑	↑
AV (in design) ↓	↑ in OBC, mixture properties change through the binder content		

*Deduced from analysis for the hypothetical scenarios in this study.

Lastly, there are some statistical analysis methods that can be borrowed by other researchers or practitioners, especially on constructing a meaningful experimental design and how to deal with variability introduced by the air voids content variation.

APPENDICES

APPENDIX A: BINDER VOLUME AND WEIGHT CONVERSION

Appendix A-1: Conversion Table for Aggregate Effective Specific Gravity (ESG): 2.70

Air Voids Content (%)	Binder Content (%)					
	4.00	4.50	5.00	5.50	6.00	6.50
2.5	2.377	2.360	2.342	2.325	2.308	2.291
3.0	2.365	2.347	2.330	2.313	2.296	2.280
3.5	2.353	2.335	2.318	2.301	2.284	2.268
4.0	2.341	2.323	2.306	2.289	2.273	2.256
4.5	2.329	2.311	2.294	2.277	2.261	2.244
5.0	2.316	2.299	2.282	2.265	2.249	2.233
5.5	2.304	2.287	2.270	2.253	2.237	2.221
6.0	2.292	2.275	2.258	2.242	2.225	2.209
6.5	2.280	2.263	2.246	2.230	2.213	2.197
7.0	2.268	2.251	2.234	2.218	2.202	2.186
7.5	2.255	2.239	2.222	2.206	2.190	2.174
8.0	2.243	2.226	2.210	2.194	2.178	2.162
8.5	2.231	2.214	2.198	2.182	2.166	2.150
9.0	2.219	2.202	2.186	2.170	2.154	2.139
9.5	2.207	2.190	2.174	2.158	2.142	2.127
10.0	2.194	2.178	2.162	2.146	2.131	2.115

Appendix A-2: Conversion Chart for Aggregate Effective Specific Gravity (ESG): 2.70

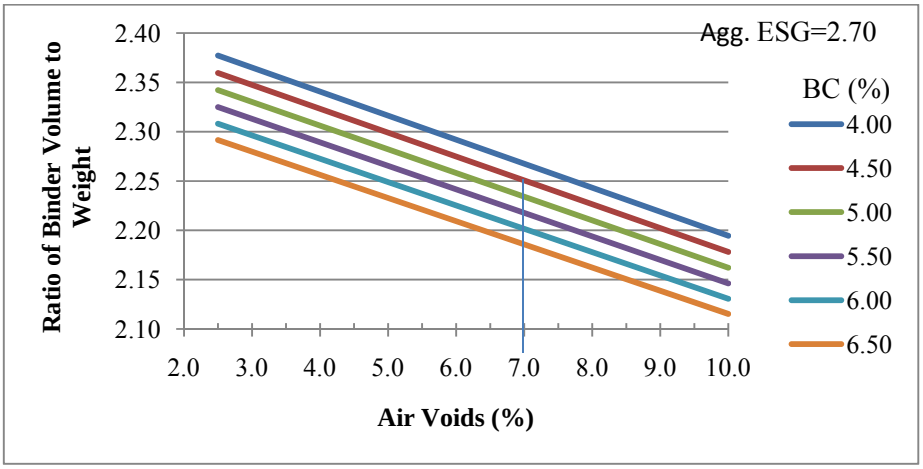

Appendix A-3: Conversion Table for Aggregate Effective Specific Gravity (ESG): 2.65

Air Voids Content (%)	Binder Content (%)					
	4.00	4.50	5.00	5.50	6.00	6.50
2.5	2.337	2.321	2.304	2.288	2.271	2.255
3.0	2.325	2.309	2.292	2.276	2.260	2.244
3.5	2.313	2.297	2.280	2.264	2.248	2.232
4.0	2.302	2.285	2.268	2.252	2.236	2.221
4.5	2.290	2.273	2.257	2.241	2.225	2.209
5.0	2.278	2.261	2.245	2.229	2.213	2.198
5.5	2.266	2.249	2.233	2.217	2.201	2.186
6.0	2.254	2.237	2.221	2.205	2.190	2.174
6.5	2.242	2.225	2.209	2.194	2.178	2.163
7.0	2.230	2.213	2.198	2.182	2.167	2.151
7.5	2.218	2.202	2.186	2.170	2.155	2.140
8.0	2.206	2.190	2.174	2.158	2.143	2.128
8.5	2.194	2.178	2.162	2.147	2.132	2.117
9.0	2.182	2.166	2.150	2.135	2.120	2.105
9.5	2.170	2.154	2.139	2.123	2.108	2.093
10.0	2.158	2.142	2.127	2.112	2.097	2.082

Appendix A-4: Conversion Chart for Aggregate Effective Specific Gravity (ESG): 2.65

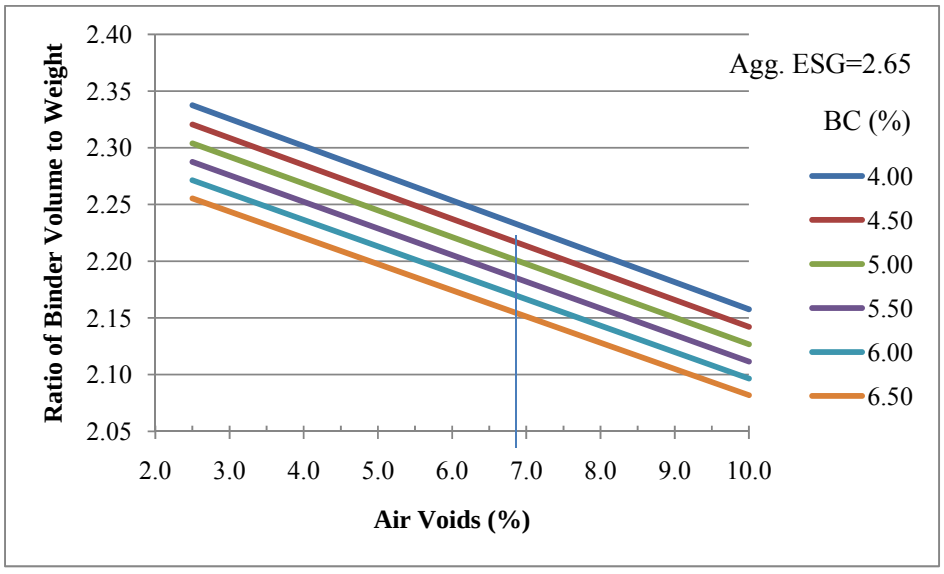

APPENDIX B: AGGREGATE GRADATIONS

Appendix B-1: Gradation Table for APA Tests

Standard Sieve	Mesh Size (mm)	Percent Passing (%)			
		Aggregate A		Aggregate B	
		Fine-Graded	Coarse-Graded	Fine-Graded	Coarse-Graded
1"	25	100.0	100.0	100.0	100.0
3/4"	19	100.0	100.0	100.0	100.0
1/2"	12.5	95.0	91.0	96.0	95.0
3/8"	9.5	81.0	78.0	87.0	78.0
No. 4	4.75	60.0	60.0	60.0	49.0
No. 8	2.36	40.0	34.0	40.0	29.0
No.16	1.18	33.0	22.0	30.0	20.0
No. 30	0.6	23.5	16.0	22.0	14.0
No. 50	0.3	15.0	11.5	16.0	9.0
No. 100	0.15	8.0	8.0	8.0	6.5
No. 200	0.075	4.0	4.0	4.0	4.0
Lime*		(1.0)	(1.0)	(1.0)	(1.0)

* Lime is part of the gradation passing No. 200 sieve size.

Appendix B-2: Gradation Table for IDT Tests

Standard Sieve	Mesh Size (mm)	Percent Passing (%)					
		Aggregate A		Aggregate B		Aggregate C	
		Fine-Graded	Coarse-Graded	Fine-Graded	Coarse-Graded	Fine-Graded	Coarse-Graded
1"	25	100	100.0	100.0	100.0	100.0	100.0
3/4"	19	99.0	99.0	100.0	100.0	99.8	99.8
1/2"	12.5	93.4	92.4	96.0	95.0	96.5	96.6
3/8"	9.5	87.0	85.1	87.0	78.0	89.0	87.1
No. 4	4.75	55.7	50.1	60.0	49.0	63.8	53.4
No. 8	2.36	39.7	32.9	40.0	29.0	43.8	32.8
No.16	1.18	-	-	30.0	20.0	30.0	22.2
No. 30	0.6	24.4	20.2	22.0	14.0	22.0	16.4
No. 50	0.3	-	-	16.0	9.0	14.9	11.2
No. 100	0.15	6.7	5.7	8.0	6.5	8.6	6.8
No. 200	0.075	3.3	3.3	4.0	4.0	4.5	3.8
Lime*		(1.0)	(1.0)	(1.0)	(1.0)	(1.0)	(1.0)

* Lime is part of the gradation passing No. 200 sieve size.

APPENDIX C: LINEAR CONTRASTS CONSTRUCTION FOR 2^{4TH} FACTORIAL DESIGN

Appendix C-1: Linear Contrasts Table

	Contrasts											
	A	B	C	D	AB	AC	BC	ABC	ABD	ACD	BCD	ABCD
(1)	-	-	-	-	+	+	+	-	-	-	-	+
a	+	-	-	-	-	-	+	+	+	+	-	-
b	-	+	-	-	-	+	-	+	+	-	+	-
ab	+	+	-	-	+	-	-	-	-	+	+	+
c	-	-	+	-	+	-	-	+	-	+	+	-
ac	+	-	+	-	-	+	-	-	+	-	+	+
bc	-	+	+	-	-	-	+	-	+	+	-	+
abc	+	+	+	-	+	+	+	+	-	-	-	-
d	-	-	-	+	+	+	+	-	+	+	+	-
ad	+	-	-	+	-	-	+	+	-	-	+	+
bd	-	+	-	+	-	+	-	+	+	+	-	+
abd	+	+	-	+	+	-	-	-	+	-	-	-
cd	-	-	+	+	+	-	-	+	-	-	-	+
acd	+	-	+	+	-	+	-	-	-	+	-	-
bcd	-	+	+	+	-	-	+	-	-	-	+	-
abcd	+	+	+	+	+	+	+	+	+	+	+	+

APPENDIX D: MINITAB STATISTICAL RESULTS—RUTTING

Appendix D-1: Preliminary ANOVA Results [Gradation (C vs. F)]

Factor	Type	Levels	Values
Aggregate	fixed	2	A, B
Gradation	fixed	2	F, C
AV	fixed	2	0.04, 0.07
BCc	fixed	2	H, L

Analysis of Variance for Rut Depth, using Adjusted SS for Tests

Source	DF	Seq SS	Adj SS	Adj MS	F	P
Aggregate	1	0.8237	0.7402	0.7402	1.05	0.311
Gradation	1	0.2336	1.2479	1.2479	1.78	0.190
AV	1	54.7324	54.4117	54.4117	77.45	0.000
BCc	1	10.3416	11.2989	11.2989	16.08	0.000
Aggregate*Gradation	1	18.6185	18.5370	18.5370	26.38	0.000
Aggregate*AV	1	4.0589	3.7792	3.7792	5.38	0.026
Aggregate*BCc	1	0.4213	0.4786	0.4786	0.68	0.414
Gradation*AV	1	0.0506	0.1351	0.1351	0.19	0.663
Gradation*BCc	1	0.0467	0.0135	0.0135	0.02	0.890
AV*BCc	1	0.0924	0.0399	0.0399	0.06	0.813
Aggregate*Gradation*AV	1	2.0664	1.7611	1.7611	2.51	0.121
Aggregate*Gradation*BCc	1	0.0571	0.1147	0.1147	0.16	0.688
Aggregate*AV*BCc	1	0.0480	0.0972	0.0972	0.14	0.712
Gradation*AV*BCc	1	0.1129	0.0332	0.0332	0.05	0.829
Aggregate*Gradation*AV*BCc	1	8.8564	8.8564	8.8564	12.61	0.001
Error	39	27.4000	27.4000	0.7026		
Total	54	127.9606				

S = 0.838191 R-Sq = 78.59% R-Sq(adj) = 70.35%

Appendix D-2: Analysis of Covariance for Rutting Assessment

Factor	Type	Levels	Values
Aggregate	fixed	2	A, B
Gradation	fixed	2	Bad, Good
BC	fixed	2	H, L

Analysis of Variance for Rut, using Adjusted SS for Tests

Source	DF	Seq SS	Adj SS	Adj MS	F	P
AV (covariance)	1	76.115	60.363	60.363	63.98	0.000
Aggregate	1	1.106	0.482	0.482	0.51	0.478
Gradation	1	14.554	16.025	16.025	16.99	0.000
BC	1	5.666	6.791	6.791	7.20	0.010
Aggregate*Gradation	1	1.469	1.597	1.597	1.69	0.200
Aggregate*BC	1	1.870	1.881	1.881	1.99	0.165
Gradation*BC	1	0.322	0.204	0.204	0.22	0.644
Aggregate*Gradation*BC	1	0.437	0.437	0.437	0.46	0.499
Error	46	43.399	43.399	0.943		
Total	54	144.939				

S = 0.971316 R-Sq = 70.06% R-Sq(adj) = 64.85%

Appendix D-3: Tukey's Multiple Comparisons for the 3-way Interaction

At 7% AV level

```
Source  DF      SS     MS     F      P
G & BC   3  13.703  4.568  6.56  0.002
Error   23  16.024  0.697
Total   26  29.727

S = 0.8347   R-Sq = 46.09%   R-Sq(adj) = 39.06%


                          Individual 95% CIs For Mean Based on
                          Pooled StDev
Level  N    Mean   StDev  ---+---------+---------+---------+------
BH     7  5.2798  0.8542                      (-------*-------)
BL     7  5.3587  1.0366                       (-------*-------)
GH     7  5.3991  0.7497                       (-------*--------)
GL     6  3.6355  0.6044  (-------*--------)
                          ---+---------+---------+---------+------
                           3.20      4.00      4.80      5.60

Pooled StDev = 0.8347
Note: BH=Bad Gradation & High BC; BL=Bad Gradation & Low BC;
      GH=Good Gradation & High BC; GL=Good Gradation & Low BC.
```

At 4% AV level

```
Source      DF      SS     MS      F      P
trt g & Bc   3  25.593  8.531  11.31  0.000
Error       24  18.106  0.754
Total       27  43.698

S = 0.8686   R-Sq = 58.57%   R-Sq(adj) = 53.39%


                          Individual 95% CIs For Mean Based on
                          Pooled StDev
Level  N    Mean   StDev  ------+---------+---------+---------+---
BH     7  4.5571  0.5740                          (------*-----)
BL     7  2.8803  1.1479          (------*------)
GH     7  2.3545  0.8017     (------*-----)
GL     7  2.1038  0.8531  (------*------)
                          ------+---------+---------+---------+---
                              2.0       3.0       4.0       5.0

Pooled StDev = 0.8686
Note: BH=Bad Gradation & High BC; BL=Bad Gradation & Low BC;
      GH=Good Gradation & High BC; GL=Good Gradation & Low BC.
```

Appendix D-4: Regression Analysis for Eq 5.5

The regression equation is

Rut = - 7.25 + 0.757 VTM + 0.619 Vbe + 1.01 $P_{ba,n}$

55 cases used, 1 cases contain missing values

Predictor	Coef	SE Coef	T	P
Constant	-7.253	2.287	-3.17	0.003
VTM	0.75716	0.08174	9.26	0.000
Vbe	0.6188	0.2268	2.73	0.009
Pba,n	1.0134	0.3295	3.08	0.003

S = 0.982031 R-Sq = 66.1% R-Sq(adj) = 64.1%

PRESS = 56.7100 R-Sq(pred) = 60.87%

Analysis of Variance

Source	DF	SS	MS	F	P
Regression	3	95.755	31.918	33.10	0.000
Residual Error	51	49.184	0.964		
Total	54	144.939			

Source	DF	Seq SS
VTM	1	76.115
Vbe	1	10.516
Pba,n	1	9.124

Appendix D-5: Regression Analysis for Eq 5.6

The regression equation is

Rut = - 6.10 + 1.58 Ln(VTM-2.8) + 0.779 Vbe + 0.277 ssa* $P_{ba,n}$

55 cases used, 1 cases contain missing values

Predictor	Coef	SE Coef	T	P
Constant	-6.103	2.064	-2.96	0.005
Ln(VTM-2.8)	1.5770	0.1605	9.83	0.000
Vbe	0.7793	0.2106	3.70	0.001
ssa* $P_{ba,n}$	0.27683	0.07514	3.68	0.001

S = 0.914031 R-Sq = 70.6% R-Sq(adj) = 68.9%

PRESS = 49.7587 R-Sq(pred) = 65.67%

Analysis of Variance

Source	DF	SS	MS	F	P
Regression	3	102.330	34.110	40.83	0.000
Residual Error	51	42.608	0.835		
Total	54	144.939			

Source	DF	Seq SS
Ln(VTM-2.8)	1	77.621
Vbe	1	13.369
ssa* $P_{ba,n}$	1	11.341

APPENDIX E: MINITAB STATISTICAL RESULTS—TENSILE CRACKING

Appendix E-1: Gradation Effects on ITS, Deformation, and Fracture Energy

```
Factor     Type   Levels  Values
Gradation  fixed       2  C, F
Block      fixed       6  AH, AL, BH, BL, CH, CL


Analysis of Variance for ITS, using Adjusted SS for Tests

Source     DF   Seq SS   Adj SS  Adj MS     F      P
Gradation   1   182373   173887  173887  5.14  0.028
Block       5  1002919  1002919  200584  5.93  0.000
Error      44  1488645  1488645   33833
Total      50  2673938


S = 183.937   R-Sq = 44.33%   R-Sq(adj) = 36.74%



Analysis of Variance for deformation, using Adjusted SS for Tests

Source     DF   Seq SS   Adj SS  Adj MS     F      P
Gradation   1   1.0800   1.0260  1.0260  3.81  0.057
Block       5   4.8239   4.8239  0.9648  3.58  0.008
Error      44  11.8569  11.8569  0.2695
Total      50  17.7608


S = 0.519111   R-Sq = 33.24%   R-Sq(adj) = 24.14%



Analysis of Variance for Fracture Energy, using Adjusted SS for Tests

Source     DF   Seq SS  Adj SS  Adj MS     F      P
Gradation   1    32.33   34.07   34.07  1.83  0.183
Block2      5   301.41  301.41   60.28  3.23  0.014
Error      44   820.12  820.12   18.64
Total      50  1153.86


S = 4.31731   R-Sq = 28.92%   R-Sq(adj) = 19.23%
```

Appendix E-2: Aggregate Effect on ITS, Deformation, and Fracture Energy

```
Factor     Type   Levels  Values
Aggregate  fixed       3  A, B, C
Block      fixed       8  C4%H, C4%L, C7%H, C7%L, F4%H, F4%L, F7%H, F7%L


Analysis of Variance for ITS, using Adjusted SS for Tests

Source     DF   Seq SS   Adj SS  Adj MS      F      P
Aggregate   2   783256   778152  389076  34.45  0.000
Block       7  1427596  1427596  203942  18.06  0.000
Error      41   463086   463086   11295
Total      50  2673938


S = 106.277   R-Sq = 82.68%   R-Sq(adj) = 78.88%


Analysis of Variance for Deformation, using Adjusted SS for Tests

Source     DF   Seq SS  Adj SS  Adj MS     F      P
Aggregate   2   2.5987  2.5775  1.2888  7.03  0.002
Block       7   7.6496  7.6496  1.0928  5.96  0.000
Error      41   7.5124  7.5124  0.1832
Total      50  17.7608


S = 0.428053   R-Sq = 57.70%   R-Sq(adj) = 48.42%


Analysis of Variance for Fracture Energy, using Adjusted SS for Tests

Source     DF   Seq SS  Adj SS  Adj MS     F      P
Aggregate   2   266.03  268.61  134.31  8.88  0.001
Block       7   267.86  267.86   38.27  2.53  0.029
Error      41   619.97  619.97   15.12
Total      50  1153.86


S = 3.88862   R-Sq = 46.27%   R-Sq(adj) = 34.48%
```

Appendix E-3: Regression Analysis: dry ITS (kPa) versus P_b, AV

The regression equation is
ITS (kPa) = 2549 - 223 P_b - 86.4 AV

Predictor	Coef	SE Coef	T	P
Constant	2549.02	95.50	26.69	0.000
P_b	-222.76	16.00	-13.92	0.000
AV	-86.422	5.876	-14.71	0.000

S = 81.6934 R-Sq = 88.7% R-Sq(adj) = 88.2%

Analysis of Variance

Source	DF	SS	MS	F	P
Regression	2	2410006	1205003	180.56	0.000
Residual Error	46	306995	6674		
Total	48	2717001			

Source	DF	Seq SS
Pb	1	966433
AV	1	1443573

Appendix E-4: Regression Analysis: Deformation (mm) versus P_b, AV

The regression equation is
Deformation (mm) = - 0.515 + 0.462P_b + 0.175 AV

Predictor	Coef	SE Coef	T	P
Constant	-0.5151	0.4819	-1.07	0.291
P_b	0.46151	0.08073	5.72	0.000
AV	0.17538	0.02965	5.91	0.000

S = 0.412236 R-Sq = 56.4% R-Sq(adj) = 54.5%

Analysis of Variance

Source	DF	SS	MS	F	P
Regression	2	10.1222	5.0611	29.78	0.000
Residual Error	46	7.8172	0.1699		
Total	48	17.9394			

Source	DF	Seq SS
Pb	1	4.1770
AV	1	5.9453

Appendix E-5: Regression Analysis: Deformation (mm) versus ITS (kPa)

The regression equation is
Deformation (mm) = 4.67 - 0.00198 ITS (kPa)

Predictor	Coef	SE Coef	T	P
Constant	4.6657	0.2172	21.48	0.000
ITS (kPa)	-0.0019819	0.0002385	-8.31	0.000

S = 0.393208 R-Sq = 59.5% R-Sq(adj) = 58.6%

Analysis of Variance

Source	DF	SS	MS	F	P
Regression	1	10.673	10.673	69.03	0.000
Residual Error	47	7.267	0.155		
Total	48	17.939			

Appendix E-6: Regression Analysis: FE(N/m) versus ITS, Deformation

The regression equation is
FE(N/m) = - 1545 + 2.57 ITS (kPa) + 721 Deformation (mm)

Predictor	Coef	SE Coef	T	P
Constant	-1544.6	326.2	-4.74	0.000
ITS (kPa)	2.5745	0.1711	15.04	0.000
Deformation (mm)	720.88	66.60	10.82	0.000

S = 179.542 R-Sq = 83.2% R-Sq(adj) = 82.5%

Analysis of Variance

Source	DF	SS	MS	F	P
Regression	2	7343098	3671549	113.90	0.000
Residual Error	46	1482824	32235		
Total	48	8825923			

Source	DF	Seq SS
ITS (kPa)	1	3566760
Deformation (mm)	1	3776338

Appendix E-7: Regression Analysis: FE(N/m) versus P_b, AV

The regression equation is
FE(N/m) = 4847 - 279 P_b - 96.0 AV

Predictor	Coef	SE Coef	T	P
Constant	4847.2	403.1	12.03	0.000
P_b	-279.08	67.52	-4.13	0.000
AV	-96.01	24.80	-3.87	0.000

S = 344.806 R-Sq = 38.0% R-Sq(adj) = 35.3%

Analysis of Variance

Source	DF	SS	MS	F	P
Regression	2	3356932	1678466	14.12	0.000
Residual Error	46	5468991	118891		
Total	48	8825923			

Source	DF	Seq SS
Pb	1	1575190
AV	1	1781742

Appendix E-8: Alternative Statistical Analysis for Interaction Effects

General Linear Model: ITS, Deformation, FE versus Aggregate, Gradation, BC, and AV:)

```
Factor     Type   Levels  Values
Aggregate  fixed       3  A, B, C
Gradation  fixed       2  C, F
AV         fixed       2  0.04, 0.07
BC         fixed       2  H, L
```

Analysis of Variance for ITS, using Adjusted SS for Tests

```
Source                    DF   Seq SS  Adj SS  Adj MS       F      P
Aggregate                  2   783256  775184  387592   49.64  0.000
Gradation                  1   177257  157167  157167   20.13  0.000
AV                         1   953378  995277  995277  127.47  0.000
BC                         1   246512  237012  237012   30.36  0.000
Aggregate*Gradation        2    74534   64551   32276    4.13  0.027
Aggregate*AV               2     7475    8536    4268    0.55  0.585
Aggregate*BC               2    16077   16058    8029    1.03  0.371
Gradation*AV               1       74      92      92    0.01  0.914
Gradation*BC               1    16885   18516   18516    2.37  0.135
AV*BC                      1       78      14      14    0.00  0.967
Aggregate*Gradation*AV     2    68514   68021   34010    4.36  0.023
Aggregate*Gradation*BC     2    48309   48347   24174    3.10  0.062
Aggregate*AV*BC            2       61     285     143    0.02  0.982
Gradation*AV*BC            1    27840   26125   26125    3.35  0.078
Aggregate*Gradation*AV*BC  2    42872   42872   21436    2.75  0.082
Error                     27   210814  210814    7808
Total                     50  2673938

S = 88.3625   R-Sq = 92.12%   R-Sq(adj) = 85.40%
```

Analysis of Variance for Deformatin, using Adjusted SS for Tests

```
Source                    DF   Seq SS  Adj SS  Adj MS      F      P
Aggregate                  2   2.5987  2.5813  1.2907   8.76  0.001
Gradation                  1   1.0626  0.8585  0.8585   5.83  0.023
AV                         1   3.6903  3.7277  3.7277  25.30  0.000
BC                         1   2.2769  2.3927  2.3927  16.24  0.000
Aggregate*Gradation        2   0.6472  0.5257  0.2628   1.78  0.187
Aggregate*AV               2   0.4249  0.4754  0.2377   1.61  0.218
Aggregate*BC               2   0.2483  0.2284  0.1142   0.78  0.471
Gradation*AV               1   0.0290  0.0617  0.0617   0.42  0.523
Gradation*BC               1   0.1932  0.1429  0.1429   0.97  0.334
AV*BC                      1   0.3297  0.2950  0.2950   2.00  0.169
Aggregate*Gradation*AV     2   0.1112  0.0821  0.0411   0.28  0.759
Aggregate*Gradation*BC     2   1.4718  1.5035  0.7517   5.10  0.013
Aggregate*AV*BC            2   0.3973  0.3736  0.1868   1.27  0.298
Gradation*AV*BC            1   0.0045  0.0033  0.0033   0.02  0.882
Aggregate*Gradation*AV*BC  2   0.2960  0.2960  0.1480   1.00  0.380
```

Error	27	3.9790	3.9790	0.1474
Total	50	17.7608		

S = 0.383888 R-Sq = 77.60% R-Sq(adj) = 58.51%

Analysis of Variance for FE (N/m), using Adjusted SS for Tests

Source	DF	Seq SS	Adj SS	Adj MS	F	P
Aggregate	2	2101982	2121809	1060904	10.13	0.001
Gradation	1	278274	273702	273702	2.61	0.118
AV	1	1171718	1476551	1476551	14.10	0.001
BC	1	324734	203316	203316	1.94	0.175
Aggregate*Gradation	2	13516	16206	8103	0.08	0.926
Aggregate*AV	2	291436	206614	103307	0.99	0.386
Aggregate*BC	2	2738	4580	2290	0.02	0.978
Gradation*AV	1	133150	212892	212892	2.03	0.165
Gradation*BC	1	176803	114919	114919	1.10	0.304
AV*BC	1	1167	1631	1631	0.02	0.902
Aggregate*Gradation*AV	2	440673	360263	180132	1.72	0.198
Aggregate*Gradation*BC	2	978135	984669	492334	4.70	0.018
Aggregate*AV*BC	2	205229	218266	109133	1.04	0.366
Gradation*AV*BC	1	27752	26000	26000	0.25	0.622
Aggregate*Gradation*AV*BC	2	141941	141941	70970	0.68	0.516
Error	27	2827703	2827703	104730		
Total	50	9116950				

S = 323.620 R-Sq = 68.98% R-Sq(adj) = 42.56%

APPENDIX F: MINITAB STATISTICAL RESULTS—STRIPPING

Appendix F-1: Regression Analysis: Wet Samples ITS_{wet} versus P_b, AV

The regression equation is
$ITS_{wet} = 1030 - 155\ P_b + 67.3\ AV$

Predictor	Coef	SE Coef	T	P
Constant	1029.75	98.61	10.44	0.000
P_b	-154.57	13.80	-11.20	0.000
AV	67.272	8.148	8.26	0.000

S = 52.3270 R-Sq = 90.4% R-Sq(adj) = 89.6%

Analysis of Variance

Source	DF	SS	MS	F	P
Regression	2	592945	296473	108.28	0.000
Residual Error	23	62977	2738		
Total	25	655922			

Source	DF	Seq SS
P_b	1	406323
AV	1	186622

Appendix F-2: Deformation and FE Comparison between Dry and Wet Samples

Aggregate Sources	Coarse-Graded		Fine-Graded	
	OBC+0.25%	OBC-0.25%	OBC+0.25%	OBC-0.25%
	Percentage of Flow Loss (%)			
A	7.0	2.0	2.0	-31.0
B	3.0	14.9	-21.0	-27.0
C	1.0	7.0	13.0	-4.0
	Percentage of Fracture Energy Loss (%)			
A	13.0	7.0	17.0	-4.0
B	4.0	21.0	-7.0	-14.0
C	7.0	-12.0	2.0	18.0

APPENDIX G: MECHANICAL TEST RESULTS

Appendix G-1 Aggregate A Rutting Test Results

Code	sample #	P_b(%)	BSG	V_b(%)	VTM (%)	VMA (%)	V_{be} (%)	VFA (%)	Rut Depth (mm)	Adj'd Rut Depth (mm)
C7%-5.9	1	5.90	2.321	13.2	8.3	18.1	9.8	54.1	5.1	4.3
C7%-5.9	2	5.90	2.332	13.2	7.9	17.7	9.9	55.6	5.4	4.9
C7%-5.9	3	5.90	2.336	13.2	7.7	17.6	9.9	56.2	6.6	6.2
C7%-5.9	4	5.90	2.362	13.4	6.7	16.7	10.0	59.9	4.6	4.8
C4%-5.4	1	5.40	2.438	12.6	4.4	13.6	9.1	67.3	3.0	2.7
C4%-5.4	2	5.40	2.443	12.7	4.2	13.7	9.1	66.7	2.0	1.8
C4%-5.4	3	5.40	2.444	12.7	4.2	13.6	9.1	67.0	3.8	3.7
C4%-5.4	4	5.40	2.453	12.7	3.9	13.3	9.2	68.7	1.3	1.4
F4%-5.9	1	5.90	2.416	13.7	4.7	14.7	10.0	67.9	4.0	3.6
F4%-5.9	2	5.90	2.416	13.7	4.7	14.7	10.0	68.0	5.1	4.7
F4%-5.9	3	5.90	2.415	13.7	4.8	14.8	10.0	67.7	4.7	4.3
F4%-5.9	4	5.90	2.426	13.7	4.3	14.4	10.0	69.8	5.4	5.2
F7%-5.4	1	5.40	2.367	12.3	7.4	16.0	8.6	53.9	4.5	4.3
F7%-5.4	2	5.40	2.369	12.3	7.3	15.9	8.7	54.3	6.3	6.2
F7%-5.4	3	5.40	2.359	12.2	7.7	16.3	8.6	52.8	4.6	4.2
F7%-5.4	4	5.40	2.374	12.3	7.1	15.8	8.7	55.0	5.6	5.6
C7%-5.4	1	5.90	2.360	13.4	6.8	16.4	10.0	60.7	3.5	2.8
C7%-5.4	2	5.90	2.375	13.5	6.2	15.9	10.0	63.1	4.5	4.2
C7%-5.4	3	5.90	2.369	13.4	6.4	16.1	10.0	62.2	3.4	2.9
C7%-5.4	4	5.90	2.363	13.4	6.6	16.3	10.0	61.3	4.8	4.2
C4%-5.9	1	5.40	2.459	12.8	3.6	13.1	9.2	70.0	1.4	2.4
C4%-5.9	2	5.40	2.460	12.8	3.6	13.1	9.2	70.3	0.9	2.0
C4%-5.9	3	5.40	2.456	12.7	3.7	13.2	9.2	69.5	1.6	2.6
C4%-5.9	4	5.40	2.458	12.7	3.7	13.2	9.2	69.8	2.6	3.6
F7%-5.9	1	5.90	2.326	13.2	8.3	17.9	9.6	53.8	5.5	4.8
F7%-5.9	2	5.90	2.340	13.3	7.7	17.4	9.7	55.6	5.9	5.4
F7%-5.9	3	5.90	2.315	13.1	8.7	18.3	9.6	52.4	5.9	4.9
F7%-5.9	4	5.90	2.335	13.2	7.9	17.6	9.7	55.0	4.4	3.9
F4%-5.4	1	5.40	2.399	12.4	6.1	14.9	8.8	58.8	3.9	2.6
F4%-5.4	2	5.40	2.382	12.4	6.8	15.5	8.7	56.2	4.2	2.6
F4%-5.4	3	5.40	2.402	12.5	6.0	14.8	8.8	59.5	3.5	2.3
F4%-5.4	4	5.40	2.406	12.5	5.8	14.6	8.8	60.0	5.3	4.2

Appendix G-2 Aggregate B Rutting Test Results

Code	sample #	P_b (%)	BSG	V_b(%)	VTM (%)	VMA (%)	V_{be} (%)	VFA (%)	Rut Depth (mm)	Adj'd Rut Depth[2] (mm)
F4%-4.45	1	4.45	2.500	10.7	3.3	13.7	10.4	76.0	2.3	2.9
F4%-4.45	2	4.45	2.492	10.7	3.6	14.0	10.4	74.2	0.9	1.2
F4%-4.45	3	4.45	2.485	10.6	3.9	14.2	10.4	72.8	1.7	1.8
F7%-4.1[1]	1	4.10	2.418	9.5	7.0	16.2	9.27	57.1	5.1	-
F7%-3.95	2	3.95	2.428	9.2	6.8	15.8	8.95	56.7	3.7	3.8
F7%-3.95	3	3.95	2.428	9.2	6.8	15.8	8.95	56.7	3.7	3.8
C4%-4.45	1	4.45	2.513	10.7	3.9	13.5	9.59	71.0	4.7	4.8
C4%-4.45	2	4.45	2.530	10.8	3.3	12.9	9.65	74.6	1.4	2.1
C4%-4.45	3	4.45	2.519	10.8	3.7	13.3	9.61	72.3	1.4	1.7
C7%-4.95	1	4.95	2.434	11.6	6.2	16.7	10.5	62.8	5.0	5.7
C7%-4.95	2	4.95	2.436	11.6	6.1	16.6	10.5	63.1	4.9	5.7
C7%-4.95	3	4.95	2.428	11.5	6.5	16.9	10.4	61.8	6.1	6.6
C7%-4.45	1	4.45	2.457	10.5	6.1	15.4	9.38	60.7	6.3	7.1
C7%-4.45	2	4.45	2.449	10.5	6.4	15.7	9.35	59.4	4.6	5.2
C7%-4.45	3	4.45	2.450	10.5	6.4	15.7	9.35	59.5	4.5	5.0
C4%-4.95	1	4.95	2.506	11.9	3.4	14.2	10.8	75.8	4.6	5.1
C4%-4.95	2	4.95	2.514	12.0	3.1	13.9	10.8	77.5	3.4	4.2
C4%-4.95	3	4.95	2.507	11.9	3.4	14.2	10.8	76.0	4.4	4.9
F4%-3.95	1	3.95	2.511	9.5	3.6	12.9	9.26	71.7	1.7	2.0
F4%-3.95	2	3.95	2.513	9.5	3.5	12.8	9.27	72.2	1.2	1.6
F4%-3.95	3	3.95	2.517	9.5	3.4	12.7	9.28	72.9	0.9	1.4
F7%-4.45	1	4.45	2.423	10.4	6.3	16.3	10.1	61.8	5.6	6.3
F7%-4.45	2	4.45	2.418	10.3	6.5	16.5	10.1	61.0	5.2	5.6
F7%-4.45	3	4.45	2.425	10.4	6.2	16.3	10.1	62.1	5.0	5.7

Note: 1. the binder content of that sample was wrong and it was not included in the statistical analysis.

2. Adjustment is referred to Chapter IV (Analysis of Covariance section), as well as with all other tables.

Appendix G-3 Aggregate A Dry IDT Test Results

Code	sample #	P_b(%)	VTM (%)	ITS (kPa)	Deformation (mm)	FE (N/m)	ITS Adj'd (kPa)	Deformation Adj'd (mm)	FE Adj'd (N/m)
C4%-6.25	1	6.25	4.0	755	2.5	2301	755	2.5	2301
C4%-6.25	2	6.25	3.9	735	3.0	2710	727	3.1	2712
C7%-6.25	1	6.25	6.9	554	3.9	2589	546	4.0	2592
C7%-6.25	2	6.25	6.6	544	3.8	2542	518	4.0	2549
C4%-5.75	1	5.75	3.6	844	2.5	2431	825	2.6	2438
C4%-5.75	2	5.75	3.9	876	2.8	2790	874	2.8	2791
C7%-5.75	1	5.75	8.3	657	3.7	2903	714	3.4	2882
C7%-5.75	2	5.75	7.8	680	3.2	2361	714	3.0	2348
F4%-6.25	1	6.25	3.6	846	3.2	3054	801	3.3	2942
F4%-6.25	2	6.25	4.4	818	3.2	3004	858	3.1	3102
F7%-6.25	1	6.25	7.7	447	4.2	2065	520	4.0	2245
F7%-6.25	2	6.25	6.1	548	3.6	2358	448	3.8	2113
F4%-5.75	1	5.75	4.6	1026	2.5	2989	1093	2.4	3089
F4%-5.75	2	5.75	4.8	1014	2.3	2703	1095	2.2	2824
F7%-5.75	1	5.75	6.1	642	3.6	2690	553	3.7	2558
F7%-5.75	2	5.75	8.7	617	2.9	2245	791	2.7	2781

Appendix G-4 Aggregate B Dry IDT Test Results

Code	sample #	P_b (%)	VTM (%)	ITS (kPa)	Deformation (mm)	FE (N/m)	ITS Adj'd (kPa)	Deformation Adj'd (mm)	FE Adj'd (N/m)
F4%-3.95*	1	4	4.3	919	2.286	3431	935	2.3	3515
F4%-3.95	2	4	4.171	1385	2.286	3627	1394	2.3	3675
F4%-4.45	1	4.5	4.333	1146	2.54	3408	1183	2.5	3476
F4%-4.45	2	4.5	4.512	1253	2.54	3649	1310	2.5	3753
F7%-3.95	1	4	6.967	1026	2.54	3001	1024	2.5	2992
F7%-3.95	2	4	7.674	969	2.159	2426	1006	2.2	2614
F7%-4.45	1	4.5	7.185	875	3.048	3175	896	3.0	3185
F7%-4.45	3	4.5	7.553	851	2.667	2718	913	2.6	2749
C4%-4.45	1	4.5	4.944	1297	2.794	3848	1443	2.6	3901
C4%-4.45	2	4.5	4.672	1209	2.032	2723	1313	1.9	2761
C4%-4.95	1	5	3.086	1108	2.794	3459	1020	2.9	3297
C4%-4.95	2	5	3.47	1126	2.286	2989	1075	2.3	2895
C7%-4.45	1	4.5	6.844	917	3.175	3315	892	3.2	3307
C7%-4.45	2	4.5	7.288	869	2.794	2934	913	2.7	2950
C7%-4.95	1	5	7.382	748	2.921	2394	785	2.9	2461
C7%-4.95	2	5	6.502	755	3.048	2883	707	3.1	2796

* This sample was identified as an outlier; it was not included in the regression analysis.

Appendix G-5 Aggregate C Dry IDT Test Results

Code	sample #	P_b (%)	VTM (%)	ITS (kPa)	Deformation (mm)	FE (N/m)	ITS Adj'd (kPa)	Deformation Adj'd (mm)	FE Adj'd (N/m)
C4%-6.05	1	6.05	3.4	866	2.8	2672	826	3.0	2661
C4%-6.05	2	6.05	3.2	869	3.4	3260	818	3.6	3245
C7%-6.05	1	6.05	7.0	630	3.8	2755	630	3.8	2755
C7%-6.05	2	6.05	7.7	592	4.4	3006	636	4.3	3019
C4%-5.55	1	5.55	3.7	1196	2.5	2956	1166	2.6	2918
C4%-5.55	2	5.55	3.5	1001	2.5	2911	942	2.6	2836
C7%-5.55	1	5.55	7.4	661	3.4	2790	704	3.4	2845
C7%-5.55	2	5.55	6.5	724	2.0	1766	662	2.1	1687
F4%-5.05*	1	5.05	8.6	711	2.5	2291	1151	1.9	2501
F4%-5.05	1	5.05	3.5	1158	1.9	2328	1112	2.0	2306
F4%-5.05	2	5.05	4.6	1076	2.5	2981	1137	2.4	3010
F7%-5.05	1	5.05	10.2	516	3.8	2363	821	3.4	2509
F7%-5.05	2	5.05	6.3	906	2.5	2657	838	2.6	2624
F4%-4.55	1	4.55	3.5	1083	3.2	3617	1029	3.3	3536
F4%-4.55	2	4.55	3.9	1209	2.2	2999	1200	2.2	2986
F7%-4.55	1	4.55	10.6	617	3.2	2419	971	2.4	2956
F7%-4.55	2	4.55	10.5	630	3.8	2903	981	3.1	2980
F7%-4.55	3	4.55	5.5	1158	2.4	3117	1013	2.7	3257
F7%-4.55	4	4.55	5.1	1076	2.2	2723	892	2.6	2868

* This sample was identified as an outlier and was not included in the regression analysis.

Appendix G-6 Wet IDT Test Results

Code	Agg.	sample #	P_b (%)	VTM (%)	ITS (kPa)	Deformat-ion (mm)	FE (N/m)	ITS Adj'd (kPa)	Deformation Adj'd (mm)	FE Adj'd (N/m)
F7%-3.95	B	1	3.95	7.4	919	2.9	3236	887	3.0	3219
F7%-3.95	B	2	3.95	7.3	964	2.9	3173	941	3.0	3161
F7%-4.45	B	1	4.45	7.3	839	3.4	3435	819	3.5	3425
F7%-4.45	B	2	4.45	7.4	798	3.3	2937	766	3.4	2920
C7%-4.45	B	1	4.45	7.1	796	2.5	2506	791	2.5	2504
C7%-4.45	B	2	4.45	7.2	793	2.5	2465	777	2.6	2457
C7%-4.95	B	1	4.95	6.9	667	2.8	2368	671	2.8	2371
C7%-4.95	B	2	4.95	6.6	718	3.0	2669	748	3.0	2688
C7%-6.25	A	1	6.25	7.5	491	3.9	2337	449	4.0	2314
C7%-6.25	A	2	6.25	6.5	514	3.4	2137	553	3.4	2160
C7%-5.75	A	1	5.75	8.0	667	2.5	2039	588	2.7	1993
C7%-5.75	A	2	5.75	7.8	692	3.6	2892	628	3.7	2856
F7%-6.25	A	1	6.25	6.5	573	3.8	2606	611	3.7	2630
F7%-6.25	A	2	6.25	6.6	516	3.9	2468	545	3.9	2486
F7%-5.75	A	1	5.75	8.1	619	4.2	3000	533	4.4	2951
F7%-5.75	A	2	5.75	8.3	619	3.8	2676	523	4.0	2621
C7%-6.05	C	1	6.05	7.0	588	4.3	2794	591	4.3	2797
C7%-6.05	C	2	6.05	7.2	560	3.8	2596	546	3.8	2589
C7%-5.55	C	1	5.55	6.7	686	3.0	2483	707	3.0	2496
C7%-5.55	C	2	5.55	6.8	667	3.2	2566	684	3.1	2577
F7%-5.05	C	1	5.05	6.6	781	2.8	2654	815	2.7	2675
F7%-5.05	C	2	5.05	6.6	749	2.5	2325	783	2.5	2345
F7%-4.55	C	1	4.55	11.5	1121	2.3	2917	775	2.9	2716
F7%-4.55	C	2	4.55	10.3	1053	2.0	2272	796	2.5	2123
F7%-4.55	C	3	4.55	5.5	598	3.0	2282	712	2.8	2350
F7%-4.55	C	4	4.55	5.0	661	3.2	2551	816	2.9	2643

REFERENCES

AASHTO. (2003). *Standard method of test for determining rutting susceptibility of hot mix asphalt (HMA) using the asphalt pavement analyzer (APA)* (2003 ed.). Virginia: American Association of State Highway and Transportation Officials (AASHTO).

AASHTO. (2004). Standard specification for Superpave volumetric mix design (M 323-04). In *Standard specifications for transportation materials and methods of sampling and testing* (24th ed.). Washington, D.C.: American Association of State Highway and Transportation Officials.

Archilla, A. R., & Madanat, S. (2001). Statistical model of pavement rutting in asphalt concrete mixes. Paper presented at the (1764) 70-77.

Asphalt Institute. (2001). *Superpave mix design, Superpave series no. 2 (SP-2)* (2nd ed.). Lexington, Kentucky: Asphalt Institute.

Asphalt Pavement Research and Technology. (1997). *National asphalt roadmap: A commitment to the future.* Lanham, Maryland: National Asphalt Pavement Association.

Baladi, G. Y., Schorsch, M., & Svasdisant, T. (2002). Determining the causes of top-down cracking in bituminous pavements. *Final Report for Michigan Department of Transportation, Department of Civil and Environmental Engineering, Michigan State University, East Lansing, MI.*

Bazin, P., & Saunier, J. (1967). Deformability, fatigue and healing properties of asphalt mixes. Paper presented at the *Intl Conf Struct Design Asphalt Pvmts.*

Birgisson, B., Montepara, A., Napier, J., Romeo, E., Roncella, R., & Tebaldi, G. (2006). Micromechanical analyses for measurement and prediction of hot-mix asphalt fracture energy. Paper presented at the *Bituminous Paving Mixtures,* (1970) 186-195.

Brown, E. R., Collins, R., & Brownfield, J. R. (1989). Investigation of segregation of asphalt mixtures in the state of georgia. *Transportation Research Record* (1217)

Brown, E. R., & Cross, S. A. (1989). *A study of in-place rutting of asphalt pavements.* Auburn, AL: National Center for Asphalt Technology.

Carpenter, S. H., & Shen, S. (2006). Dissipated energy approach to study hot-mix asphalt healing in fatigue. Paper presented at the *Bituminous Paving Mixtures,* (1970) 178-185.

Chatti, K., & El Mohtar, C. S. (2004). Effect of different axle configurations on fatigue life of asphalt concrete mixture. *Transportation Research Record,* (1891) 121-130.

Choubane, B., Page, G. C., & Musselman, J. A. (2000). Suitability of asphalt pavement analyzer for predicting pavement rutting. *Transportation Research Record,* (1723), 107-115.

Choubane, B., Gokhale, S., Sholar, G., & Moseley, H. (2006). Evaluation of coarse- and fine-graded superpave mixtures under accelerated pavement testing. Paper presented at the *Pavement Management; Monitoring,* (1974) 120-127.

Christensen, D. W., & Bonaquist, R. F. (2004). *Evaluation of indirect tensile test (IDT) procedures for low-temperature performance of hot mix asphalt*. Washington, D.C.: Transportation Research Board National Research.

Christensen, D. W., & Bonaquist, R. F. (2006). *Volumetric requirements for Superpave mix design.* Transportation Research Board National Academy of Sciences.

Cominsky, R. J., Killingsworth, B. M., Anderson, R. M., Anderson, D. A., & Crockford, W. W. (1998). *NCHRP report 409: Quality control and acceptance of Superpave-designed hot mix asphalt.* Washington, D.C.: Transportation Research Board National Academy Press.

Davis, R. (2001). Discussions. *Proceedings, Association of Asphalt Paving Technologists, 70* 700-707.

Elliott, R. P., Ford, M. C., Jr., Ghanim, M., & Tu, Y. F. (1991). Effect of aggregate gradation variation on asphalt concrete mix properties. *Transportation Research Record,* (1317), 52-60.

Epps, J. A., & Monismith, C. L. (1972). Fatigue of asphalt concrete mixtures-summary of existing information. *Fatigue of Compacted Bituminous Aggregate Mixture* , 19.

Finn, F. N., & Epps. J.A. (1980). *Compaction of hot mix asphalt concrete (research report 214-21).* College Station: Texas Transportation Institute, Texas A&M University.

Ford, M. C. J. (1988). *Pavement densification related to asphalt mix characteristics*. Washington, D.C.: Transportation Research Board.

Freddy L. Roberts, Prithvi S. Kandhal, E. Ray Brown, Dah-Yinn Lee, Thomas W. Kennedy. (1996). *Hot mix asphalt materials, mixture design, and construction* (2nd ed.). Lanham, Maryland: National Asphalt Pavement Association Research and Education Foundation.

Grenfell, J. R. A., Taherkhani, H., Collop, A. C., Airey, G. D., & Scarpas, A. (2008). Deformation characterization of asphalt concrete behavior. Paper presented at the *2008 Annual Meeting of the Association of Asphalt Paving Technologists, AAPT, April 25, 2008 - April 30 , 77* 479-516.

Harmelink, D., Shuler, S., & Aschenbrener, T. (2008). Top-down cracking in asphalt pavements: Causes, effects, and cures. *Journal of Transportation Engineering, 134*(1), 1-6.

Harmelink, D., Aschenbrener, T., & Shuler, S. (2007). Achieving 4% air voids in real pavements with Superpave. *Transportation Research Record,* (2040), 115-122.

Huber, G. A., & Heiman, G. H. (1987). Effect of asphalt concrete parameters on rutting performance: A field investigation. Paper presented at the *Proceedings, Association of Asphalt Paving Technologists, 56* 33-61.

Kandhal, P. S. (1994). Field and laboratory investigation of stripping in asphalt pavements: State of the art report. *Transportation Research Record,* (1454), 36-47.

Kandhal, P. S., & Cooley, L. A. (2003). *Accelerated laboratory rutting tests: Evaluation of the asphalt pavement analyzer, NCHRP report 508.* Washington, D.C.: Transportation Research Board.

Kandhal, P. S., & Cooley Jr., L. A. (2002). Coarse-versus fine-graded Superpave mixtures comparative evaluation of resistance to rutting. *Transportation Research Record,* (1789), 216-224.

Kandhal, P. S., & Cooley Jr., L. A. (2006). Simulative performance test for hot mix asphalt using asphalt pavement analyzer. *Journal of ASTM International, 3*(5)

Kandhal, P. S., & Mallick, R. B. (2001). Effect of mix gradation on rutting potential of dense-graded asphalt mixtures. *Transportation Research Record,* (1767), 146-151.

Kassem, E., Masad, E., Chowdhury, A., & Claros, G. (2008). Influence of field compaction pattern on asphalt pavement uniformity. Paper presented at the *2008 Annual Meeting of the Association of Asphalt Paving Technologists, AAPT, April 25, 2008 - April 30, , 77* 257-298.

Leiva, F., & West, R. C. (2008). Relationships between laboratory measured characteristics of HMA and field compactability. Paper presented at the *2008 Annual Meeting of the Association of Asphalt Paving Technologists, AAPT, April 25, 2008 - April 30, , 77* 183-219.

Linden, R. N., Mahoney, J. P., & Jackson, N. C. (1989). Effect of compaction on asphalt concrete performance. *Transportation Research Record,* (1217)

Monismith, C. L., Epps, J. A., & Finn, F. N. (1985). Improved asphalt mix design. Paper presented at the *Proceedings of the Association of Asphalt Paving Technologists , 54* 347-406.

Monismith, C. L., Popescu, L., & Harvey, J. (2004). Performance-based pay factors for asphalt concrete construction; comparison with a currently used experience-based approach. Paper presented at the *Asphalt Paving Technology 2004, March 8, 2004 - March 10 , 73* 147-194.

Myers, L. A., Roque, R., & Ruth, B. E. (1998). Mechanisms of surface-initiated longitudinal wheel path cracks in high-type bituminous pavements. *Journal of the Association of Asphalt Paving Technologists, 67*, 401-432.

Pellinen, T. K., Xiao, S., Carpenter, S., Masad, E., Di Benedetto, H., & Roque, R. (2005). Relationship between triaxial shear strength and indirect tensile strength of hot mix asphalt. Paper presented at the *2005 Meeting of the Association of Asphalt Paving Technologists, March 7, 2005 - March 9, 74* 347-379.

Prowell, B. D., & Brown, E. R. (2007). Verification of the N design levels. Paper presented at the *Asphalt Paving Technology 2007 AAPT, March 11, 2007 - March 14, 76* 771-821.

Prowell, B. D., & Dudley, M. C. (2002). Evaluation of measurement techniques for asphalt pavement density and permeability. *Transportation Research Record,* (1789), 36-45.

Puangchit, P., Hicks, R. G., Wilson, J. E., & Bell, C. (1982). *Impact of variation in material properties on asphalt pavement life.* Salem, Oregon: Oregon Department of Transportation.

R. Lyman Ott, Michael Longnecker. (2001). *An introduction to statistical methods and data analysis* (5th ed. ed.). California: Duxbury.

Roque, R., Birgisson, B., Drakos, C., & Dietrich, B. (2004). Development and field evaluation of energy-based criteria for top-down cracking performance of hot mix asphalt. Paper presented at the *Asphalt Paving Technology 2004, March 8, 2004 - March 10 , 73* 229-260.

Santucci, L. E., Allen, D. D., & Coats, R. L. (1985). The effects of moisture and compaction on the quality of asphalt pavements. *Proc. Asphalt Paving Technologists, 54*

SC DOT. (2009). *Standard method of test for laboratory determination of moisture susceptibility based on retained strength of asphalt concrete mixture (SC designation: SC-T-70 (07-09)).*South Carolina Department of Transportation.

SC DOT. (2010). *South Carolina department of transportation qualified coarse aggregate sources*

SC DOT. (2011). *South Carolina department of transportation qualified fine aggregate sources*

SC DOT. (2009). *Supplemental technical specification for hot-mix asphalt material properties-designation: SC-M-402 (03/11).* Columbia, SC: South Carolina Department of Transportation.

Shen, S., & Carpenter, S. H. (2006). *Dissipated energy concepts for HMA performance: Fatigue and healing. Dissertation Abstracts International, 67*(11)

Shen, S., & Carpenter, S. H. (2007). Development of an asphalt fatigue model based on energy principles. Paper presented at the *Asphalt Paving Technology 2007 AAPT, March 11, 2007 - March 14, 76* 525-573.

Shen, S., Chiu, H., & Huang, H. (2010). Characterization of fatigue and healing in asphalt binders. *Journal of Materials in Civil Engineering, 22*(9), 846-852.

Tam, K. K., Raciborski, R., & Lynch, D. F. (1989). Performance of 18 bituminous test sections on a major urban freeway during 11 years of service. *Transportation Research Record,* (1217), 65-79.

Tashman, L., Masad, E., Little, D., & Lytton, R. (2004). Damage evolution in triaxial compression tests of HMA at high temperatures. Paper presented at the *Asphalt Paving Technology 2004, March 8, 2004 - March 10, 73* 53-87.

Toler, J. (2008). *Design and analysis of experiments*

Tran, N., West, R., Powell, B., & Kvasnak, A. (2009). Evaluation of AASHTO rut test procedure using the asphalt pavement analyzer. Paper presented at the *Asphalt Paving Technology 2009, AAPT, March 15, 2009 - March 18, 78* 1-24.

Uhlmeyer, J. S., Willoughby, K., Pierce, L. M., & Mahoney, J. P. (2000). Top-down cracking in Washington state asphalt concrete wearing courses. *Transportation Research Record: Journal of the Transportation Research Board, 1730*, 110-116.

Vavrik, W. R., Pine, W. J., Huber, G., Carpenter, S. H., & Bailey, R. (2002). The bailey method of gradation evaluation: The influence of aggregate gradation and packing characteristics on

voids in the mineral aggregate. Paper presented at the *Asphalt Paving Technology 2001, March 19, 2001 - March 21, 70* 132-175.

Vivar, E., & Haddock, J. E. (2007). Hot-mix asphalt permeability and porosity. Paper presented at the *Asphalt Paving Technology 2007 AAPT, March 11, 2007 - March 14 , 76* 953-979.

Wen, H., & Kim, Y. R. (2002). Simple performance test for fatigue cracking and validation with WesTrack mixtures. *Transportation Research Record: Journal of the Transportation Research Board, 1789*, 66-72.

William Mendenhall, T. S. (1996). *A second course in statistics: Regression analysis* (5th ed.). New Jersey: Prentice-Hall, Inc.

Williams, R. C., & Prowell, B. D. (1999). Comparison of laboratory wheel-tracking test results with WesTrack performance. *Transportation Research Record,* (1681), 121-128.

Xiao, F., Zhao, W., Gandhi, T., & Amirkhanian, S. N. (2011). Laboratory investigation of moisture susceptibility of long-term saturated warm mix asphalt mixtures. *International Journal of Pavement Engineering, in print*

Xiao, F., Zhao, W., & Amirkhanian, S. N. (2009). Fatigue behavior of rubberized asphalt concrete mixtures containing warm asphalt additives. *Construction and Building Materials, 23*(10), 3144-3151.

Xiao, F., Zhao, W., & Amirkhanian, S. N. (2011). Laboratory investigation of fatigue characteristics of rubberized asphalt mixtures containing warm asphalt additives at a low temperature. *Journal of Testing and Evaluation, 39*(2), 290-295.

Xiao, F., Zhao, W., Gandhi, T., & Amirkhanian, S. N. (2010). Influence of antistripping additives on moisture susceptibility of warm mix asphalt mixtures. *Journal of Materials in Civil Engineering, 22*(10), 1047-1055.

Yoder, E. J., & Witczak, M. W. (1975). *Principles of pavement design* (2nd ed.). New York: John Wiley & Sons, Inc.

Yoo, P. J., & Al-Qadi, I. (2008). The truth and myth of fatigue cracking potential in hot-mix asphalt: Numerical analysis and validation. Paper presented at the *2008 Annual Meeting of the Association of Asphalt Paving Technologists, AAPT, April 25, 2008 - April 30 , 77,* 549-590.

Zhang, J., Cooley Jr., L. A., Hurley, G., & Parker, F. (2004). Effect of Superpave defined restricted zone on hot-mix asphalt performance. Paper presented at the (1891) 103-111.

Zhang, Z., Roque, R., Birgisson, B., & Sangpetngam, B. (2002). Identification and verification of a suitable crack growth law. Paper presented at the *Asphalt Paving Technology 2001, March 19, 2001 - March 2 , 70* 206-241.

Zube, E. (1962). Compaction studies of asphalt concrete pavements as related to the water permeability test. *Highway Research Board*, Bulletin, 358